

November 2022

L-Ergothioneine Treatment in Old CBA/CaJ Male Mice Slows the Progression of Age-related Hearing Loss

Mark A. Bauer
University of South Florida

Follow this and additional works at: <https://digitalcommons.usf.edu/etd>



Part of the [Speech Pathology and Audiology Commons](#)

Scholar Commons Citation

Bauer, Mark A., "L-Ergothioneine Treatment in Old CBA/CaJ Male Mice Slows the Progression of Age-related Hearing Loss" (2022). *USF Tampa Graduate Theses and Dissertations*.
<https://digitalcommons.usf.edu/etd/10376>

This Dissertation is brought to you for free and open access by the USF Graduate Theses and Dissertations at Digital Commons @ University of South Florida. It has been accepted for inclusion in USF Tampa Graduate Theses and Dissertations by an authorized administrator of Digital Commons @ University of South Florida. For more information, please contact digitalcommons@usf.edu.

L-Ergothioneine Treatment in Old CBA/CaJ Male Mice

Slows the Progression of Age-related Hearing Loss

by

Mark A. Bauer

A dissertation submitted in partial fulfillment
of the requirements for the degree of
Doctor of Philosophy
Department of Medical Engineering
College of Engineering
University of South Florida

Major Professor: Robert D. Frisina, Ph.D.
Joseph Walton, Ph.D.
Mark Jaroszeski, Ph.D.
Bo Ding, M.D.
Victoria Sanchez, Ph.D.

Date of Approval:
October 25, 2022

Keywords: Anti-Oxidant, Sex Selectivity, Thresholds, Tissue Analysis, Correlation

Copyright © 2022, Mark A. Bauer

Dedication

I'd like to dedicate this dissertation to the many people who have encouraged me throughout my time in grad school. Your words have meant so much to me as I've gone through challenges in my years of graduate school. Those conversations were pivotal in my completion of a PhD. In no particular order, these are some of the people that I'd like to honor: Rich Seidler, James Burke, Pastor Zhivago, Arnie Gulley, Nicole Febles, Parveen Bazard, and most importantly my parents, Roland and Jackie Bauer. Thank you, thank you for your encouragement; I couldn't have done it without you.

Acknowledgments

There are many people that I'd like to acknowledge for their help in various parts of my dissertation. I'd first like to acknowledge the contribution of undergraduates who have meaningfully provided data for my dissertation through analysis of animal data collected over the course of 3 years. As one can imagine, this data analysis required multiple generations of lab assistants where they had analyzed the data in one form or another. Many, many thanks to these undergraduate helpers, Alejandro A. Acosta, Nidhi Bangalore, Lina Elessaway, Mark Thivierge, and Moksheta Chellani, y'all are the best!

Secondly, I'd like to thank Dr. Laurent Calcul for his incredible help in teaching me LC-MS/MS. He was always available for questions whenever I had them and helped to guide me through some of the pain points in my experiments. Thank you Dr. Calcul!

I'd also like to acknowledge Dr. Walton's help in initial discussions about Ergothioneine and guiding me through some of the finer points of ABR waveforms. Thank you!

Lastly, I'd like to acknowledge Dr. Frisina for helping to guide me through my project and this last bit of the journey with my dissertation and defense. Thanks again!

Table of Contents

List of Tables	iii
List of Figures	iv
Abstract.....	vi
Chapter 1: Introduction	1
Chapter 2: Materials and Methods.....	16
2.1 Subjects.....	16
2.2 Dosing Scheme.....	16
2.3 Hearing Tests.....	17
2.3.1 Auditory Brainstem Response (ABR)	17
2.3.2 Data Analysis: Auditory Brainstem Response (ABR) Thresholds	18
2.3.3 Data Analysis: Auditory Brainstem Response (ABR) Peak Picking.....	19
2.3.4 Distortion Product Otoacoustic Emissions (DPOAE).....	20
2.3.5 Data Analysis: Distortion Product Otoacoustic Emission (DPOAE).....	21
2.4 Blood Sampling	22
2.5 LC-MS/MS-Blood Preparation.....	22
2.6 LC-MS/MS-EGT Quantification.....	22
2.7 Gene Expression - RT-PCR.....	23
2.8 Reagents.....	24
2.9 Survival Analyses.....	25
Chapter 3: Results	29
3.1 ABR Threshold Analysis.....	29
3.2 DPOAE Amplitude and Threshold Analysis	32
3.3 ABR Amplitude and Latency Analysis.....	34
3.4 EGT Uptake - LC-MS/MS Analysis - Whole Blood Sampling.....	36
3.5 EGT Blood Levels and ABR Threshold Correlation Analysis	38
3.6 Cochlear Tissue Analysis: RT-PCR Results	40
3.7 Survival Analyses.....	42
Chapter 4: Discussion.....	60
4.1 Sex Differences in EGT Treatments and Auditory Measures.....	60
4.2 Underlying Mechanisms	66

Chapter 5: Conclusion	71
References	72
Appendix A: EGT Injection Calculations	88
Appendix B: Compiled Group Results for ABR and DPOAE.....	90
Appendix C: Peak Picking Results-Peak 1.....	96

List of Tables

Table 2.1: Primer List for Gene Expression Targets.....	28
---	----

List of Figures

Figure 2.1: Hearing Testing, Blood Sampling and EGT Treatment Timeline.....	26
Figure 2.2: ABR Amplitude and Latency Example Analysis.....	27
Figure 3.1: Male ABR Results.	45
Figure 3.2: Female ABR Results.....	46
Figure 3.3: Male DPOAE Results.	47
Figure 3.4: Female DPOAE Results.....	48
Figure 3.5: ABR Amplitude Analysis Peak 1.....	49
Figure 3.6: ABR Latency Analysis Peak 1.	50
Figure 3.7: Whole Blood Analysis.....	51
Figure 3.8: Baseline Values Analysis.	52
Figure 3.9: EGT Levels in Blood and ABR Thresholds Correlation-2 nd Month.	53
Figure 3.10: EGT Blood Levels and ABR Thresholds Correlation-4 th Month.....	54
Figure 3.11: SV Gene Expression.....	55
Figure 3.12: OC Gene Expression.	56
Figure 3.13: MD Gene Expression.....	57
Figure 3.14: Male Survival Analysis.....	58
Figure 3.15: Female Survival Analysis.	59
Figure 4.1: Conceptual Model of EGT Therapy.....	69
Figure 4.2: OCTN1 Relative Expression in Three Different Tissue Types.....	70

Figure B.1: Combined ABR Thresholds for All Test Groups.	90
Figure B.2: Combined ABR Threshold Shifts for All Test Groups.	91
Figure B.3: Combined DPOAE Amplitudes for All Test Groups.....	92
Figure B.4: Combined DPOAE Amplitude Shifts for All Test Groups.	93
Figure B.5: Combined DPOAE Thresholds for All Test Groups.....	94
Figure B.6: Combined DPOAE Threshold Shifts for All Test Groups.	95
Figure C.1: ABR Amplitude Shift Analysis Peak 1.	96
Figure C.2: ABR Latency Shift Analysis Peak 1.	97

Abstract

The naturally occurring amino acid, L-Ergothioneine (EGT), has immense potential as a therapeutic, having shown promise in the treatment of other disease models, including neurological disorders. EGT is naturally uptaken into cells via its specific receptor, OCTN1, suggesting that it is highly conserved, to be utilized by cells as an antioxidant and anti-inflammatory, particularly under stressed conditions. In our current study, EGT was administered over a period of 6 months to 25-26 month old CBA/CaJ mice as a possible treatment for age-related hearing loss (ARHL), since presbycusis has been linked to higher levels of cochlear oxidative stress, apoptosis and chronic inflammation. Results from the current study indicate that EGT can prevent aging declines of some key features of ARHL. However, we found a distinct sex difference for the response to the treatments, for hearing measurements – Auditory Brainstem Responses (ABRs) and Distortion Product Otoacoustic Emissions (DPOAEs). Males exhibited improvements in both low dose (LD) and high dose (HD) test groups throughout the entire testing period for both DPOAEs and ABRs and did not display the characteristic aging declines in hearing seen in Control animals. In contrast, female mice did not show any improvements with either treatment dose. Further confirming this sex difference, EGT levels in whole blood sampling throughout the testing period showed greater uptake of EGT in males compared to females. Additionally, RT-PCR results from three tissue types of the inner ear confirmed EGT activity in the cochlea in both males and females. Here, both males and females exhibited significant differences in biomarkers related to apoptosis,

inflammation, oxidative stress, and mitochondrial health: Cas-3, TNF- α , SOD2, and PGC1 α , respectively. Taken together, these findings suggest that EGT has a future as a naturally derived therapeutic for slowing down the progression of ARHL, and possibly other neurodegenerative diseases. EGT, while seemingly effective in the treatment of presbycusis in aging males, could also be modified into a general prophylaxis for other age-related disorders where treatment protocols would include eating a larger proportion of EGT-rich foods or supplements. Lastly, the sex difference discovered here, needs further investigation [1] to see if therapeutic conditions can be developed where females show responsiveness to EGT, similar to the dramatic effects seen here in the aging males.

Chapter 1: Introduction

Age-Related Hearing Loss (ARHL) or presbycusis is one of the most prevalent age-related neurodegenerative disorders affecting our older population. It is estimated that over 40% of the population will experience hearing loss by the age of 65, with that number exceeding 70% by age 75 [2]–[6]. ARHL is characterized by initial high frequency deficits (> 6 kHz) with a later progression to the low frequency range (1-4 kHz), when thresholds decline across all frequencies [7]–[10]. The perceptual aspects of age-linked hearing loss are especially evident in acoustic environments where background noise is elevated, resulting in perceptual deficits and inability to understand speech, even for those few older persons with normal audiograms or good peripheral sensitivity [11].

Aside from affecting communication abilities, ARHL is also highly associated with other disorders of aging such as loneliness, depression, and the onset of senile dementia [12]–[16]. In fact, the 2020 Lancet Commission on Dementia named ARHL as the top modifiable risk factor for dementia [17]. Therefore, it is important to note that ARHL, with its own detrimental aspects, also has other significant negative cascading downstream effects for our expanding older population. ARHL contributes to the economic burden through loss of productivity, reductions in quality of life, as well as additional healthcare costs related to poor health in those with hearing loss. Cost estimates have put the total bill between 750 to 980 billion dollars annually, in the US alone [18], [19]. Unfortunately, there are no FDA approved drugs/treatments that can slowdown or cure ARHL. In the present report, we investigate the

potential role of the novel amino acid L-Ergothioneine (EGT) in preventing some key aspects of ARHL in aging mammals.

To begin, a brief discussion of the etiologies of ARHL is beneficial. The auditory system can be broken into main two levels, peripheral and central. The peripheral auditory system includes the ear canal and drum (outer ear), middle ear bones (ossicles of the middle ear), and the cochlea (auditory portion of the inner ear), which receives the sound energy from the outer and middle ears. The inner ear structures housed within the cochlea are then stimulated through fluidic (endolymph, perilymph) movement delivered by the ossicles through the stapes footplate. More specifically, this acoustic-mechanical movement results in a traveling wave along the basilar membrane where specific regions are activated according to the frequency of the sound being transmitted to the cochlea. The inner hair cells and outer hair cells are then stimulated in the appropriate frequency region; where outer hair cells provide amplification gain, according to the intensity of the sound input. Concurrently, the inner hair cells are also activated by the traveling wave where the amplified signal is processed and transmitted to the auditory nerve, and then analyzed and interpreted further in the central auditory system. Lastly, it is important to note that the stria vascularis, a specialized region on the lateral wall of scala media, maintains a K^+ gradient in the endolymph that is needed to drive sound transduction in the hair cells [20]–[22].

Any dysfunction within these cochlear physiological systems can result in reductions in hearing abilities, which have been the focus of many studies related to ARHL [9], [11]. For example, in pioneering work, Schuknecht proposed a framework for the progression of peripheral ARHL which is manifested in three ways: Sensory, characterized by inner (IHC) and

outer hair cell (OHC) degeneration; Neural, characterized by a loss of radial afferent neurons connected primarily to IHCs; and Strial, seen with thinning and degeneration of the stria vascularis, including a loss of marginal cells which normally push K^+ up a concentration and voltage gradient into scala media. Schuknecht's overall theoretical framework was a pioneering effort to identify clinically relevant mechanisms for hearing loss, which are related to elevated hearing thresholds and declines in supra-threshold sound perception. However, it is likely that most clinical cases of ARHL are characterized by a combination of all three of these cochlear etiological phenomena. [23]–[26]

Regarding Schuknecht's model, it is often widely accepted that sensory and neural presbycusis can be related, since loss of IHC can induce auditory nerve fiber degeneration over time; i.e., loss of synapses and nerve fibers since they are no longer being stimulated. This type of degeneration may take years to progress due to a redundancy of neurons. [27]–[30] Strial presbycusis, another proximate cause of ARHL hearing loss, involves reduction of the endocochlear potential (EP) due to strial impairment. Specifically, since strial marginal cells help to maintain a K^+ gradient within the endolymph of scala media, resulting in approximately an +80 mV charge, they are often referred to as generating the "cochlear battery". This cochlear battery provides the driving force for proper acoustic transduction and hair cell functioning. Reductions in the EP reduce the OHCs mechanical amplification ability, as well as the stimulus coding properties of the IHCs. [31]–[33]

Central auditory presbycusis is also involved in reduced speech and complex sound perception in many cases, and this brain degeneration can be a part of age-related declines of the brain, and/or a secondary response to peripheral cochlear degeneration due to loss of

inputs [34]. In humans, brain structures that carry auditory information are often shown to be reduced in overall volume with an associated decline in neuronal size and vascular capillary density. This degeneration corresponds with declines in processing speed and speech perception [35]. Additionally, age-related changes have also been linked to functional changes in neurotransmitters, such as the inhibitory neurotransmitters GABA and glycine, and associated receptors/synapse systems, in addition to neuronal loss [36]. For example, Frisina's group demonstrated some of the functional deficits in human hearing that appear when the central auditory system is dysfunctional. They performed Speech-in-Noise Testing (SPIN test) on aged participants with normal audiograms from 0.25 to 4 kHz; i.e., thresholds were within 15 dB HL. The participants were asked to distinguish speech in various levels of background noise, and older subjects needed a higher signal-to-noise ratio to fully understand speech, even when their audiograms were within the normal range, indicating deficits in the central auditory system, likely involving the midbrain and cortical regions.

Contralateral suppression of OHCs is also reduced as aging occurs. Contralateral suppression is an efferent feedback mechanism whereby the brainstem, in response to a sound stimulus from one side, will limit the amount of amplification produced by the OHCs, as measured with distortion-product otoacoustic emissions. This decline in suppression with age is indicative of a decline in the processing abilities of the medial olivocochlear region of the brainstem auditory pathway, which can impair speech perception in background noise and auditory attention capabilities. Additionally, cortical declines have also been observed in older subjects, where tasks involving temporal processing, like the previously mentioned SPIN test and gap detection, show significant deficits. [37]–[40] However, it can be difficult to distinguish

peripheral and central auditory processing declines from cognitive declines associated with aging in some cases. [8], [40]

It is important to mention briefly and non-comprehensively, some of the testing modalities used to measure health and function of these important peripheral and central auditory structures. Cochlear health is generally measured using auditory brainstem responses (ABRs) and distortion product otoacoustic emissions (DPOAEs) clinically, in infants and adults, and in animal models. To measure DPOAEs, two simultaneous pure tones are presented at set frequencies, with f_2 being greater than f_1 . Based on basilar membrane mechanics, these pure tones elicit a nonlinear response or physical vibration of the basilar membrane, a distortion product. The distortion product is then measured with a microphone placed at the external auditory meatus (ear canal). DPOAE responses are indicators of the health and functionality of the OHC system near the tonotopic area of the stimulus tones presented. Reduced amplitudes and elevated thresholds of DPOAEs indicate the presence of hearing loss and possible loss of OHCs and/or reduction in their functionality. Declines in DPOAEs are a biological mechanism of ARHL. Many processes of the peripheral auditory system are OHC driven and thus it is important to maintain integrity of these structures for normal hearing. This underscores the importance of DPOAEs as a diagnostic tool in determining onset and severity of presbycusis in human and animal subjects [41]–[43].

Useful peripheral and central auditory functionality can be determined with ABRs. ABRs comprise a far field, evoked potential brain recording with sound as the stimulus. The stimulus is adjusted by frequency and intensity (dB SPL) to obtain threshold and amplitude measures. The resultant EEG-like scalp-recorded voltage readings show individual waves comprising

waveform features that correspond to different processing stages of the auditory system. So, each individual wave corresponds to a region within the auditory pathway, where the number and shape of the waves is species dependent, ranging from five to seven. For most mammals, the waves from I-V have a rough correspondence to: the auditory nerve, cochlear nucleus, superior olivary complex, lateral lemniscus, and inferior colliculus, respectively; where more information is known about ABR generation sites in certain mammals relative to others. Again, with this test, any reduction in the amplitudes, increasing of latencies and elevation of thresholds is indicative of damage or degradation of the auditory pathway. This test also gives a bit of specificity to where in the system the dysfunction may be occurring [44], [45].

While these tests are used clinically, much of what we know about hearing has been determined through lab animal testing. Animal models have allowed us to understand both the physiology of hearing as well as the “under-the-hood” structural and molecular underpinnings which induce some of the previously discussed pathologies. Of particular use are inbred mouse strains which are genetically identical and bred to be homozygous. Using these strains, genetic and physiological traits can be selected for, allowing for a reduction in confounding factors as well as reducing genetic drift. For example, the CBA/CaJ mouse strain utilized in our lab, has been bred to lose hearing slowly with age on an overall time-course analogous to most humans (after correcting for absolute lifespan differences of humans and mice). This strain also shows some strial presbycusis, involving characteristic thinning of the stria vascularis, which is related to EP reductions and elevations in hearing thresholds with age. Mice are extremely useful in the study of presbycusis as they are both structurally and genetically similar enough to relate

findings to humans, particularly at subcortical and peripheral levels of our hearing system [42], [46].

The discussed physiological changes have a biological biomarker basis with aging. Unfortunately, many aspects of aging are still poorly understood, as many theories have been proposed to explain age-related alterations in the brain and sensory systems. Aging then is not just simply the occurrence of one event but a confluence of many, for example, telomere shortening due to a reduction in telomerase activity, increased apoptosis and apoptotic biomarkers, over-production of reactive oxygen species, declines in antioxidant systems, “inflammaging”, mitochondrial damage, etc. [7], [8], [16], [47], [48]. For the purposes of this dissertation however, particular focus will be given to measuring inflammatory biomarkers and changes in metabolic activity that affect cell genetics and functionality.

Chronic, low grade inflammation, or inflammaging, is a characteristic marker of aged tissue. With aging, the body exhibits immunosenescence, an inability to manage the inflammatory response both during and after an immune response. This often results in a sustained increase in pro-inflammatory markers like IL-6, TNF- α , and TGF- β . Inflammation is inherently not always a negative event, as it is beneficial, mostly in the short run, for tissue repair through clearance of pathogens and cellular debris. Upregulation of inflammatory markers recruits various leukocytes and macrophages designed to mitigate acute immune responses. However, in an acquired chronic inflammatory state, tissues become damaged through the accumulation of cellular debris and maladaptive cellular responses, which in turn continues to recruit the innate immune response. Then, instead of, or in addition to, targeting pathogens as designed, it damages healthy tissue. Chronic inflammation is likely a key player in

some age-related declines observed in hearing loss models [49]–[51]. Evidence points to immune responses originating in the organ of Corti, stria vascularis, spiral ligament, and lateral wall of the cochlea. Specifically, cells within the stria vascularis have been shown to release pro-inflammatory cytokines that recruit the innate immune response [52]. Interestingly, long-term age-related inflammation studies within the cochlea are understudied, with more significant investigations needing to be done. One human epidemiological study, however, linked increased serum inflammatory markers with ARHL, providing pioneering evidence that reducing inflammation could be an effective target for future biotherapeutics [53]. Additionally, clues can be taken from studies involving noise-induced hearing loss (NIHL), which has mechanistically similar inflammatory responses to ARHL. For example, it has been shown that inhibition of the IL-6 pathway in NIHL, can improve hearing after noise trauma [50], [54], [55].

A second common aging event implicated in the progression of ARHL is the formation of reactive oxygen species (ROS) and oxidative stress. ROS are free radicals or molecular species which exist in an unpaired electron state. Free radicals act as electron donors or acceptors and can impact cells and tissue negatively through DNA, protein, and lipid degradation. Free radicals and ROS are produced through normal cellular, metabolic activities as well as exposure to environmental factors like UV light or pollutants [56], [57]. In aged animals, oxidative stress, often linked to inflammation, is often poorly controlled and damaging. In normally functioning systems, such as for most young adults, oxidative stress due to the overproduction of ROS from environmental insults, is managed through ROS metabolism and free-radical scavenging. These endogenous antioxidant defense systems utilize enzymes like SOD1 and glutathione peroxidase

in the cochlea, to turn harmful hydrogen peroxide into water. Additionally, ROS are important cellular signaling molecules needed for maintaining homeostasis [27], [57].

As mentioned, uncontrolled ROS management and oxidative stress produce negative effects within the body. Oxidative stress contributes to protein degradation, lipid peroxidation, and DNA mutation, elevating apoptotic biomarkers (e.g., Cas-3, Cas-8, Bcl-2) and leading to eventual cellular death. Lipid peroxidation leads to the degradation of the lipid bilayer of the cell, while mutations in DNA coding cause dysfunctional synthesis of proteins [8]. However, of major interest is the effect that oxidative stress has on the mitochondria of the cell.

Mitochondria are often termed the powerhouse of the cell since they synthesize the ATP needed to drive many molecular reactions and cell functions. These highly metabolic organelles produce ROS as a byproduct and are even thought to be the main source of ROS. Therefore, chronic unmanaged ROS stress interrupts the electron transport chain, possibly resulting in the release of the mitochondria's own native apoptotic factors, AIF and cytochrome c, ultimately leading to cell death. ROS can also cause mitochondrial DNA (mtDNA) damage much like that seen for nuclear DNA. However, unlike nuclear DNA, mtDNA does not have as effective self-repair mechanisms in the event of miscopies/mutations. These mutations can then be passed on in future cellular replications rendering cells bioenergetically ineffective as aging occurs and mtDNA mutations accumulate [57]–[61]. These phenomena are hallmarks of aging as it is seen throughout the body and not solely in the cochlea.

Interestingly, there have been multiple studies utilizing antioxidants as treatments for ARHL, some of which have had limited success. In a longitudinal study (0-25 months) using Fischer 344 rats performed by Seidman [62], the following antioxidants: vitamin C, vitamin E,

lazaroid, and melatonin, individually, showed benefits in improving auditory thresholds and reducing the number of mtDNA deletions. Similarly Seidman's team also found hearing and mitochondrial benefits when feeding 18-20 month old Fischer 344 rats with lecithin for a period of 6 months [63]. Another group took these ideas further and combined antioxidants, where C57BL/6 mice were fed chow supplemented with L-cysteine-glutathione mixed disulfide, ribose cysteine, NW-nitro-L-arginine methyl ester, folate, vitamin C, and vitamin B12. Results from the treatment group again showed significant decreases in threshold shifts from 3-12 months of age [64]. Someya's group also found that the mitochondrial antioxidants α -lipoic acid and coenzyme Q₁₀ were effective in preventing some aspects of ARHL, while also lowering hair cell and spiral ganglion nerve (SGN) apoptosis through the suppression of Bak-dependent mitochondrial apoptosis [65]. However, it should be noted that not all antioxidant studies revealed positive results; as Fischer 344 rats supplemented with L-carnitine did not slow the progression of ARHL [66]. As well, Sha et al.'s [67] comprehensive study showed negative results for slowing ARHL and preservation of hair cells and SGNs in 10 month old CBA/J mice when fed chow combined with vitamins A, C, and E, α -lipoic acid, and L-carnitine. Indeed, all human FDA clinical trials have failed to show success using antioxidants alone.

L-ergothioneine (EGT), appears well suited to tackle some of the challenges of slowing the progression of ARHL due to its combination of antioxidant and anti-inflammatory properties, allowing it to function in multiple positive capacities and affecting several key cochlear cellular pathways simultaneously [68]–[72] related to ARHL. The focus of the present study will mainly reside on the structures within the cochlea: the stria vascularis (SV), organ of Corti (OC), and modiolus (MD) [9], [23], [73]–[77]. So, EGT is unique in that it is able to

potentially treat multiple pathways and mechanisms which contribute to ARHL. Because of this unusual ability, many of the previously mentioned aging processes such as chronic low-grade inflammation (inflammaging), increased oxidative stress and ROS production, increased apoptosis, and finally DNA and mitochondrial DNA (mtDNA) damage can be addressed with EGT treatment [77]–[82].

In this study, the overall hypothesis is that EGT's properties will positively impact key auditory markers of the aging auditory system. For example, in other models where EGT has been used as a treatment for inflammation, EGT has shown usefulness in preventing induction of pro-inflammatory cytokines as well as a depression in the expression of VCAM-1, ICAM-1, E-selectin in a human aortic endothelial cell model. EGT effectively prevented monocytes from binding to the endothelium [83]. In another study using mouse myoblasts, EGT prevented the upregulation of IL-6 when challenged with palmitic acid, which has been correlated to the modeling of insulin resistance and type 2 diabetes [84]–[86]. EGT works *in vivo* as well, as healthy human subjects were administered EGT and checked for oxidative burden biomarkers, among others. Urine samples showed reduction in the DNA damage product, 8OHdG; protein carbonyls, which indicate protein damage; F₂ isoprostanes, indicating non-enzymatic peroxidation; and the inflammatory marker, C-reactive protein [87].

Therefore, we hypothesize that EGT can aid in reducing some of these individual damaging events such as inflammaging, increased ROS, and accumulated mitochondrial damage. Also, it is hypothesized that these events are interconnected, acting in a cyclic nature, where one mechanism influences another which ultimately leads to more damage. For example, mitochondrial damage can activate inflammation through pathology-associated

molecular events that recruit neutrophils and cytokines during cellular trauma [79], [88]–[90]. Again, EGT's properties align with our overall hypothesis, as EGT has been shown to protect cells from DNA damage, both nuclear and mitochondrial [91]. This dual protection comes from the translocation of EGT into both the nucleoplasm as well as into the mitochondria. Mitochondria then are protected from ROS damage to their electron transport chain as well as safeguarding its unique mtDNA code [92], [93].

It should be noted that this cyclic nature is yet to be fully established explicitly in the aging auditory system, where evidence of these mechanisms exists between ROS and mitochondria, and inflammation in the aging cochlea. In fact, it has recently been shown in our lab that mitochondrial mutations and inflammation occur in the cochlea of aging CBA/CaJ mice [94], [95]. Further evidence from Menardo's group [96] supports this correlation between oxidative stress, inflammation and mitochondrial damage as being critical mechanisms for premature ARHL in the SAMP8 mouse model.

EGT's therapeutic potential lies in its chemical structure as it exists as a thione-thiol tautomer. At physiological pH, EGT is positively charged with a preference for its thione conformation. These attributes allow for EGT to be highly stable and resist auto-oxidation unlike the structurally similar cochlear antioxidant glutathione [97]. However, like glutathione, its sulfhydryl group supports a role as an antioxidant with higher redox potentials (-0.06 V vs -0.2 to -0.32 V for other antioxidants thiols like glutathione) [98]. The sulfhydryl group acts by oxidizing and conjugating reactions of peroxides and other ROS until EGT is rapidly reduced back to its original tautomeric state. Glutathione, in contrast, is quickly and completely

depleted under the same circumstances and generates more free radicals in the process [87], [93], [97], [99].

Interestingly, L-ergothioneine is a dietary amino acid that can only be obtained in food products since it is unable to be synthesized in the body. The highest concentrations of EGT are found in specific types of mushrooms like the king bolete or oyster mushroom and is also found in selected meat products, some vegetables, and various types of grains [100]. Additionally, EGT is also unique in that it possesses its own highly specific cell transporter, organic cation transporter novel-1 (OCTN1) [68], [87], [101]–[103]. EGT is impermeable to plasma membranes, so a transporter is needed for the cellular uptake through the cell membrane, and utilization of EGT intracellularly [104]. Uptake through OCTN1 is largely dependent on temperature, sodium concentrations, and pH, but proceeds as expected under normal physiological conditions. In support of this, studies involving OCTN1 negative cells and knockout animal models, show little uptake of EGT [68], [105], [106]. OCTN1 is encoded by the *SLC22a4* gene and is found throughout the body. High expression of these transporters is generally found in areas of the body that have high metabolic activity, as EGT has been shown to reduce oxidative stress in these regions, as described above [87], [102], [107]. Moreover, consistent with increased transporter concentration, EGT is also found in areas such as the liver and blood, and also present in lesser amounts in other areas of the body such as the spleen, kidney, lungs, heart, eyes, intestines, and brain [71], [87], [101]. It should be noted that EGT is likely found in high concentrations within whole blood due to its affinity to the divalent ion, Fe^{2+} [108]–[110], which is found in erythrocytes and bone marrow, implying a possible role in erythropoiesis [101], [111], [112]. These properties then hint at another one of EGT's natural

advantages, namely EGT's high uptake and low excretion which contributes to a long half-life in the body of up to 30 days [70], [71]. Even more exciting, EGT has an excellent safety profile as there has been no reported toxicity for any dosage utilized so far. In fact, EGT has been assigned a No Observed Adverse Effect Level (NOAEL) = 800mg/kg BW/day [113].

Research within the last several years has shown its effectiveness in chronic neurodegenerative disorders. For example, EGT declines with age, specifically, beyond 60 years and lower levels of EGT are associated with greater incidence of mild cognitive impairment [114]. Beyond cognitive function, low blood levels of EGT are associated with increased incidence of other aging pathologies such as coronary artery disease, cardiovascular problems, mortality, prostate cancer, breast cancer and total mortality [115]–[118]. Interestingly, Smith et al.'s longitudinal study [115] found that EGT was an independent biomarker for a lower risk of cardiometabolic disease and mortality among 112 plasma metabolites (n = 3236, mean age: 57 years old). As EGT has many benefits and virtually no side effects, the European Food Safety Authority (EFSA) granted its use as a supplement for pregnant and breast-feeding moms, children, and infants [119]. There are clinical studies going on to investigate therapeutic effects of EGT for reducing cognitive decline in Singapore (Phase 3) [120]. A study was registered for EGT clinical trials in USA in Sept. 2020 to study its effect on cognition, mood and sleep but, unfortunately, the study was terminated due to recruitment issues amidst the COVID pandemic. We anticipate an increase in EGT clinical studies in the coming years [121].

EGT has additionally been nicknamed as a "longevity" vitamin, because of the human body's specific EGT transporter and its potential physiological and therapeutic roles in many aging diseases [122], [123]. Given all these promising benefits of EGT, including for age-related

neurological disorders, EGT is a great candidate for therapeutic interventions in the aging auditory system. To the best of our knowledge, there is no study of the effects of EGT on hearing to date, so, this is the first ever report about EGT's possible therapeutic roles in the aging auditory system. Here, aged rodent animals were treated with EGT and various hearing and biomarker measurements were performed in a longitudinal, interventional study design.

Chapter 2: Materials and Methods

2.1 Subjects

Aging CBA/CaJ mice (aged 25-26 months), bred in-house or delivered from Jackson Labs as young adults, were divided into three test groups per sex: Control, Low Dose, and High Dose. Control animals received only saline injections throughout the testing period while Low Dose and High Dose groups were given L-Ergothioneine (EGT) in differing amounts. Testing proceeded until about 31 months of age or for approximately 24 weeks; however, a number of animals died prior to completing the full 6-month study.

It should be noted that only in the Control groups, mice not acquired at baseline ages, i.e. 25-26 months, but still within the age range of testing, were included in the study. The results from these animals were only included in aggregate calculations such as thresholds-by-month, and not included in calculations which required baseline data, like threshold-shifts-from-baseline. For additional reference, the N of each graph, by group and analysis is included. So, the Control thresholds-by-month graph will have different N values than the Control threshold-shifts-from-baseline.

2.2 Dosing Scheme

For the first experimental group (Low Dose), subcutaneous injections (0.1 mL) of L-Ergothioneine at a dosage of 35 mg/kg were given daily for the first seven days of testing (dosage volume adjusted according to animal weight). Thereafter, a maintenance dose of 70 mg/kg (approx. 0.1 mL injection) was administered every seventh day until the conclusion of

the study. The second experimental group (High Dose) followed the same dosing routine but with increased dosages at every dosing cycle. Here, subcutaneous injections were administered daily with 70 mg/kg (approx. 0.1 mL) for the first seven days with a maintenance dose of 140 mg/kg every seventh day thereafter (approx. 0.2 mL injection, volume again adjusted according to body weight). This was continued until the conclusion of the study. Control mice followed the same dosing time schedule but were given saline. These dosages were chosen by following the dosage amount outlined in Tang et al., 2018. [124] The dosage scheme was then determined by utilizing the 30 day half-life of EGT. The first seven days of injection acted as a loading dose, where the subsequent weekly doses were essentially maintenance doses. [70] Please refer to Figure 2.1 below. All of the animal protocols were approved by the University of South Florida Institutional Animal Care and Use Committee (IACUC).

2.3 Hearing Tests

2.3.1 Auditory Brainstem Response (ABR)

Mice were anesthetized using a ketamine/xylazine mixture (120 and 10 mg/kg body weight) intraperitoneal injection, prior to all experimental sessions. Acoustic stimuli were then synthesized digitally using the System III Tucker-Davis Technology (TDT, Alachua FL) signal-processing platform. The stimuli were then attenuated and filtered (low pass cutoff at 5 kHz). Stimulus sounds were presented through an electrostatic speaker (TDT EC1) connected to the external ear canal by 4 cm tubes, so via a calibrated, closed system. A ¼" B&K microphone (Type 4938, Bruel & Kjaer, Naerum, Denmark) attached to a 0.1 cm³ coupler was used to calibrate the TDT system daily. The mice were placed on a heating pad inside a soundproof booth. Three sub-cutaneous needle electrodes were inserted at the vertex (non-inverted) and

in the mastoid area muscle of the ipsilateral (testing) side (inverted), with a ground inserted in the muscle posterior to the contralateral pinna to record the ABR responses of each mouse. These electrodes were connected to a bioamp headstage (HS4 Fiber Optic, TDT). For ABR threshold experiments, the subjects were presented with tonal stimuli in the frequency range of 3 to 48 kHz at various sound levels (starting at 90 dB with 5 dB intensity steps). Each intensity was duplicated and threshold was determined as the lowest intensity at which a response is replicated. A wide band noise (WBN) stimulus, having a bandwidth from 0 to 48 kHz, was also used. The duration for each ABR stimulus was 5 msec (0.5 msec. rise and fall time) with \cos^2 envelope, presented at a repetition rate of 21/s [125].

2.3.2 Data Analysis: Auditory Brainstem Response (ABR) Thresholds

For ABR testing, thresholds were read at all measured frequencies by three independent experimenters for all animal groups, blinded to the animal's age and treatments. Thresholds were defined as the lowest sound level at which a distinct ABR wave could be identified. ABR recordings for all 9 tonal stimuli (3-48 kHz), along with WBN stimuli, were evaluated and compared for all groups, in both male and female mice. More specifically, age-related declines were evaluated relative to baseline thresholds. Since these aged mice showed normal variability of hearing declines characteristic of old human and animal subjects, the best way to compare mice between groups was to determine threshold shifts from baseline readings. So, for subsequent testing periods, i.e. 1st month, 2nd month, 4th month, and 6th month ABR results are presented as absolute ABR values, as well as ABR baseline-shift values. GraphPad Prism 9 statistical analysis software was used. Dunnett's multiple comparisons *post-hoc* tests (MCT)

were used to assess pairwise comparisons between conditions when the ANOVA main effects were statistically significant [125].

Data were also evaluated with a Linear Mixed Model since animal numbers in each test group changed month-to-month, due to attrition of these very old mice, and therefore violated the rules of a Repeated Measure Model. In essence, a Linear Mixed Model (LMM) allowed for a more robust study as all data points were able to be analyzed; where in a Repeated Measure Model, only animals that started and finished the entire testing period (6 months) would have been able to be included in the analysis, thus limiting the statistical power of the results [126]–[128]. Due to the advanced age of these animals, resulting in attrition, and inclusion of some additional Control mice (male and female) not present at baseline, but with ages that matched various timepoints in the study, the N for some of the animal groups changed from timepoint to timepoint. Lastly, it should be noted that aggregate ABR thresholds were calculated using all available data points. However, ABR threshold shift analysis used only data from animals that were started from the very beginning at baseline.

2.3.3 Data Analysis: Auditory Brainstem Response (ABR) Peak Picking

ABR analysis was not only limited to thresholds, as both amplitudes and latencies for Peaks 1 and 2 were also analyzed. For amplitudes, the respective peaks were analyzed by selecting the top of the wave (peak) and the bottom of the wave (trough) as seen in Figure 2.2, where the white markers denote the areas selected. The trough is then subtracted from the peak to get the amplitude value (nV/ μ V) for the respective Peak. Latency is found by selecting the maximum of each peak and noting the timepoint (ms) relative to stimulus onset, as shown in Figure 2.2 by the blue arrows and lettering. Lastly, Interpeak Analysis between Peak 1 and

Peak 2 was performed by subtracting Peak 2 latency from Peak 1 latency. A two-way analysis of variance (ANOVA) was used to statistically analyze the amplitude levels and latency values for the older age groups. Dunnett's multiple comparisons *post-hoc* tests (MCT) were used to assess pairwise comparisons between conditions when the ANOVA main effects were statistically significant [125]. GraphPad Prism 9 statistical analysis software was used.

2.3.4 Distortion Product Otoacoustic Emissions (DPOAE)

Mice were anesthetized with ketamine-xylazine (120 and 10 mg/kg body weight, respectively) by intraperitoneal injection before experimental sessions. All recording sessions were completed in a soundproof acoustic chamber (IAC lined with Sonex) with body temperature maintained with a heating pad. Before recording, the stimulus probe and microphone coupler were placed in the test ear near the tympanic membrane with the aid of an operating stereoscope. Ipsilateral acoustic stimulation and simultaneous measurement of DPOAEs was accomplished with a TDT BioSig System III. Stimuli were digitally synthesized at 200 kHz using SigGen software with the ratio of f_2/f_1 constant at 1.25, and $L_1 = 65$ dB and $L_2 = 50$ dB SPL, as calibrated in a 0.1 cc coupler simulating the mouse ear canal. Signal duration was 84 msec and repetition rate was 21/sec. After synthesis, f_1 and f_2 were each passed through an RP2.1 D/A converter to PA5 programmable attenuators. Following attenuation, the signals went to ED1 speaker drivers which fed into the EC1 electrostatic loudspeakers coupled to the ear canal via short flexible tubes with rigid plastic tapering tips. For DPOAE measurements, the resulting ear canal sound pressure was recorded with an ER10B+ low noise microphone (gain 20 \times) and probe (Etymotic, Elk Grove Village, IL) housed in the same coupler as the f_1 and f_2 speakers. The output of the ER10B+ amplifier was input to an MA3 microphone amplifier, the

output of which went to an RP2.1 A/D converter for sampling at 200 kHz. A fast Fourier transform (FFT) was performed on the resultant waveform. The magnitude of f_1 , f_2 , the $2f_1-f_2$ distortion product, and the noise floor of the frequency bins surrounding the $2f_1-f_2$ component were measured from the FFT. The procedure was repeated for geometric mean frequencies ranging from 5.6 to 44.8 kHz (8 frequencies/octave) to assess adequately the neuroethologically functional range of mouse hearing. Duration of the testing was approximately one hour per animal [42]. For scheduling time points of both ABR and DPOAE tests please refer to Figure 2.1.

2.3.5 Data Analysis: Distortion Product Otoacoustic Emission (DPOAE)

Much like ABR testing, DPOAE amplitudes and thresholds were analyzed for all animal groups. Amplitudes were defined as the measured response from the OHC system for a set stimulus at a given frequency. Thresholds were defined as the lowest sound level at a specific frequency at which a distinct response could be identified. Age-related decline was evaluated with respect to the baseline testing. Since these aged mice showed various stages of hearing decline, the best way to compare mice between groups was to determine amplitude and threshold shifts relative to baseline readings. Subsequent testing periods, i.e. 1st month, 2nd month, 4th month, and 6th month DPOAE results are represented as absolute DPOAE values as well as shift values from the baseline. Dunnett's multiple comparisons *post-hoc* tests (MCT) were used to assess pairwise comparisons between conditions when the ANOVA main effects were statistically significant [125]. GraphPad Prism 9 statistical analysis software was used. It should be noted that the data from this analysis was also treated like that of ABR thresholds using the LMM for analysis.

2.4 Blood Sampling

All mice underwent the same blood sampling protocol. No more than 100 μL of whole blood was collected at each time point. Samples were collected at the beginning of the six-month testing period (baseline), then also at Day 7, Month 1, Month 2, Month 4, and Month 6. Blood draws were performed using the facial vein collection method. Blood was collected into K_2EDTA vials and then, stored in a $-80\text{ }^\circ\text{C}$ freezer until ready for analysis. Please refer to Figure 2.1 which illustrates the timeline of dosing, blood sampling, and hearing measures.

2.5 LC-MS/MS-Blood Preparation

Whole blood samples were taken out of the $-80\text{ }^\circ\text{C}$ freezer, thawed, and vortexed. 10 μL aliquots were taken from each sample and combined with EGT-d9 and LC-MS/MS quality pure water to a total volume of 100 μL . Samples were then, heated to $80\text{ }^\circ\text{C}$ for 15 min, which allowed EGT/EGT-d9 to elute out of the mixture into the supernatant. Ice cold acetone was added to each sample and allowed to sit overnight in a $-20\text{ }^\circ\text{C}$ freezer. Next day, samples were vortexed and centrifuged at 17,000g for 10 min to make sure that any debris was at the bottom of the tube. The supernatant was then placed into a separate tube and evaporated using N_2 streaming. Once dry, the samples were reconstituted to 100 μL and centrifuged at 17,000g for a short time. The supernatant without any debris was finally placed into a silanized glass insert within its appropriate vial [124].

2.6 LC-MS/MS-EGT Quantification

Chromatographic separation and mass spectroscopy were performed using an Agilent 1260 HPLC connected to an Agilent 6460 Triple Quad mass spectrometer. For proper separation, 5 μL of sample was passed through a Kinetex 2.6 μM Polar C18 column and used in

conjunction with two mobile phases, Solvent A (0.1% formic acid in water and Solvent B (acetonitrile) with a gradient elution. Gradient elution was as follows: 15% of Solvent B (0 min), 15% of Solvent B (0 to 1 min), 15% to 35% Solvent B (1 to 4 min), 35% to 90% of Solvent B (4 to 5 min), 90% of Solvent B (5 to 8.5 min), 90% to 15% of Solvent B (8.5 to 9 min), 15% of Solvent B (9 to 12 min). Sample separation was performed at a fixed flow rate of 0.5 mL/min with column temperature set at 30°C. The retention time was 2.15 min for both EGT and its isotope-labeled IS, EGT-d9.

Mass spectrometry was performed using positive ion, electrospray ionization mode, with samples quantified using MRM (Multiple Reaction Monitoring) for target ions. Settings for the related test set up are as follows: Capillary Voltage-3200V, Nitrogen Sheath Gas Pressure-50 psi, gas temperature-350°C, gas flow rate-12 L/min, with Ultra-High purity nitrogen used as collision gas. Lastly, expected precursor and product ion transitions with the associated fragmentor voltages (V)/collision energies (eV) for EGT and EGT-d9 are here: EGT; 230.1, 103V to 127, 9eV. EGT-d9; 239.1, 98V to 195.1, 9eV. [124]

2.7 Gene Expression - RT-PCR

Animals were euthanized and decapitated as per the NIH guide for Care and Use of Laboratory Animals as well as University of South Florida IACUC protocols. Cochlear Tissue samples – Stria Vascularis, Modiolus and Organ of Corti were collected. It should be noted that modiolar dissections do not include vestibular tissue. Real-time quantitative RT-PCR analysis was performed as previously described (Ding et al., 2013; 2016). In brief, total RNA is extracted using the RNeasy Mini Kit (Qiagen, Valencia, CA). Samples were vortexed for 1 min to shear genomic DNA before loading onto the RNeasy mini columns, and then eluted in a minimum

volume of 30 μ L and a maximum volume of $2 \times 50 \mu$ L RNase-free water. RNA obtained with this procedure was essentially free of genomic DNA. 25 ng of RNA was reverse transcribed with complementary DNA being subjected to PCR amplification. The reverse transcript (RT) reaction proceeds at room temperature for 5 min, 46°C for 20 min, and then 90°C for 1 min to complete the RT. The competition between primer sets was excluded by adjusting the reaction condition. The qPCR was performed on an Analytik Jena AG qTOWER³ Real-Time PCR Thermal Cycler (Jena, Germany). Each set of reactions always includes a no-sample negative Control. We also performed a negative Control containing RNA instead of cDNA to rule out genomic DNA contamination. The quantitative real-time RT-qPCR reaction mixture was prepared using the EvaGreen PCR Master Mix. Thermal cycling conditions were as follows: Initial heating step at 94°C for 2 min, followed by looped steps at 94°C for 15 seconds, 55°C for 30 seconds, and 68°C for 1 minute. After the final loop, the cycler was held at 68°C for 5 min. Amplification specificity was checked using melting curves. Both negative and positive Controls were included in each PCR reaction. All assays were carried out in triplicates as independent PCR runs for each cDNA sample. Gene expression was referenced to the expression of GAPDH as the housekeeping gene. Each gene expression value was then normalized with respect to GAPDH mRNA content. Gene expression candidates can be found in Table 2.1. Calculations of expression were performed using the Relative Standard Curve Method [129].

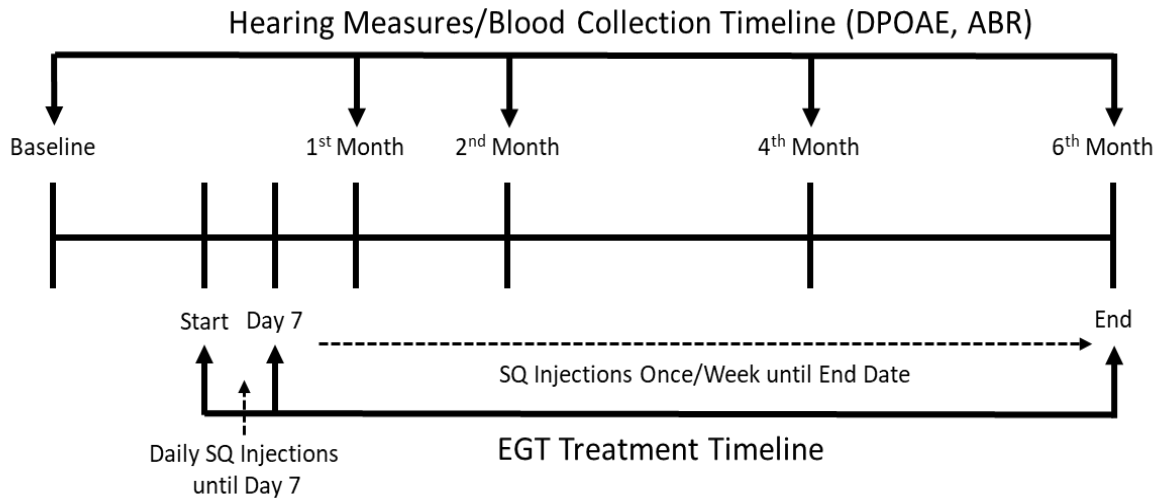
2.8 Reagents

L-Ergothioneine(EGT) was purchased from Cayman Chemicals. (Ann Arbor, MI). L-Ergothioneine-d9 (EGT-d9) was obtained from Tetrahedron (Toronto, ON, CA). RNeasy Minikit was obtained from Qiagen (Valencia, CA). Evagreen cDNA kit and Evagreen Supermix were

purchased from Bio-Rad (U.S.). All other chemical reagents, unless otherwise noted, were purchased from Thermo Fisher Scientific (Waltham, MA).

2.9 Survival Analyses

In survival analyses, 'death' events were tracked and analyzed using the Kaplan-Meier Method along the treatment and testing timeline of the present investigation. All mice included in this analysis were those that started their hearing measures at Baseline (25-26 months). Events were classified as "censored" when the reason for death was user error (e.g., ketamine overdoses related to large liver tumors), or if the mice lived long enough to complete the six month study where they were subsequently euthanized. Events were considered "death events" when mice were either found dead in their cage or they were ethically euthanized as recommended by veterinarians under our IACUC protocol guidelines. (Mantel-Cox) Log-rank tests for trends was then performed on the resulting data.



Control: 0.1mL SQ saline through Day 7, 0.2mL saline SQ once/week until testing end date
Low-Dose: 35mg/kg SQ through Day 7, 70mg/kg SQ once a week until testing end date
High-Dose: 70mg/kg SQ through Day 7, 140mg/kg SQ once/week until testing end date.

Figure 2.1: Hearing Testing, Blood Sampling and EGT Treatment Timeline. SQ=Subcutaneous Injections.

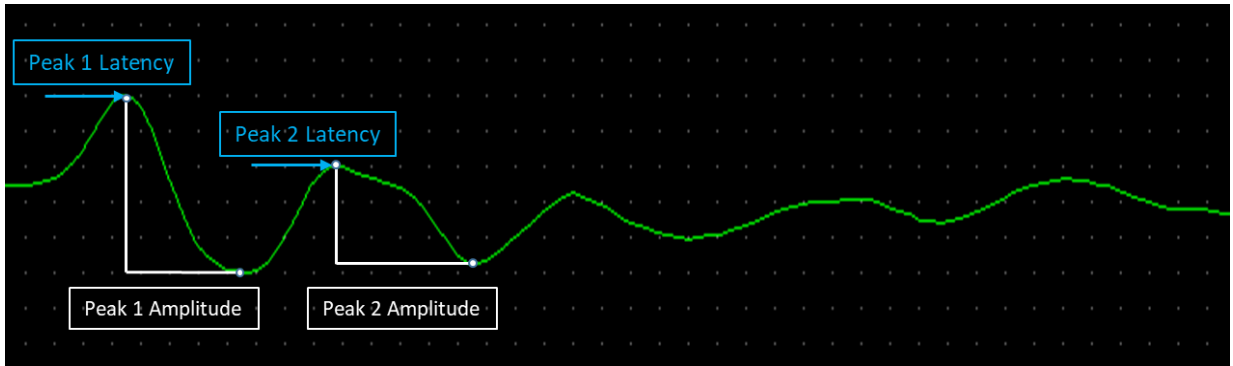


Figure 2.2: ABR Amplitude and Latency Example Analysis. Amplitudes calculated as peak-to-trough; latencies calculated by selecting the maximum of each wave for their respective peaks, and recording the timepoint relative to stimulus onset.

Table 2.1: Primer List for Gene Expression Targets.

	Forward Primer Sequence	Reverse Primer Sequence	Accession Number
GAPDH	CCTGCGACTTCAACAGCAAC	TTCATTGTCATACCAGGAAATGAGC	
OCTN1	GCCCCCTATTTGTTTTACCT	TGCATCTGCTCCAAGTTCTC	AB016257.1
Cas-3	TGGCTTGCCAGAAGATACCG	CCAGGAATAGTAACCAGGTGCT	XM_017312543.3
TNF-a	TCCCAGGTTCTCTTCAAGGGA	GGTGAGGAGCACGTAGTCGG	NM_013693.3
PGC1a	CGGAAATCATATCCAACCAG	TGAGGACCGCTAGCAAGTTTG	NM_008904.2
SOD2	CCGAGGAGAAGTACCACGAG	GCTTGATAGCCTCCAGCAAC	NM_013671.3

Chapter 3: Results

3.1 ABR Threshold Analysis

Male and Female mice were tested at five time points over the course of a 6 months study – baseline, 1st, 2nd, 4th and 6th month as noted in Figure 3.1. Here, data analysis was divided according to sex; male and female, with each grouped analysis relating to the three distinct test groups, Control (Fig. 3.1(A&D)), Low Dose EGT (LD) - (Fig. 3.1(B&E)), and High Dose EGT (HD) - (Fig. 3.1(C&F)). In the left column (Fig. 3.1(A-C)), are the averaged thresholds for each group by month. Fig. 3.1(D-F), shows all tested months with the Baseline subtracted to remove its influence on threshold values – yielding baseline shift values. Beginning with male Control Values in Fig. 3.1A, the general elevation of ABR thresholds can be observed with age. Baseline values for these CBA/CaJ mice, approx. 25-26 months, distinctly show an elevation in comparison to the Young Adult Control mice, aged 5 months. All subsequent thresholds show the aging change with threshold elevations; notably significant by the 4th and 6th Month. In Fig. 3.1D, with the Baseline subtracted out (shift values), the differences between the testing time points are more evident. There is a clear separation between the 1st and 2nd Months as well as more clearly defined threshold elevations for the 4th and 6th Months. This Control analysis will serve as the basis for comparison in the next two EGT-treated mouse groups. Excitingly, male LD mice (Fig. 3.1(B&E)) exhibit completely different aging curves as compared to Control mice (Fig. 3.1B). Specifically, there was no aging threshold elevation, in contrast to the Control animals, especially during the 4th month. The 6th Month has slight threshold elevation and

breaks away from the main cluster, but the shift was less than the shift for the Control group at the same time point (6th Mon).

Also interesting, for the male treated groups, there is no significant differences present when comparing all subsequent months to baseline. Threshold shift data (Fig. 3.1E) also exhibits similar characteristics to the monthly threshold data, no significant differences, but with a little more clear separation seen. The threshold shift data clearly shows the therapeutic effects of EGT treatment in male animals. Here, one can see that by the 1st Month of treatment, there were a few frequencies that had a negative shift (below 0), while many had no shift (0 dB SPL). For example, the frequencies with a negative shift were 3K, 16K, 24K, 36K, and WBN. Frequencies with no shift were 12K, 20K, and 32K. Negative shifts indicate an improvement in hearing with time. The 2nd and 4th Month also exhibited lower thresholds, where both 2nd and 4th Months had negative shifts at 16K. 2nd Month threshold shifts still had a few frequencies near 0 but started to show negative shifts at various frequencies. 4th Month thresholds experienced +5 to +10 dB shifts on most frequencies with the exception at 16K. This shift was significantly less than Control animals (+10 to +20 dB by 4th month). 6th Month threshold shifts were all elevated and visually separated from the majority of the threshold shifts, but the treated males still showed better hearing than Control animals (+30 dB by 6th month). It should be noted that the threshold shifts for Controls are quite a bit larger than LD mice at the 4th and 6th Month. Also, notice that by the end of testing, the N for the 4th and 6th Month were lower due to aging and attrition of mice at these time points. Mice, by these two time points, are roughly 29-30 months of age by the 4th Month, and 31-32 months by the 6th Month which is roughly the equivalent of over 70-80 human years! [130]

Male HD mice (Fig. 3.1(C&F)) threshold analysis also showed a different aging pattern than the Control group. HD mice appear to cluster together until the 2nd Month, whereas the 4th Month starts to show characteristic threshold elevations. The 6th Month threshold then completely separates and shows significant differences from Baseline for most frequencies. 1st Month mice threshold shift data for HD males have no changes for most frequencies (0 dB shift) or negative shifts (below 0 – hearing improvement of around 5 dB) with 16K, 36K, and WBN. 2nd Month threshold shift data have no elevations across frequencies, with the exception of 16K (Shift around +2.5 dB). 4th and 6th Month threshold shift data showed steady aging declines, as the 6th Month threshold shift data exhibited significant differences in comparison to Baseline. However, when compared to Controls, 4th Month HD data only showed shifts of about +10 dB, whereas Control mice shifted up to +20 dB. 6th Month HD data shifts were ~ +20 to +25 dB, whereas male Control threshold shifts were more than +30 dB.

In the accompanying analysis for females, female Controls had similar ABR thresholds to male Controls (Fig. 3.2(A&D)). Female Controls had characteristic ARHL threshold elevations relative to young adult animals (5 Months old) and Baseline Controls (25-26 Months) (Fig. 3.2A). Threshold shift data (Fig. 3.2D) also show the characteristic threshold elevations which supports the findings from the monthly threshold data. In the Low Dose EGT group (Fig. 3.2(B&E)), both graphs show similar trends as the Control group. Like the Control group, LD subjects show threshold elevations – typical of the aging auditory system, with significant differences by the 4th month at various frequencies (Fig. 3.2B). The threshold shift data also confirm this threshold elevation each month, as significant differences begin to show by the 4th Month at various frequencies (Fig. 3.2E). Similar results are also found in the female High Dose EGT group (Fig.

3.2(C&F)). Threshold shift analysis (Fig. 3.2F) for female HD is consistent with what was seen in the previous graph, where significance can be seen for most frequencies by the 4th Month. Interestingly, from this whole analysis, when we compared each treatment group to Control, we can see that no hearing benefit was acquired from EGT for the females. In fact, it appears that the Control group had slightly lower thresholds than the two treated groups, suggesting that for these aged females, EGT could have somewhat of a detrimental effect on hearing.

Looking at the data for ABR thresholds, EGT clearly has more therapeutic effects for males compared to females. In fact, both LD and HD males performed well according to threshold elevation and threshold shift analysis, thus indicating better health in the cochlear nerve and throughout the brainstem central auditory pathway. Treated females in contrast did not show any benefit from EGT therapies.

3.2 DPOAE Amplitude and Threshold Analysis

Like ABRs, male and female results for DPOAEs are presented. Each column of data presents two different measurements of DPAOE, amplitude and threshold. The column on the left (Fig. 3.3(A,C,&E)) presents amplitudes while those on the right present thresholds (Fig. 3.3(B,D,&F)). Both DPOAE amplitudes and thresholds are effective measurements for determining the health of the cochlear outer hair cell system (OHC), which is responsible for modulation and amplification of cochlear sound signals [131]–[133]. In general, DPOAE amplitudes decline with age; while thresholds go up with aging, like ABR thresholds. In Fig. 3.3A, it can be seen that for monthly testing, the Control animals show a notable separation from month to month. Indeed, the 6th Month amplitudes bottom out near the recording system noise floor. Significant differences for Control animals at 6 months were present for

each frequency. Significant differences were also seen by the 4th Month at all frequencies, except for 40.2 kHz and 44.7 kHz. In Fig. 3.3C, there is a clear difference in the amplitudes as these LD mice aged. Notably, the amplitudes cluster together until the 6th Month time point, then a distinct decline in DPOAE amplitudes takes place. However, it should also be noted that the 4th Month amplitude improved; as values are lower than the baselines across most frequencies. In addition, no significant differences were observed for these treatment data indicating the effectiveness of EGT in maintaining OHC health as compared to Control mice. Male HD mice also exhibit a similar pattern as the LD test group, where the amplitudes by month are clustered together until the 6th Month. Additionally, the male HD treatment group only has minimal significant differences at the 6th Month at 17.8 and 26.8 kHz. Again, comparing these findings to Controls, positive effects of EGT therapy can be observed for male mice. Male DPOAE threshold data essentially follows their amplitude data, as both treatment groups, LD (Fig. 3.3D) and HD (Fig. 3.3F), exhibit better (lower) thresholds than Controls (Fig. 3.3B). DPOAE Control thresholds show more significant differences at the 4th and 6th months, relative to LD and HD, at 8.9, 17.8, and 44.7 kHz. LD does not have significant differences, and HD only shows an effect at 6.7 and 8.9K kHz at the 6th Month, consistent with therapeutic effects of slowing down the progression of ARHL.

Female DPOAE results are organized in the same manner as the male data. In Fig. 3.4A, female Control amplitudes have characteristic declines as expected in aging mice. Significant differences are also seen by the 4th Month into the 6th Month. Fig. 3.4(C&E) exhibits similar aging curves for DPOAE amplitudes. Both treated groups, LD and HD, have similar aging curves as Controls, indicating that EGT treatment is not beneficial to females in comparison to Control.

In Fig. 3.4(B,D,&F), DPOAE thresholds have characteristic aging threshold elevations throughout the 6 month testing period. Both Control and LD mice show similar significant differences for all frequencies by the 6th Month, and 4th Month at higher frequencies. Interestingly, the female HD group has steady elevation of thresholds as well as more significant differences at earlier time points (2nd Mon). HD mice have changes at 6th Month for all frequencies, significance at most frequencies for the 4th Month, and significance by the 2nd Month at 6.7, 8.9, and 44.7 kHz. Taken together, these results confirm that EGT treatment in comparison to Control does not positively affect female mice. Both the amplitudes and thresholds of the two treatment groups, LD and HD, are in agreement with the previous ABR findings as well for aging females. So, it is clear that EGT-treated males outperform male Controls as well as all female groups. These data from both ABR and DPOAE functional hearing measures demonstrates that EGT has promise in delaying certain key aspects of ARHL for males.

3.3 ABR Amplitude and Latency Analysis

The analysis presented in this section pertains to Peak 1 in the ABR recordings for 16 and 24 kHz. These frequencies were selected since they fall within the best range of hearing for mice. It is important to note that these mice were analyzed according to the Linear Mixed Model (LMM) as well as Figure 2.2 found in the methods section.

Peak 1 amplitudes and latencies are important for hearing, as they correlate with the health of the hair cell/auditory nerve synapses, and also are indicators of ribbon synapse loss. For example, the amplitudes decline with age as well as for cochlear insults, such as noise, that damage ribbon synapses [134], [135]. In Figure 3.5, it interesting to note the differences between males and females at 16 kHz. While not statistically significant, these Peak 1 data

confirm previous statistically significant male/female ABR threshold data differences in this dissertation, i.e., positive trends are seen here for EGT-treated males. Males (Figure 3.5A) had slightly lower amplitudes at Baseline for all groups, and they show higher amplitudes in comparison to females for all subsequent timepoints. In addition, female (Figure 3.5B) amplitudes declined faster than males; and females also did not show any separation of treatment groups from Controls. In contrast, LD males showed amplitude increases above Baseline for all months tested. The 24 kHz amplitude analysis does not show as sizeable differences between males (Figure 3.5C) and females (Figure 3.5D), however it can still be seen that males exhibit a slower rate of decline than females; where males only decline ~500 nV for all three groups during the entirety of the testing period, while females decline (~500 nV to ~1000 nV) for all three groups. Interestingly, in the female group (Figure 3.5D), the Controls outperform (higher amplitudes) the two EGT-treated female groups.

Peak 1 Latency Analysis (Figure 3.6) follows the same trends of the positive EGT treatment effects seen in Figure 3.5; where latencies from male treated groups outperform both the male control and all female groups for both frequencies, 16 and 24 kHz. For instance, when comparing Figure 3.6A and Figure 3.6B, it is apparent for males at 16 kHz, that both treated groups are outperforming the Controls, as the Controls' latency has a steady climb from ~2.68 ms at Baseline to ~2.8 ms at 6th months. Both treated groups show similar changes, having minimal increases in latency over the 6 month treatment period. In fact, the LD group actually ends the testing period with a lower latency than at Baseline; and the HD latency only increases about ~0.05 ms by the 6th month (less change than the male Controls). In Figure 3.6B, female Controls outperform (shorter latencies) than the treated female groups by the 6th

month. Both LD and HD groups show longer latencies than Controls throughout the testing period, and have a greater positive slope for latencies in comparison to males. Analysis at 24 kHz (Figures 3.6C and 3.6D) is much the same as that for 16kHz. LD and HD males are showing better (shorter) latencies throughout the entire testing period relative to Controls. Females at 24 kHz have almost the same results seen for 16 kHz; steeper slope of month-to-month latency increases compared to males and to the female Controls. Again, these ABR latency trends confirm the statistically significant findings for the ABR thresholds, despite a lack of statistical significance for Peak 1 latencies. Future studies with more animals will test these initial ABR latency results further.

3.4 EGT Uptake - LC-MS/MS Analysis- Whole Blood Sampling

Whole blood was extracted from the facial vein for each mouse at specified time points as given in Figure 2.1. Whole blood was then processed for each animal as described above, and run through an LC-MS/MS to quantify each sample for the total amount of EGT. In Fig. 3.7, data for all groups are displayed from testing start date to testing end date. On the bottom of the graph are the functions for the two Controls, male Controls and female Controls as brown and light blue curves, respectively. These two groups are relatively stable throughout testing as they have not been treated with EGT, but male Control mice have a slight downslope by the end of 6th Month. This can be attributed to general aging as it is known that EGT levels decline with age [136]. Contrastingly, all treated mice are significantly different from Control mice as early as day 7. Male mice also show greater uptake in EGT than female mice by the 1st Month, which continues throughout to the end of the study – 6th Mon. In males, EGT levels raise to over 4000 ng/mL for HD and 5000 ng/mL for LD mice. Interestingly, LD and HD for both male

and female mice mimic each other. Simply put, LD and HD for males are very similar to each other as are LD and HD for females. Additionally, it should be noted that both female EGT groups, seemed to experience a plateau in EGT uptake at a lower concentration than males. Females plateaued around 3000 ng/mL by the 1st Month with a slight decline by the 6th Month, where HD settled around 2500 ng/mL and LD stayed around 3000 ng/mL. Lastly, Baseline Values in Fig. 3.7 for all groups have variations within the sexes, as well as variation between the sexes. For clarification, these baseline data were plotted into a separate figure to see the differences at the start of the study (Fig. 3.8). Here, male test groups (Control, LD, HD) in comparison to all female test groups have concentrations of EGT higher than any female test groups. Interestingly, Control, LD, and HD male groups span a range of around 500 ng/mL from Control to HD, respectively. This variability for males did not seem to affect the LD and HD males, as both groups mimicked each other in EGT uptake. Female test groups had less variation of mean concentrations between the test groups, which apparently, did not appear to influence the time course of the longitudinal uptake. Of note, Young Adult Mice (n=3, 5 Months) were also included in this analysis to compare baseline EGT blood levels in Young Control (YC) animals and Older Control animals. As expected, both male and female YC show greater Baseline Values than the older Controls used in this study, where male YC mice have a nearly 1500 ng/mL difference in baseline values, and are significantly different from all male test groups, Control, LD, and HD. Female YC mice are also significantly different from all female test groups, Control, LD, and HD, however, female YC mice have lower concentrations of EGT relative to male YC for baseline values. Female YC are approx. 1000 ng/mL below male YC. This difference in young adult mice (5 months) holds true even into old age (25-26 Months);

indicating perhaps male CBA/CaJ mice have preferential uptake through their adult lives. This needs further investigation, and may be related to sex hormone concentration differences, or perhaps female/male muscle mass differences.

3.5 EGT Blood Levels and ABR Threshold Correlation Analysis

In this analysis, we were able to utilize our data set to examine correlations between whole blood EGT concentrations (ng/mL) and ABR thresholds at 16 kHz for the 2nd and 4th Months. 16 kHz was selected as it is one of the best frequencies for hearing in CBA/CaJ mice. In this instance, we also utilized baseline shift data where the baseline value is subtracted out from the time point of interest to remove the influence of natural variations in the initial baseline starting values. It should be noted that each individual data point on these graphs are from one animal. Any animal that was missing LCMS data or ABR thresholds, was not included in this particular analysis, which incorporated both 2nd Month and 4th Month data. In Fig. 3.9, panels A and B compare the correlation data from male Controls to the data from all EGT treated, LD and HD, mice. Panels C and D also compare the female data. Here, in 3.9(A&B), differences between the correlations for male Control and EGT-treated mice are apparent, as the Control group has a slight positive correlation while treated males have a slight negative correlation. Control mice also do not show much variability in their EGT baseline shifts as expected. However, ABR baseline shifts show elevated thresholds, as also expected; low EGT change, and higher thresholds over time. In the EGT-treated mice, ABR baseline shifts are not as drastic as those seen in the Controls, i.e., some are in fact negative, showing improved hearing performance at 16 kHz. It is clear that by the 2nd Month, either dose of EGT administered to male mice has a positive impact on auditory health.

Consistent with our previous female data, there were no apparent differences between the correlations between Control and EGT-treated females (Fig. 3.9(C&D)). Control and EGT-treated mice both have negative correlations, and do not appear to have any predictive value. Interestingly, Female Control data (Fig. 3.9C) have the same pattern as the male Control data (Fig. 3.9A) as there is very little variability in the EGT shift data, e.g., for Controls, ABR shift data shows a similarity in variability with data points going from -5 and -15 dB, a typical aging pattern. In Fig. 3.9D, Female EGT-treated mice do not display any data points that have apparent relations to improvements in ABR thresholds, i.e. no negative threshold shifts are present. Rather, the data points are distributed evenly from 0 to +15 dB as noted by the weak correlation value, $r=-0.156$. Additionally, EGT baseline shift data or changes in EGT uptake did not have any significant relations to hearing measures. Lastly, when we compared these results to the male EGT-treated group (Fig. 3.9B), the difference between treated males and females is especially apparent in the ABR threshold shift values. Treated males have quite a few data points in the 0 to negative shift range whereas female data points begin only at 0 and continue up to +15 dB.

In Fig. 3.10, we analyzed similar results as in Fig. 3.9, but instead used 4th Month data. Initial results for Fig. 3.10, show a large treatment effect for male mice (Fig. 3.10B) when compared to male Controls (Fig. 3.10A). Male Controls have a slight positive correlation with the data ($r=0.3349$) and have expected EGT baseline shift values $\sim \pm 500$ ng/mL. ABR baseline shift data are also as expected as all data points have moved into positive shift territory with a range between +5 and +25 dB. Excitingly, EGT treated males (Fig. 3.10B), have a negative correlation value ($r= -0.726$) that is statistically significant ($P= 0.041$). The data show an even

higher predictive value than that seen for the EGT treated males at the 2nd Month (Fig. 3.9). Female Control (Fig. 3.10C) data for the 4th Month are very similar to female Control data for the 2nd Month, i.e., no relation between EGT blood levels and hearing. Lastly, EGT treated females (Fig. 3.10D) also show a different profile than the 2nd Month. The hearing data correlate a little better with the measured EGT in the whole blood. The calculated r value ($r = -0.486$) confirms this better correlation. Outcomes for hearing measures do seem to be slightly weighted by the amount of EGT in the subject's system. For example, the two mice with the highest threshold shifts at +35 dB demonstrate that a lower amount of EGT in whole blood, even though it's still relatively high in comparison to Controls, can lead to poorer outcomes. One can also look to the mouse with the lowest threshold shift at just +5 dB and notice that this animal has the 2nd highest amount of EGT according to LCMS baseline shift measurements. Overall, this correlation analysis demonstrates the beneficial influence that EGT treatment has on ABR threshold shifts as mice age. This is especially seen in Fig 3.10B, where the correlation is high, and the points follow closely the line of best fit.

3.6 Cochlear Tissue Analysis: RT-PCR Results

In this portion of the study, cochleae were harvested from the mice at the conclusion of the 6-month treatment period; and structures of the cochlea were harvested individually: Stria Vascularis (SV), organ of Corti (OC), Modiolus (MD). These individual tissues were then processed and converted to cDNA for use in real-time Reverse Transcription Polymerase Chain Reaction (RT-PCR). Results were calculated using the Relative Standard Curve Method. Gene Expression was analyzed for the following genes: GAPDH (loading Control), OCTN1 (EGT receptor), Cas-3 (apoptosis marker), TNF- α (inflammation), PGC1a (mitochondrial biogenesis),

and SOD2 (antioxidant). It should also be noted that both LD and HD results were combined for this analysis since LD and HD both showed beneficial effects on hearing tests and LC-MS/MS experiments of the present investigation, as presented above.

In this first panel, Fig. 3.11, all gene expression graphs are from the SV. Noticeably, all male gene expression profiles, Tumor Necrosis Factor-Alpha (TNF- α), Superoxide Dismutase 2 (SOD2), and Caspase 3 (Cas-3), show significantly different gene expression levels relative to Controls. The reduction in TNF- α and Cas-3 are clear indicators that EGT treatment has affected the SV positively as both inflammation and apoptosis are downregulated [137]. The upregulation of SOD2 also means that EGT is working as an antioxidant. SOD2 is an antioxidant enzyme that is upregulated under cell stress, more specifically upregulated near the mitochondria to reduce the concentration of free radicals [138], [139]. Female correlates of these gene expression profiles were also included in this panel for comparison to males. Figure 3.11(D-F) do not have any significant differences compared to Controls, but do show trends that were seen more robustly in males; TNF- α and Cas-3 downregulated, and SOD2 upregulated,. These female results are important because even though they do not display statistically significant differences relative to Controls, it does show that EGT effects are mildly present in the SV, even if only slightly, consistent with our finding above that the EGT functional hearing benefits are more striking in the males.

Presented in Fig. 3.12 is RT-PCR data obtained from the OC, where significant differences were seen. In Fig. 3.12(B&C), females showed significant results for TNF- α and Cas-3 which were downregulated in the treated mice. Lastly, in Figure 3.12, the males exhibited an upregulation in gene expression which indicates an increase in mitochondrial biogenesis, as

PGC1 α has been shown in previous studies to increase expression in the presence of stressors or supplements that activate this protein [69], [140].

Lastly, Figure 3.13 shows gene expression changes in MD. Panels A&B, from male mice for SOD2 and PGC1 α exhibit significant differences, as they are both upregulated. From previous investigations, it is known that these two proteins are both antioxidants related to mitochondrial health and that they work synergistically together [69], [140]. First, in Fig. 3.13(C&F), one can see that the results favor female mice in expression of Cas-3. Females exhibit a significant reduction in Cas-3 whereas males have no significant change compared to Controls. This same trend is also found for TNF- α where females show significant reduction in this inflammatory marker, where the males show no significant change. Males were included as a comparison to convey that not all changes were positive for the males. Based on these results it appears that female mice were able to utilize EGT in the modiolar cochlear region for some regulation of inflammation and apoptosis, whereas male mice appeared to be utilizing the antioxidant pathway for their benefit. Taken together, it appears that EGT therapy is targeting multiple cochlear anti-aging mechanisms, though further investigation is needed to decipher the exact pathway mechanisms involved here in greater numbers of aging males and females.

3.7 Survival Analyses

In survival analyses, 'death' events were tracked and analyzed using the Kaplan-Meier Method along the treatment and testing timeline of the present investigation. All mice included in this analysis were those that started their hearing measures at Baseline (25-26 months). Events were classified as "censored" when the reason for death was user error (e.g.,

ketamine overdoses related to large liver tumors), or if the mice lived long enough to complete the six month study where they were subsequently euthanized. Events were considered “death events” when mice were either found dead in their cage or they were ethically euthanized as recommended by veterinarians under our IACUC protocol guidelines.

Male survival analysis (Fig. 3.14) shows a distinct separation in survival probability between male HD and Control/male LD; where male HD had a survival probability above 75% but male Control mice and male LD had probabilities that were just above 50%. Male HD began with 8 mice and had only 1 death and 1 censored subject, so by the end of testing only 6 mice were considered ‘at risk’ for a ‘death event’. Male LD began with 6 mice, had 2 deaths, 4 censored subjects and finished testing at 6 months with 2 mice at risk. The Control group began with 13 mice, had 5 death events, 8 censored subjects, and finished testing with 6 mice at risk. (Mantel-Cox) Log-rank test for trends were not significant ($P=0.543$). Female survival analysis (Fig. 3.15) showed a slight separation in survival probability between female HD and Control/female LD; female HD survival probabilities were ~75% whereas female LD and Control were both close in probabilities by the 6th month and were around 60%. Female HD began with 12 mice, had 2 deaths, 10 censored subjects, and 9 mice that finished the testing at risk. Female Control began with 6 mice, had 2 deaths, 4 censored subjects, and finished testing with 3 mice at risk. Lastly, Female LD started with 7 mice, had 2 deaths, 5 censored subjects, and finished testing with 4 mice at risk. (Mantel-Cox) Log-rank test for trends were also not significant $P=0.458$). It should be noted that for both of these analyses the High Dose had higher survival probabilities. Although none of these differences were significant, they do show trends that EGT treatment may be prolonging life in these animals. Since these results are very

preliminary, as they suffer from low sample sizes and censor bias, further study is needed to see if the EGT treatments extend lifespan.

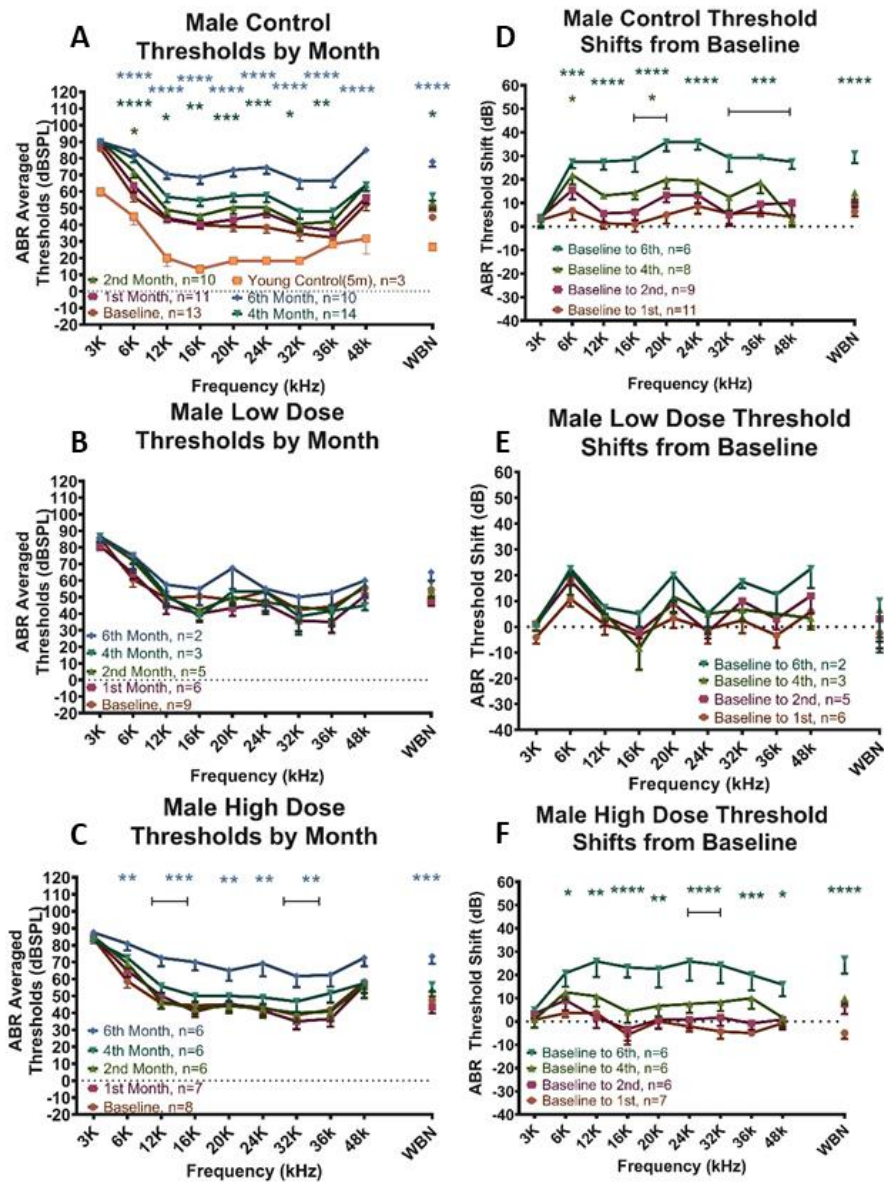


Figure 3.1: Male ABR Results. All plots describe intragroup threshold changes by month, respectively. Significant differences were determined using 2-way ANOVA with Dunnett's multiple comparison *post-hoc* corrections. All subsequent months were compared to Baseline values. Values given as means \pm SEM. Statistical significance denoted for testing month by corresponding color where * $P < .05$, ** $P < .01$, *** $P < .001$, **** $P < .0001$.

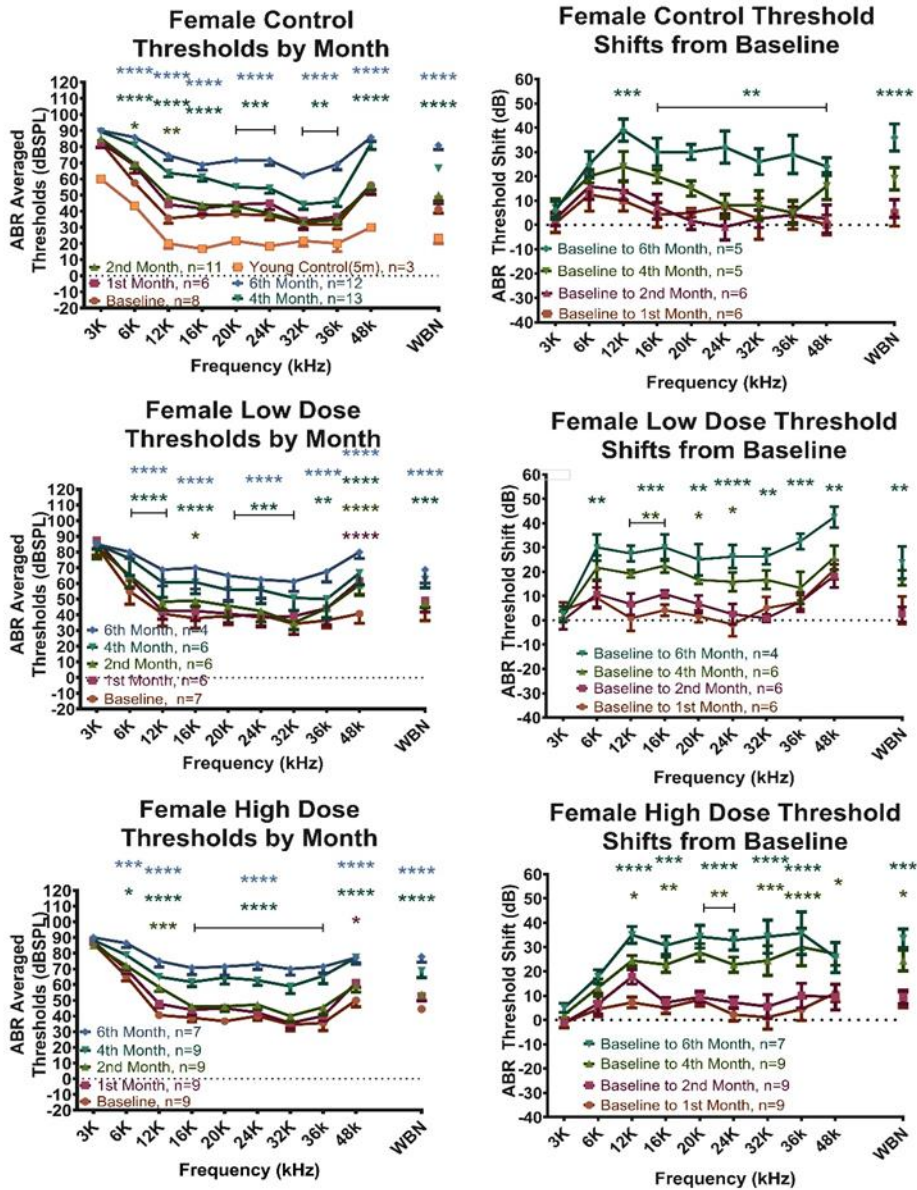


Figure 3.2: Female ABR Results. All plots describe intragroup threshold changes by month, respectively. Significant differences were determined using 2-way ANOVA with Dunnett's multiple comparison *post-hoc* corrections. All subsequent months were compared to Baseline values. Values given as means \pm SEM. Statistical significance denoted for testing month by corresponding color where * $P < 0.05$, ** $P < 0.01$, *** $P < 0.001$, **** $P < 0.0001$.

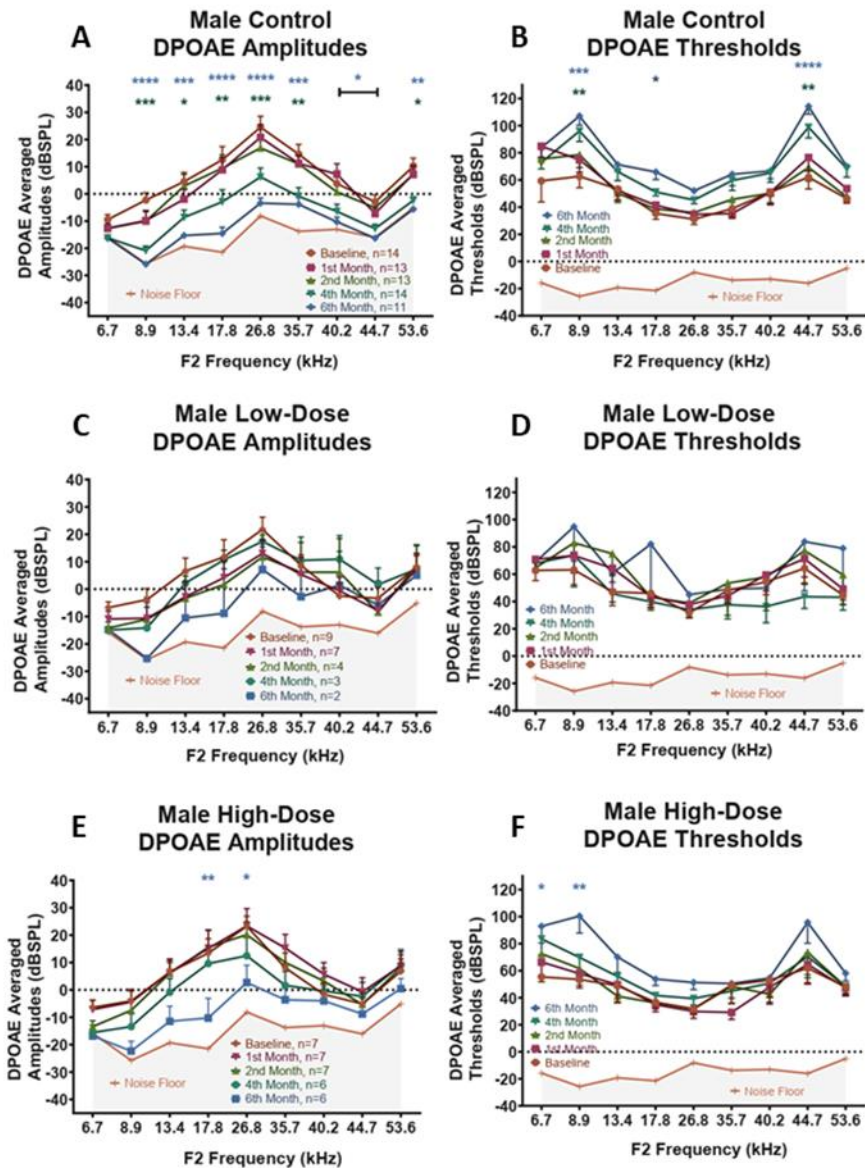


Figure 3.3: Male DPOAE Results. All plots describe intragroup threshold changes by month, respectively. Significant differences were determined using 2-way ANOVA with Dunnett's multiple comparison *post-hoc* corrections. All subsequent months were compared to Baseline values. Values given as means \pm SEM. Statistical significance denoted for testing month by corresponding color where * $P < 0.05$, ** $P < 0.01$, *** $P < 0.001$, **** $P < 0.0001$.

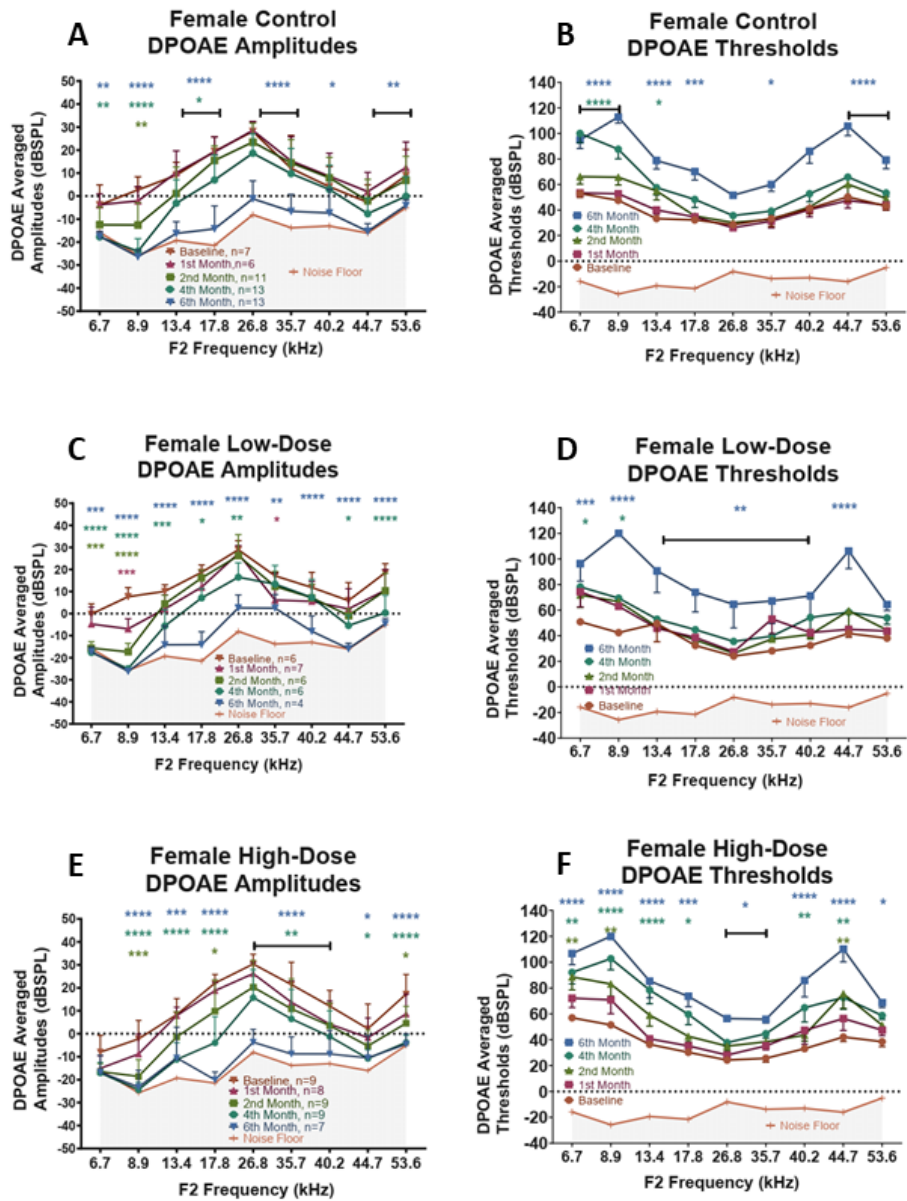


Figure 3.4: Female DPOAE Results. All plots describe intragroup threshold changes by month, respectively. Significant differences were determined using 2-way ANOVA with Dunnett's multiple comparison *post-hoc* corrections. All subsequent months were compared to Baseline values. Values given as means \pm SEM. Statistical significance denoted for testing month by corresponding color where * $P < 0.05$, ** $P < 0.01$, *** $P < 0.001$, **** $P < 0.0001$.

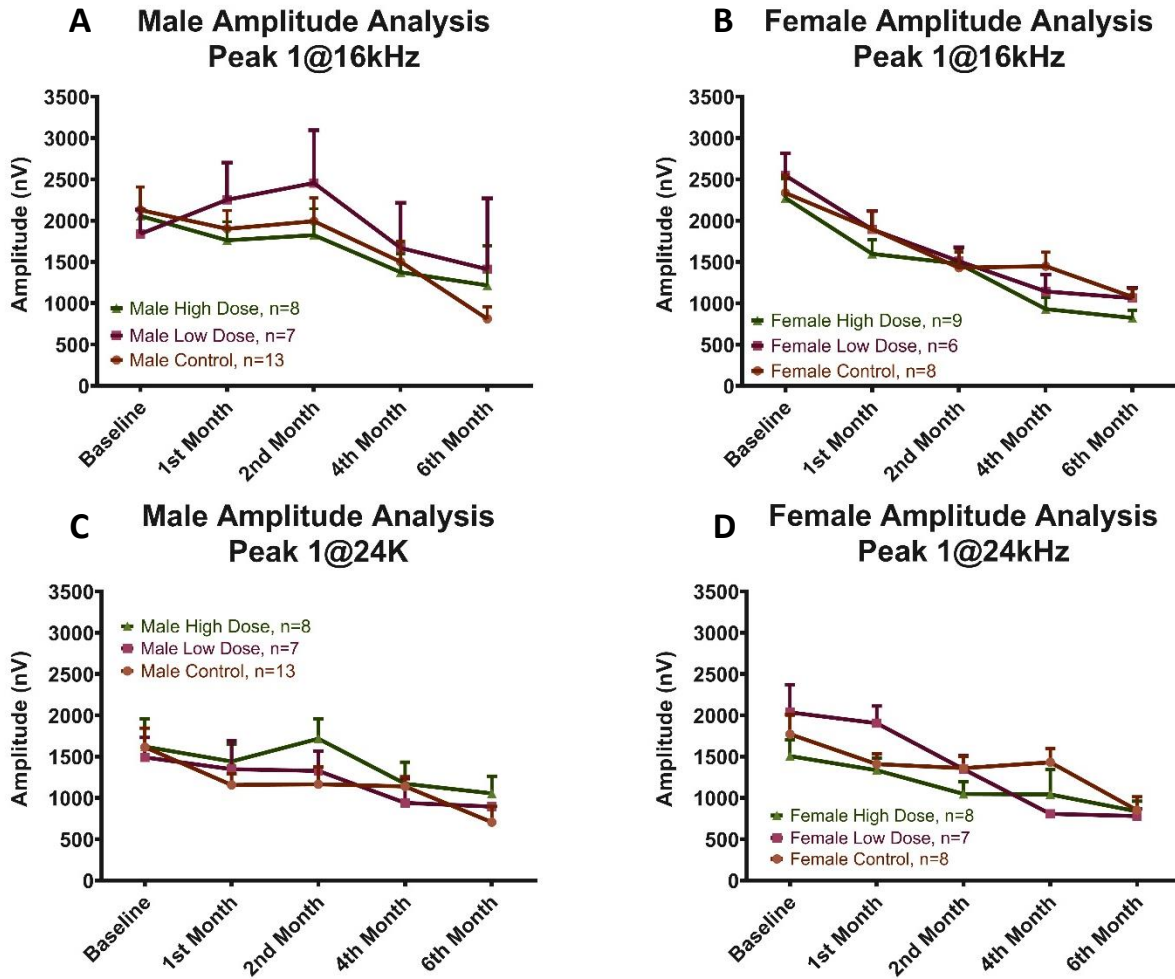


Figure 3.5: ABR Amplitude Analysis Peak 1. Treated males' amplitudes *decline less than the other subject groups*. Subject #s (n) given for each experimental group indicate the number of mice enrolled at baseline. However, it is important to note that the # in some groups changes month-to-month due to attrition from old age, as well as inclusion of age-matched Control mice acquired partway through the study. Peak 1 amplitudes were measured from ABR data at 2 specific frequencies, 16 and 24 kHz. Peak-to-trough amplitudes were measured for recordings at 85 dB SPL. Data was analyzed using 2-way ANOVA with Dunnett's multiple comparison *post-hoc* corrections. Each dataset is compared to every other dataset and analyzed for significance.

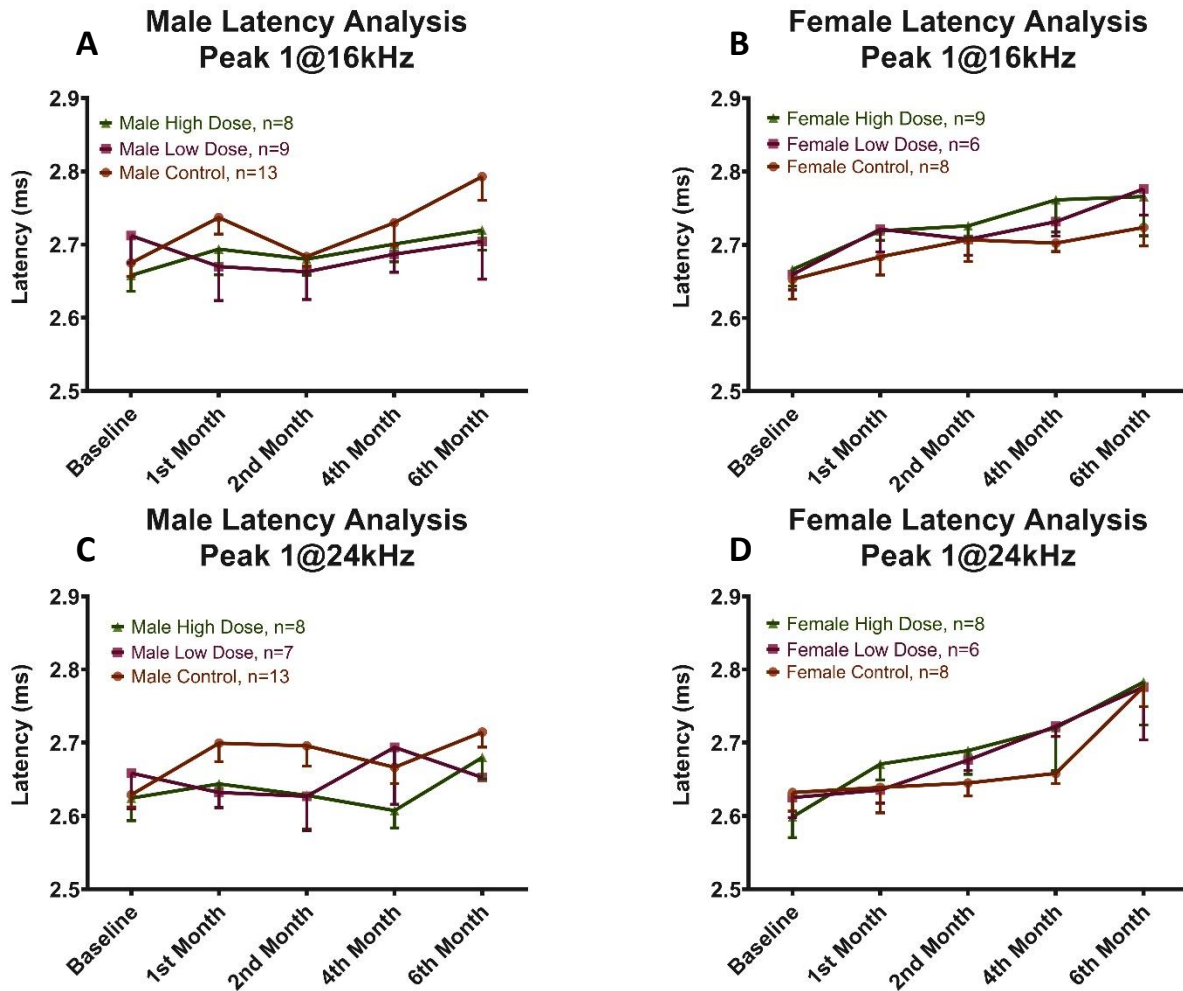


Figure 3.6: ABR Latency Analysis Peak 1. Treated males have *shorter latencies than the other subject groups*. Peak 1 latencies were measured from ABR data at 2 specific frequencies, 16 and 24 kHz. Peaks were selected using recordings at 85 dB SPL. Subject #s (n) given for each subject group indicate the #of mice at baseline. However, note that the N# of each group changes month-to-month due to attrition from old age, as well as inclusion of mice (age-matched male and female Controls) acquired partway through the study. Data were analyzed using 2-way ANOVA with Dunnett’s multiple comparison *post-hoc* corrections. Each dataset was compared to every other dataset and analyzed for significance.

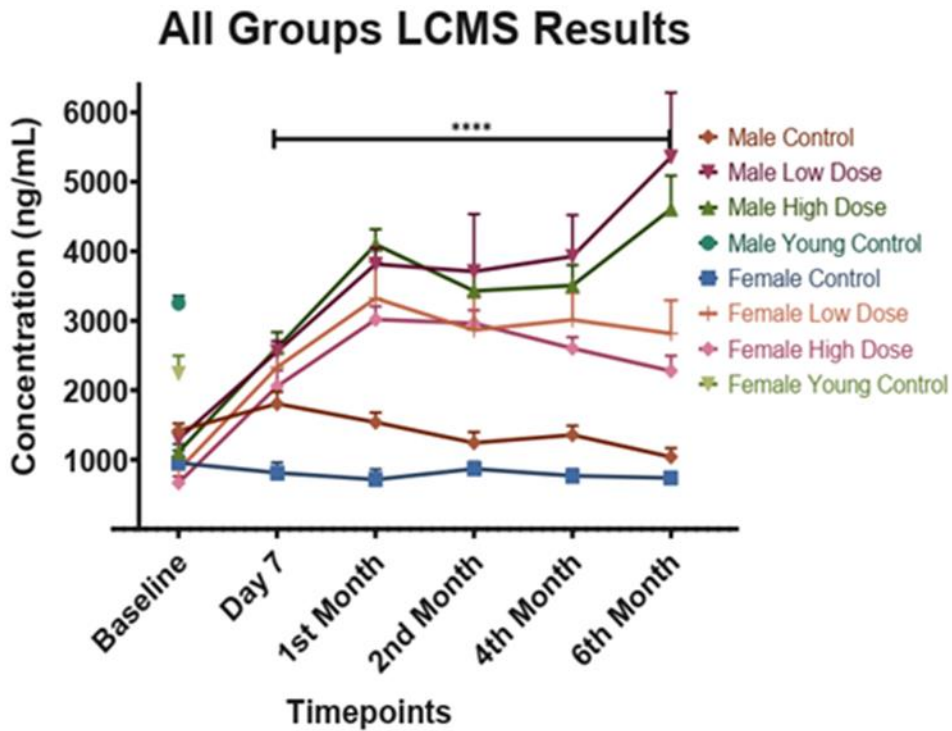


Figure 3.7: Whole Blood Analysis. LCMS results show the differences in uptake between male and female, as well as the changes in EGT uptake over time. All treated groups show significant differences by Day 7 in comparison to male and female Controls. Significant differences were determined using 2-way ANOVA with Dunnett's multiple comparison *post-hoc* corrections.

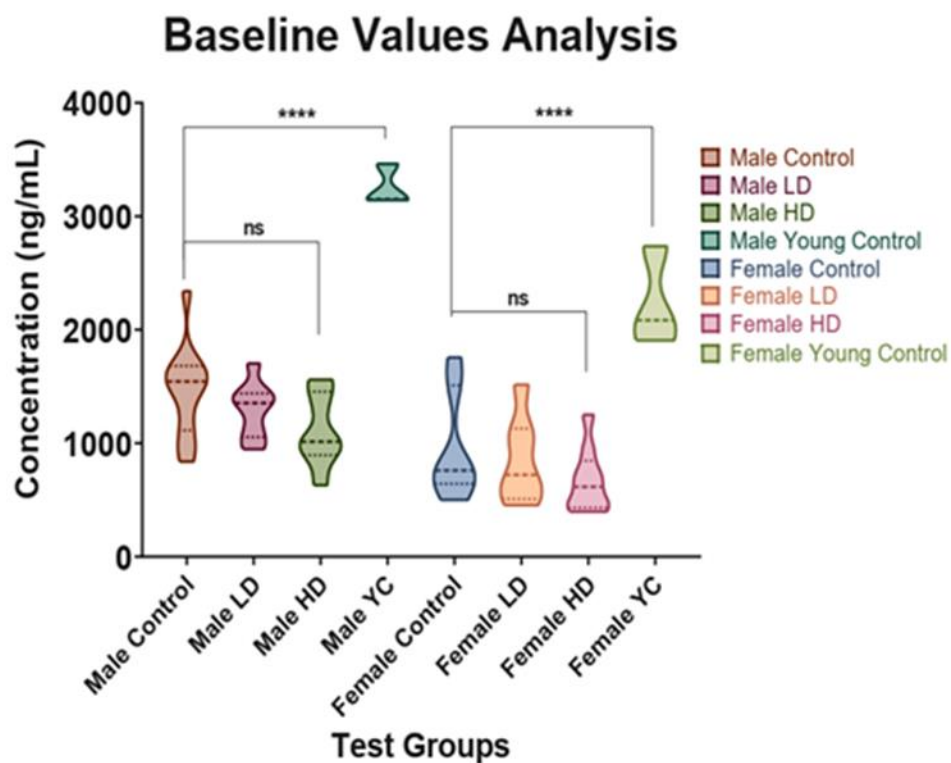


Figure 3.8: Baseline Values Analysis. LCMS results show the differences in baseline values for male and female, where male Control, LD, and HD start with higher baseline EGT than female test groups. Also included are samples from Young Control mice (n=3, 5 months) from both sexes to compare young EGT baselines to the older test group. Young adults have much higher naturally occurring levels of EGT. For both young adults and old age, males have higher levels than females. There were no significant differences for the old experimental groups at baseline. Significant differences were determined using 1-way ANOVA with Tukey's multiple comparison *post-hoc* corrections.

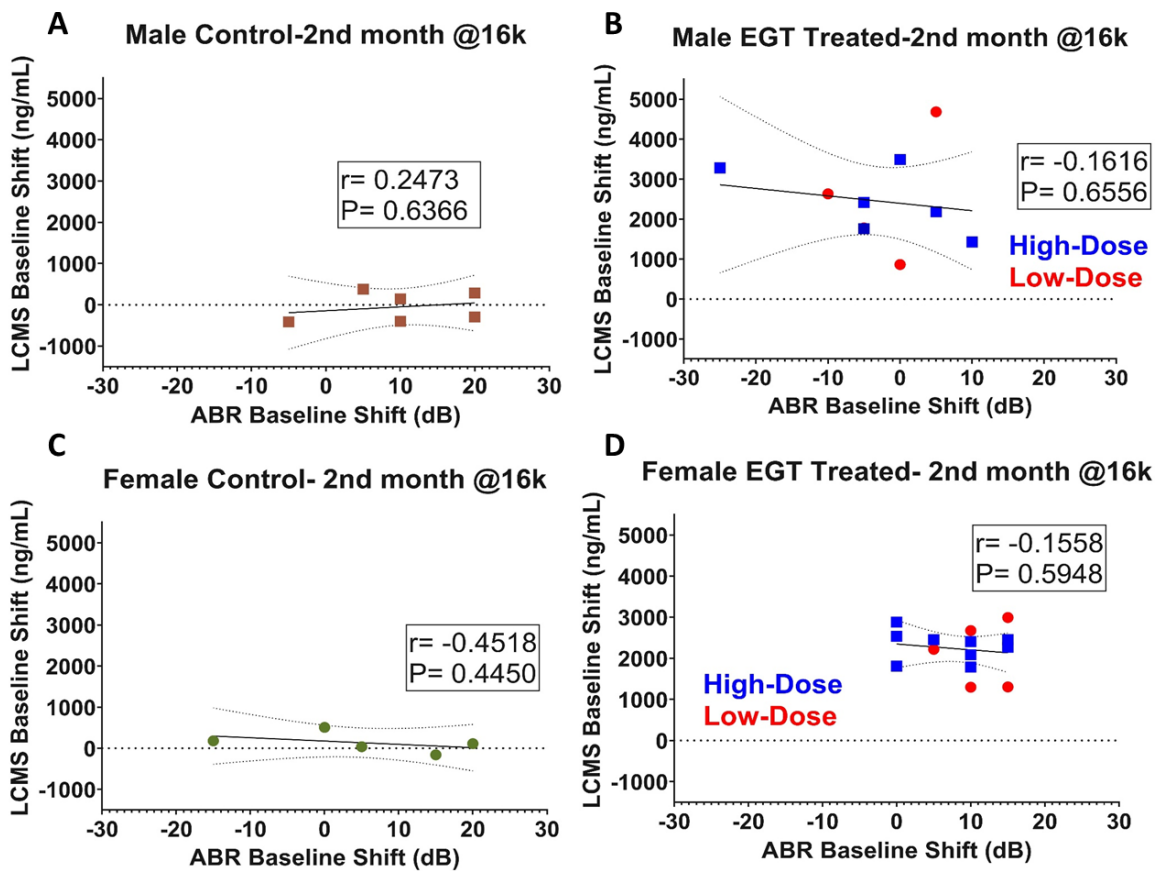


Figure 3.9: EGT Levels in Blood and ABR Thresholds Correlation-2nd Month. 2nd Month correlations are relative to the start of EGT treatment. They show slight slopes in lines of best fit. However, Male EGT-Treated animals show the most beneficial outcome among the respective groups, showing some negative shifts by the 2nd month.

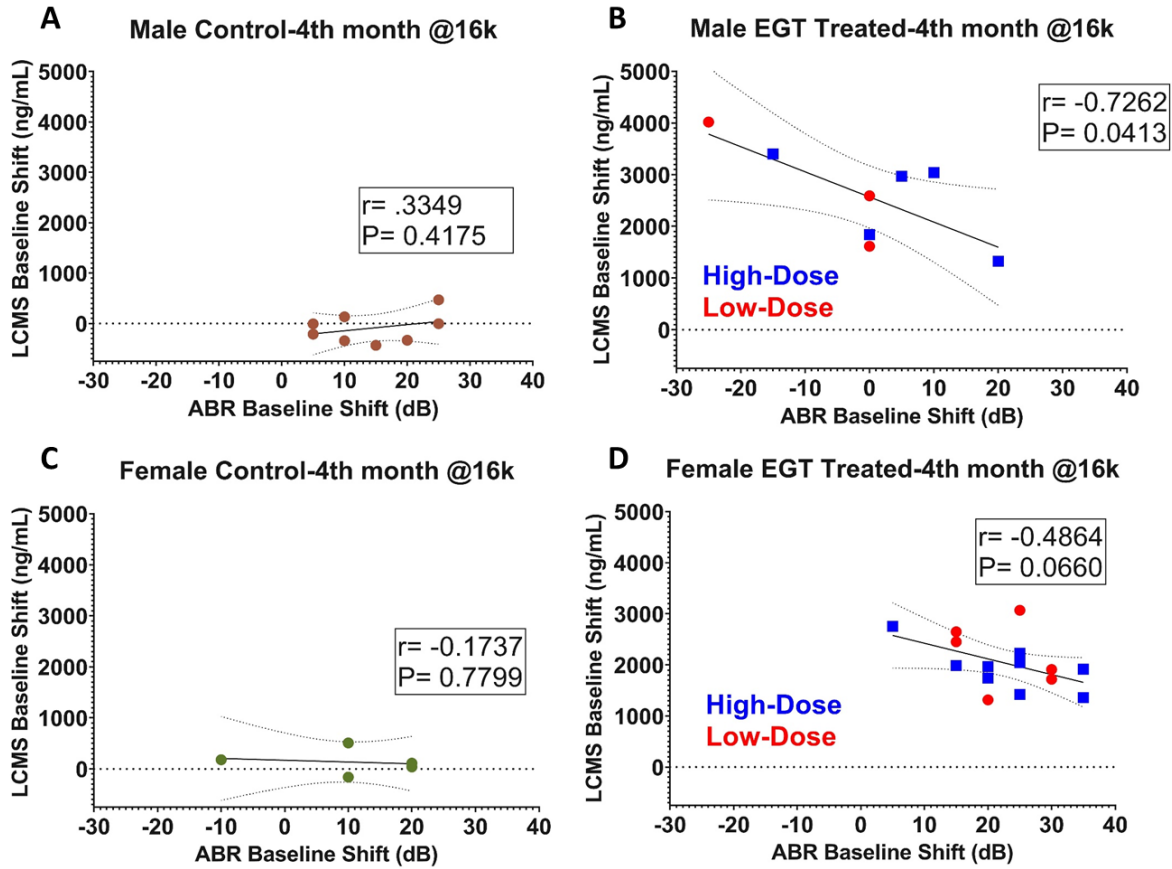


Figure 3.10: EGT Blood Levels and ABR Thresholds Correlation-4th Month. These correlations display similar trends for Controls as for the 2nd Month. However, both male and female treated groups have negative slopes of their lines of best fit. Interestingly, the male group shows statistically significant correlation between the two variables, demonstrating that higher levels of EGT in the blood correlates to lower ABR thresholds.

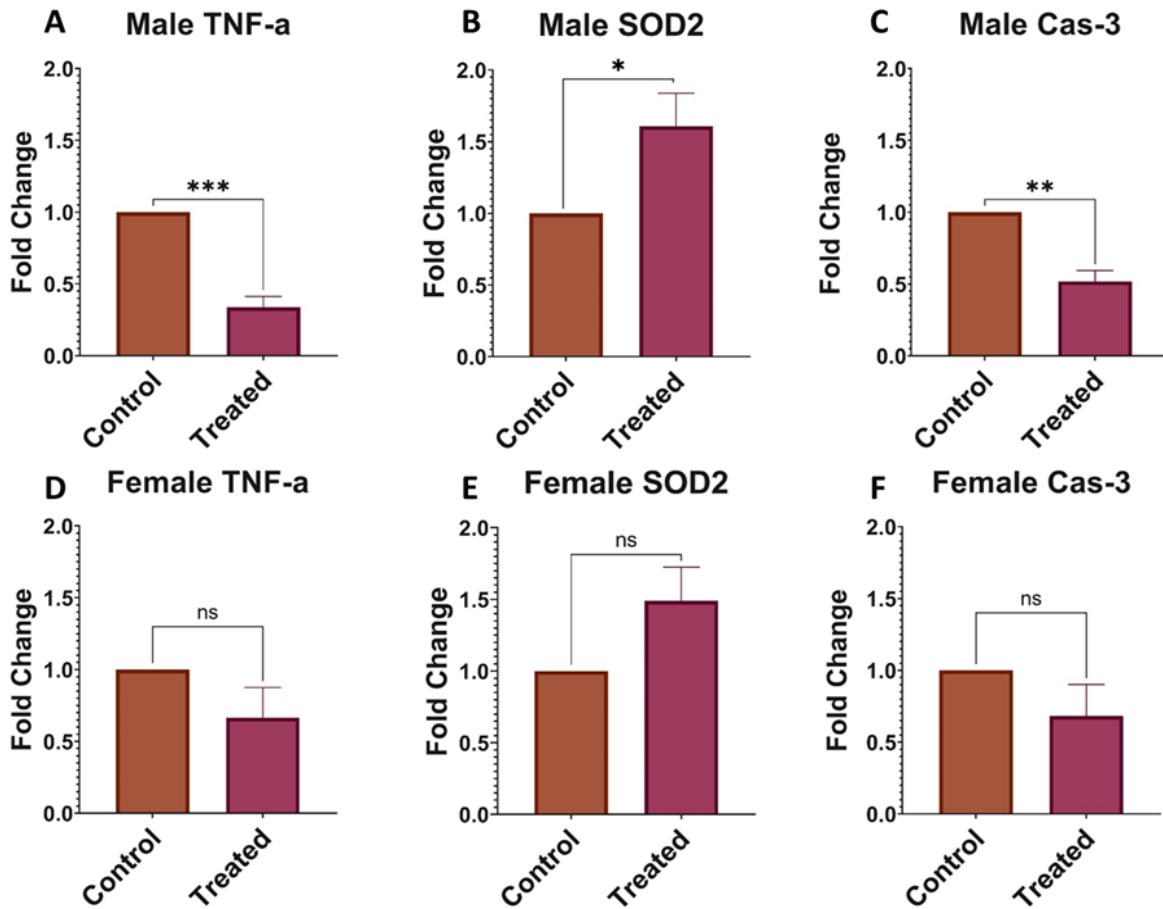


Figure 3.11: SV Gene Expression. Tissue harvested from Stria Vascularis (SV), EGT Therapeutic Effects; TNF- α , Cas-3: Downregulated; SOD2: Upregulated. Values given as means \pm SEM. * $P > 0.05$, ** $P > 0.01$, *** $P > 0.001$ Unpaired t-test with Welch's correction.

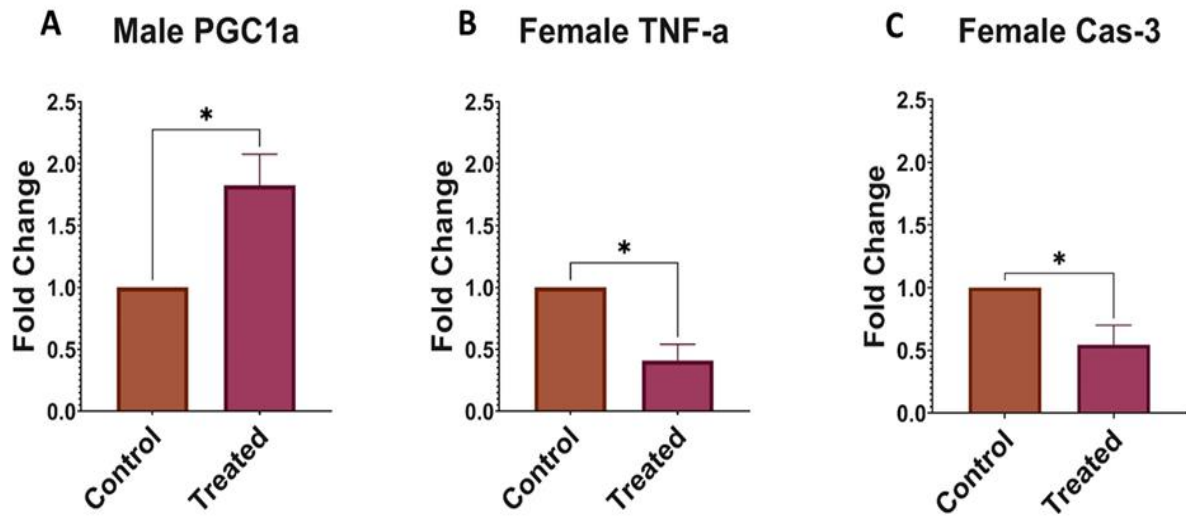


Figure 3.12: OC Gene Expression. Tissue harvested from Organ of Corti (OC), EGT Therapeutic Effects; TNF- α , Cas-3: Downregulated; PGC1 α : Upregulated. Values given as means \pm SEM. *P>0.05, **P>0.01, ***P>0.001 Unpaired t-test with Welch's correction.

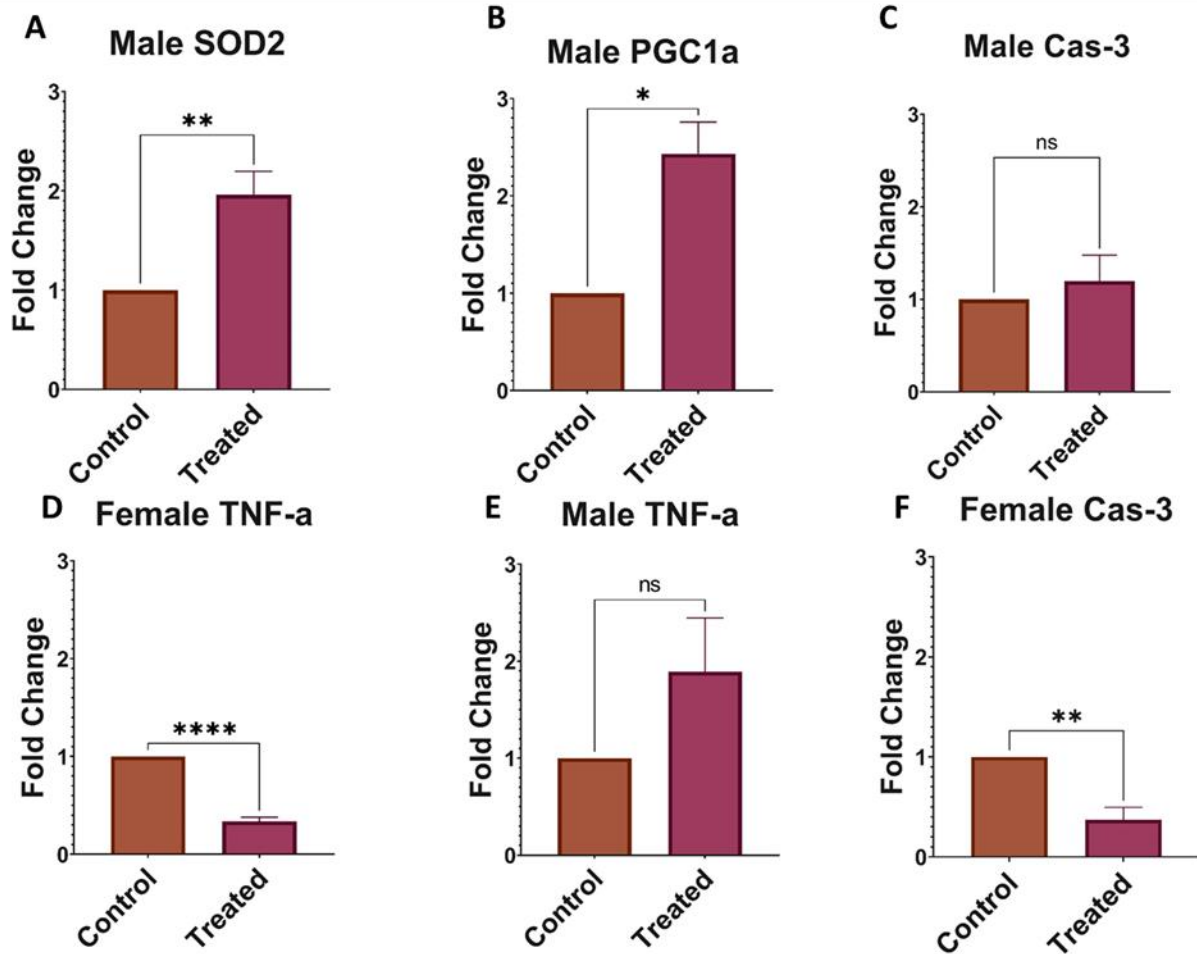


Figure 3.13: MD Gene Expression. Tissue harvested from Modiolus (MD), EGT Therapeutic Effects; TNF- α , Cas-3: Downregulated; PGC1 α , SOD2: Upregulated. Values given as means \pm SEM. *P>0.05, **P>0.01, ***P>0.001 Unpaired t-test with Welch's correction.

Survival Analysis: Males

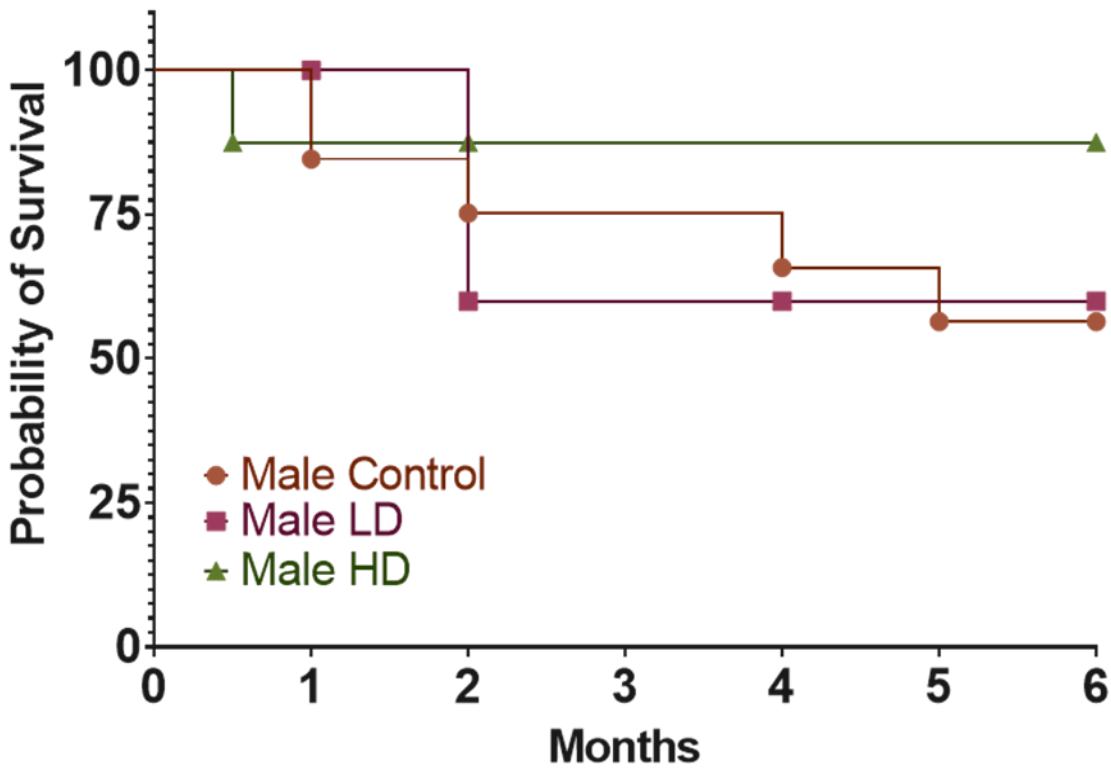


Figure 3.14: Male Survival Analysis. Male Control (n=13, 6 survived the 6 month test period); Male LD (n=6, 2 survived the test period); Male HD (n=8, 6 survived the test period). It should be noted that at timepoint 0 (Beginning of EGT Treatment), the age of mice was 25, 26 months. By the end of the testing period at 6 months from the start of treatment, the mice were at 31, 32 months of age.

Survival Analysis: Females

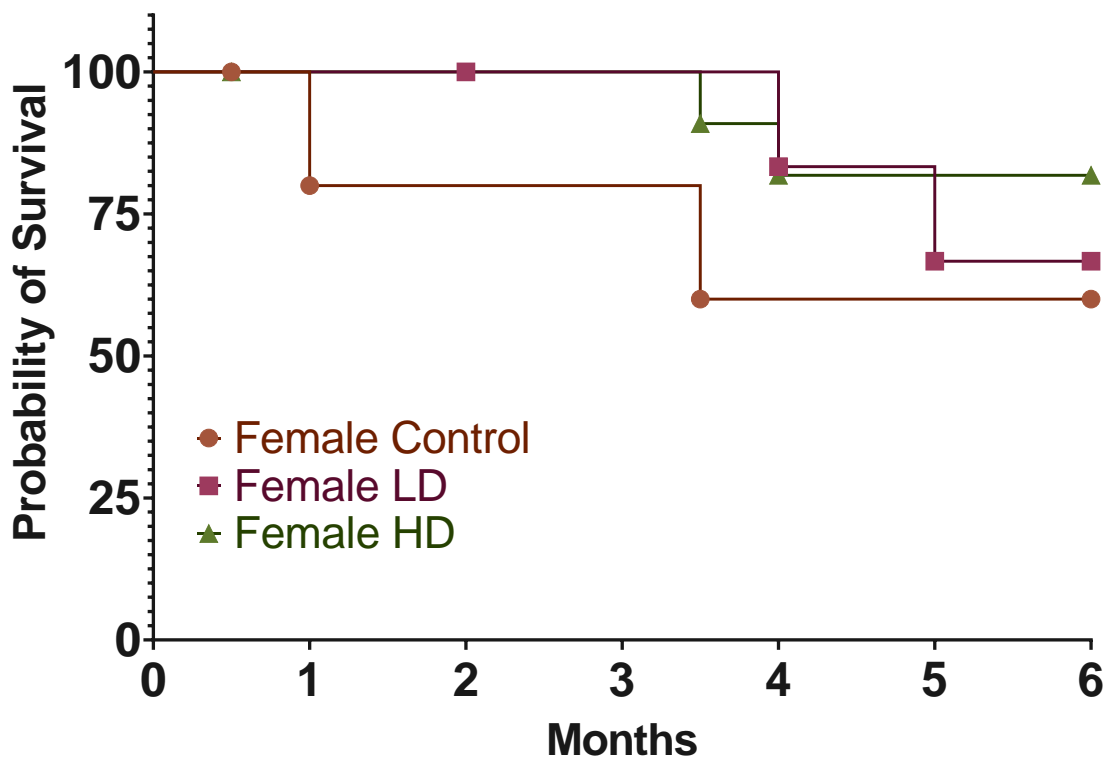


Figure 3.15: Female Survival Analysis. Female Control (n=6, 3 survived the 6 month test period); Female LD (n=7, 4 survived the test period); Female HD (n=12, 9 survived the test period). It should be noted that at timepoint 0 (Beginning of EGT Treatment), the age of mice was 25, 26 months. By the end of the testing period at 6 months from the start of treatment, the mice were at 31, 32 months of age.

Chapter 4: Discussion

In this study, we demonstrated for the first time, that EGT supplementation in old male mice had significant positive effects on objective, physiological hearing measures. For both ABR and DPOAE measurements, EGT-treated male mice showed significantly different aging curves compared to male Controls and all female groups. Considering these test groups' ages, and the fact that they were already experiencing noticeable ARHL, these findings are both novel and ground breaking. To the best of our knowledge, EGT has never been used as a possible pre-clinical treatment for any type of hearing loss including ARHL, nor have positive results been found using other antioxidants such as glutathione, in such advanced aged mouse populations (25-26 months to 30-31 months) which is the equivalent of over ~80 human years.

Furthermore, results from our study will be possible to translate to humans as well, because EGT is highly safe and already approved by the FDA as a dietary supplement. So, toxicology issues will be minor relative to many other newer pharmaceuticals under consideration for preventing or treating hearing loss. Hence, our findings give novel insights into greater possibilities for EGT, as these initial results will be a springboard for future work.

4.1 Sex Differences in EGT Treatments and Auditory Measures

Analysis of the hearing measures in this study found significant effects for males but no/minimal effects for female mice, which raises important questions about the origins behind this sex selectivity. LC-MS/MS testing of whole blood samples for EGT levels revealed intriguing results which supported our hearing measure findings, and were consistent with currently

available scientific literature. LC-MS/MS testing showed baseline values for all groups that were roughly equivalent, except that male baseline values were slightly higher than the females, indicating a difference in EGT uptake for these old animals prior to treatments. To further understand baseline differences in both sexes, young adult mice were tested at the age of 5 months, again revealing a natural advantage of males for EGT uptake. Specifically, males showed an uptake nearly 1000 ng/mL greater than females. For the old animals receiving EGT supplementation, treated males showed an advantage; where the differences in uptake were apparent by the 2nd month of treatment, and continued until the end of the study. There are multiple possibilities for explaining these sex differences. In Mackenzie and Mackenzie's early study into EGT uptake back in 1957 [141], the researchers found that testosterone was a main facilitator for EGT uptake. They noted that in rats, by the time they reached sexual maturity, EGT uptake in males was nearly double that of females. Interestingly, females injected with testosterone showed a similar uptake as males, whereas males injected with testosterone did not show any appreciable increase in EGT uptake. Lastly, male rats castrated by the age of 5 weeks, did not show any difference in EGT uptake in comparison to non-castrated males. Taken together, these results certainly support those seen in this current study, however they do not address how aging plays a role in EGT uptake over a lifespan. In the case of our aging study, it can safely be assumed that female mice will have undergone mouse menopause, while male mice will have experienced lowered testosterone levels in comparison to their peak adolescent and young adult years [142].

We've seen that aging affects EGT uptake, but it should also be noted that these hormonal changes also contribute to elevated hearing thresholds. In female mice, estrogen

plays an important role in cell protection in the inner ear as well as the optimal processing of neural sound information in the central auditory system. In males, much less is known about the intersection between testosterone, hearing, and aging. However, testosterone has been implicated in having protective effects against immune-mediated cochlear insults and is also known to provide neuroprotection and regeneration during development in the central nervous system [142]–[147]. Therefore, any disturbance in the protective effects or processing activities of these two sex hormones that happens during aging, will negatively affect hearing capabilities and also, likely impair EGT uptake in old age. In the case of females, assuming very little circulating estrogen and no testosterone production, it can be hypothesized that females may have lower amounts of EGT receptors in comparison to males, which may account for the inability to fully utilize the circulating EGT. Of course, future studies with younger sample groups may be able to mitigate some of these aging factors and provide a more direct understanding of the correlation between sex hormones and EGT effectiveness in protecting or improving hearing abilities.

Another item to consider is the impact that red blood cell (RBC) characteristics have on the transport of EGT throughout the body. RBCs are important carriers for oxygen to be delivered to tissues and organs throughout the body. However, since EGT's delivery system is primarily through its high affinity for RBCs, RBC health, variation with age, and sex differences then would play a major role in EGT distribution; since EGT binds highly with the Fe^{2+} found in the heme groups of hemoglobin [109]. EGT binds with Fe^{2+} at a rate of 2 EGT molecules to 1 of Fe^{2+} . In the human study performed by Zauber and Zauber, differences in both sexes were examined between very old subjects (>84 years old) and younger adult Control groups (30-50

years old). Interestingly, young female Controls when compared to young male Controls exhibited lower baseline numbers for RBC count, Hemoglobin, Hematocrit, Serum Iron, and Erythrocyte sedimentation rate, but roughly equivalent values for mean corpuscular volume, mean corpuscular hemoglobin, and mean corpuscular hemoglobin concentration. These results reveal interesting biological sex differences in RBC characteristics. When further comparing the very old population to the young Control groups for each sex, it is interesting to note that the old female group is only significantly different in two measures, Serum Iron, and Erythrocyte sedimentation rate. Males however had many significantly lower blood values, relative to the initial younger adult results, indicating changes due to aging [148]. Alis et al. confirms these age-related changes in red blood cells in both males and females. Specifically, increases in red blood cell distribution width (RDW) were significantly correlated with increasing age from <20 to 80+ years old. Their results additionally showed that the correlation was stronger in women than in men [149].

RBC mechanical properties also appear to be sex related, as pre-menopausal females exhibit better rheological properties than age-matched males. Curiously, these properties can be summarized by the age of RBCs *in vivo*, where RBCs have a lifespan of approx. 120 days. Males are found to have twice the amount of “old RBCs” compared to females, while females contain nearly twice the amount of “young RBCs”. Thus, due to monthly blood loss, pre-menopausal women contain a larger proportion of young RBCs which, in comparison to males, show increased deformability, lower mechanical fragility, and decreased aggregability. This in turn leads to a lower blood viscosity, since lower deformability and aggregability of RBCs allow for greater movement of blood within the vascular system, notably through microvasculature.

Here, RBCs need to be in balance with fragility and deformability so they do not rupture in small veins, capillaries, and arterioles before reaching their end targets: mitochondria. However, it was noted that post-menopausal females lose some of these mechanical advantages over age-matched males [150].

Further confirming the association of decline in RBC function with age, a mouse study employing C57BL/6Js from 6 to 32 weeks old as the animal model, observed similar changes in RBC characteristics such as reduce deformability, a decrease in mean height as measured by atomic force microscopy (AFM), and decreases in hemoglobin's ability to carry oxygen. These changes were found to occur due to changes in the lipid profile of RBCs as well as underlying changes in the morphology of hemoglobin [151]. In another mouse study using the same animal model, C57BL/6J, only male mice were used, and analyzed at the ages of 6 and 28 months. It was found that the old mice, while displaying anemia, also displayed key signs of aged RBCs, lower hemoglobin and erythrocyte counts, lower hematocrit, and lower serum iron and transferrin saturations. In spite of these changes, compensation factors, including erythropoietic activity and erythroid progenitors, were turned on but with no impact on anemia. Strikingly, testosterone supplementation in old mice increased splenic erythropoiesis while also returning serum iron and transferrin saturations back to baseline values found in young adult mice. Moreover, these changes allowed for greater iron availability for erythropoiesis as indicated by an increased reticulocyte hemoglobin ratio [152]. These results were corroborated in a similar study in older human males (~75 years of age) where testosterone supplementation increased the utilization of iron in erythropoiesis while also raising hematocrit and hemoglobin levels. [153]

Taken together these findings clearly indicate that age and sex are inextricably linked with RBC health and oxygen delivery. Thus by association, EGT is also inextricably linked to age, sex, and RBC health. Additionally, with the positive roles that testosterone plays in EGT uptake and RBC health in males, more investigation is required to find exact explanatory mechanisms of sex differences relating to the physiological findings in the current study. EGT has gained increased researchers' attention in the last decade or so since the discovery of its highly specific transporter (OCTN1). Additionally, the literature does exist which directly links EGT to RBC numbers and health. For example, the majority of available reports quantifies the EGT levels in RBCs and serum, along with antioxidant/anti-inflammatory effects on RBCs, and various cell types and disease states [69], [154]–[160].

Unfortunately, it appears that in-depth analysis which focuses on the interaction between RBC characteristics/morphology and EGT are lacking. Research to better understand EGT delivery by RBCs would be useful in optimizing future treatment paradigms as well as seeing the effect of EGT on RBC diseases. For example, in the erythrocyte disorder, sickle cell disease (SCD), hemoglobin (Hb) is replaced by sickle hemoglobin (HbS). A highly oxidative state is induced as compensatory mechanisms utilizing antioxidants and associated enzymes are unable to handle these stressors, resulting in inflammation, hemolytic anemia, etc. Interestingly, implicated in these antioxidant mechanisms are glutathione and EGT, where EGT is found to be the second most abundant thiol in RBCs [161]. Harnessing EGT's natural ability to bind with RBCs while understanding the underlying characteristics of RBCs could certainly prove to be an overall boon for future innovative treatments in disease models, including ARHL.

4.2 Underlying Mechanisms

We hypothesized that EGT would target key aging mechanisms such as increased apoptosis, inflammation, and oxidative stress, and declining mitochondrial health. Accordingly, biomarkers gene expression levels were measured with RT-PCR experiments: In Figure 4.1, we postulated that under the influence of EGT, a master regulator, peroxisome proliferator-activated receptor γ coactivator (PGC-1 α), would regulate multiple biological/cellular processes including the hypothesized targeted mechanisms. Therefore an increase in PGC-1 α , while being a useful marker for mitochondrial health and mitochondrial biogenesis, would then also influence the regulation of SOD2 (mitochondrial oxidative stress marker), TNF- α (inflammation biomarker), and Cas-3 (apoptotic biomarker) [162, p. 1], [163], [164].

Based on our results, elements of the proposed mechanism in Figure 4.1 were manifested in each tissue type in the cochlea – stria vascularis (SV), organ of Corti (OC) and modiolus (MD). In addition, it seems that EGT was not as preferential in its effectiveness at the mechanism level compared to the hearing measures, between the two sexes, as both male and female mice experienced some gene expression changes in all three tissues, but the overall distribution of these changes varied with tissue type. As previously mentioned for these samples, both LD and HD were combined for this analysis since LD and HD have changes in the same directions for the hearing tests and LC-MS/MS; these groups were labeled as treated.

In analyzing these results, it can be assumed that EGT is reaching the cochlea as all three tissues are showing significant changes in various biomarkers. To begin, males showed positive benefits from EGT treatment in RT-PCR biomarkers for a preferential pathway with a specific set of biomarkers. Here, males appeared to utilize EGT as mostly an antioxidant through the

upregulation of either/both SOD2 and PGC-1 α . In the SV tissue, SOD2 is significantly upregulated and both TNF- α and Cas-3 are significantly downregulated. In OC tissue, the only biomarker significantly upregulated is PGC-1 α , indicating that there is increased mitochondrial biogenesis occurring along with downstream regulation through PGC-1 α . Lastly, the MD tissue shows both SOD2 and PGC-1 α are significantly upregulated, indicating that EGT is targeting the mitochondria in this tissue type. Of note, male results revealing no changes in the inflammatory and apoptotic markers (TNF- α , Cas-3) does not support involvement of EGT treatments in modulating these pathways in MD.

Interestingly, females showed downregulation in TNF- α and Cas-3 in all three tissues, where SV was the only tissue with non-significant values, but similar downregulation as in other tissues. The SV tissue is also the only tissue where females showed a positive trend with any of the other biomarkers. The upregulation of SOD2 indicates that mitochondrial antioxidant systems have been activated. With that, EGT in females appears to be utilized to lower apoptosis and inflammation, two noted mechanisms of cochlear ARHL. Reconciling these results with those seen in the hearing measures (ABR/DPOAE) for females, one can see that even without positive results for hearing measures, the individual tissues of the cochlea still experienced some benefit from EGT treatments. This may indicate that in order to fully maximize the benefits of EGT, there must be a more effective therapeutic dose or timing, and larger elevations in whole blood EGT concentration needed to realize improvements in hearing. However, as shown by LC-MS/MS results, the carrying capacity of female whole blood is limited by the possible mechanisms outlined previously. In short, females did not reach the elevated whole blood EGT levels of males, whose hearing measures improved during treatment.

However, our biomarker analysis does provide clues as to some of the mechanisms occurring within the inner ear following EGT treatment, where further studies are needed to decipher the detailed molecular mechanisms, and optimize levels and timing of therapeutic doses.

Lastly, it should be noted that these RT-PCR results from the three tissue types are intimately tied to the density of OCTN1 in that area. For example, OC tissue which had the least amount of therapeutic effects would also then most likely have the lowest level of OCTN1 expression, the receptor responsible for transporting EGT across the cell's membrane.

Interestingly, OCTN1 results confirm this type of association as seen in Figure 4.2. Figure 4.2 indicates that expression in old control samples is greatest in the SV of the inner ear, lowest in the OC, and MD expression levels are intermediate. These findings are consistent with current literature [165]. In comparing these results to the gene expression levels and metabolic activity from each tissue: OC tissue has a lower amount of OCTN1, lower metabolic activity overall, and thus did not utilize EGT in the same way as the other tissues [166]; SV tissue, which is highly metabolic [167] and thus quite susceptible to oxidative stress and inflammation, which in turn leads to mitochondrial damage, is likely to need more EGT and thus would benefit from higher EGT receptor expression levels. MD tissue also displays relatively high metabolic activity and thus contains more OCTN1 receptors than OC tissue, but less than SV [168].

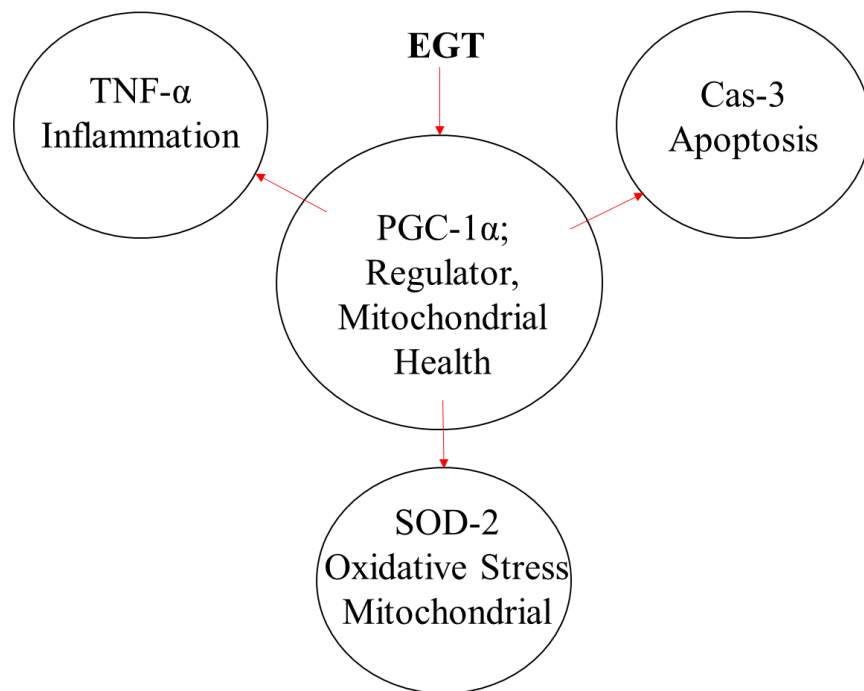


Figure 4.1: Conceptual Model of EGT Therapy. PGC-1 α , a mitochondrial biogenesis biomarker also regulates multiple mechanisms used in aging, inflammation, apoptosis, and oxidative stress.

OCTN1 Expression in Control SV, OC, MD Tissue

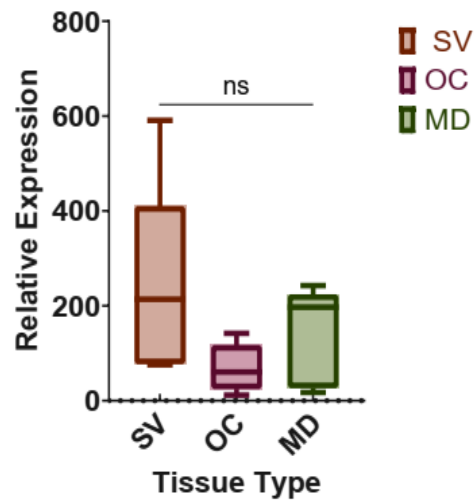


Figure 4.2: OCTN1 Relative Expression in Three Different Tissue Types. SV, n=6; OC, n=5; MD, n=5; Combined Male and Female Data (Old Control Only). Values denoted as means \pm SEM.

Chapter 5: Conclusion

Overall, for the first time, we demonstrated the therapeutic potential of EGT in treating certain key aspects of ARHL, a top communication deficit and neurodegenerative disorder of our aging population. Treatment has greater benefits for male mice as compared to females, however, further investigations are required to find out the underlying molecular mechanisms for this sex difference. Given the exciting results here, EGT's prior approval by the FDA as a dietary supplement, and emerging literature describing EGT's therapeutic roles in other diseases, including aging disorders such as cognitive deficits and declines, cardiovascular problems, life span, frailty, neurological disorders, etc.; indicates that EGT could be a potential ingredient in future drug combinations and hybrid therapies for hearing loss and other neurological conditions.

References

- [1] C. A. Pittman, R. Roura, C. Price, F. R. Lin, N. Marrone, and C. L. Nieman, "Racial/Ethnic and Sex Representation in US-Based Clinical Trials of Hearing Loss Management in Adults: A Systematic Review," *JAMA Otolaryngol Head Neck Surg*, vol. 147, no. 7, pp. 656–662, Jul. 2021, doi: 10.1001/jamaoto.2021.0550.
- [2] Q. Huang and J. Tang, "Age-related hearing loss or presbycusis," *Eur Arch Otorhinolaryngol*, vol. 267, no. 8, pp. 1179–1191, Aug. 2010, doi: 10.1007/s00405-010-1270-7.
- [3] J. T. Pacala and B. Yueh, "Hearing Deficits in the Older Patient: 'I Didn't Notice Anything,'" *JAMA*, vol. 307, no. 11, pp. 1185–1194, Mar. 2012, doi: 10.1001/jama.2012.305.
- [4] B. Gopinath *et al.*, "Hearing handicap, rather than measured hearing impairment, predicts poorer quality of life over 10 years in older adults," *Maturitas*, vol. 72, no. 2, pp. 146–151, Jun. 2012, doi: 10.1016/j.maturitas.2012.03.010.
- [5] D. R. Frisina and R. D. Frisina, "Speech recognition in noise and presbycusis: relations to possible neural mechanisms," *Hear Res*, vol. 106, no. 1–2, pp. 95–104, Apr. 1997, doi: 10.1016/s0378-5955(97)00006-3.
- [6] D. S. Dalton, K. J. Cruickshanks, B. E. K. Klein, R. Klein, T. L. Wiley, and D. M. Nondahl, "The Impact of Hearing Loss on Quality of Life in Older Adults," *The Gerontologist*, vol. 43, no. 5, pp. 661–668, Oct. 2003, doi: 10.1093/geront/43.5.661.
- [7] A. R. Fetoni, P. M. Picciotti, G. Paludetti, and D. Troiani, "Pathogenesis of presbycusis in animal models: A review," *Experimental Gerontology*, vol. 46, no. 6, Art. no. 6, Jun. 2011, doi: 10.1016/j.exger.2010.12.003.
- [8] K. K. Ohlemiller and R. D. Frisina, "Age-Related Hearing Loss and Its Cellular and Molecular Bases," in *Auditory Trauma, Protection, and Repair*, J. Schacht, A. N. Popper, and R. R. Fay, Eds. Boston, MA: Springer US, 2008, pp. 145–194. doi: 10.1007/978-0-387-72561-1_6.
- [9] G. A. Gates and J. H. Mills, "Presbycusis," *Lancet*, vol. 366, no. 9491, pp. 1111–1120, Sep. 2005, doi: 10.1016/S0140-6736(05)67423-5.

- [10] K. J. Grant *et al.*, “Predicting neural deficits in sensorineural hearing loss from word recognition scores,” *Sci Rep*, vol. 12, no. 1, Art. no. 1, Jun. 2022, doi: 10.1038/s41598-022-13023-5.
- [11] K. K. Ohlemiller and R. D. Frisina, “Age-Related Hearing Loss and Its Cellular and Molecular Bases,” in *Auditory Trauma, Protection, and Repair*, J. Schacht, A. N. Popper, and R. R. Fay, Eds. Boston, MA: Springer US, 2008, pp. 145–194. doi: 10.1007/978-0-387-72561-1_6.
- [12] S. E. Kramer, T. S. Kapteyn, D. J. Kuik, and D. J. H. Deeg, “The association of hearing impairment and chronic diseases with psychosocial health status in older age,” *J Aging Health*, vol. 14, no. 1, pp. 122–137, Feb. 2002, doi: 10.1177/089826430201400107.
- [13] K. Parham, B. J. McKinnon, D. Eibling, and G. A. Gates, “Challenges and opportunities in presbycusis,” *Otolaryngol Head Neck Surg*, vol. 144, no. 4, pp. 491–495, Apr. 2011, doi: 10.1177/0194599810395079.
- [14] A. Shukla *et al.*, “Hearing Loss, Loneliness, and Social Isolation: A Systematic Review,” *Otolaryngol Head Neck Surg*, vol. 162, no. 5, pp. 622–633, May 2020, doi: 10.1177/0194599820910377.
- [15] F. R. Lin, L. Ferrucci, E. J. Metter, Y. An, A. B. Zonderman, and S. M. Resnick, “Hearing loss and cognition in the Baltimore Longitudinal Study of Aging,” *Neuropsychology*, vol. 25, no. 6, pp. 763–770, Nov. 2011, doi: 10.1037/a0024238.
- [16] X. Z. Liu and D. Yan, “Ageing and hearing loss,” *J Pathol*, vol. 211, no. 2, pp. 188–197, Jan. 2007, doi: 10.1002/path.2102.
- [17] G. Livingston *et al.*, “Dementia prevention, intervention, and care: 2020 report of the Lancet Commission,” *Lancet*, vol. 396, no. 10248, pp. 413–446, 2020, doi: 10.1016/S0140-6736(20)30367-6.
- [18] E. C. Landry *et al.*, “Early Health Economic Modeling of Novel Therapeutics in Age-Related Hearing Loss,” *Frontiers in Neuroscience*, vol. 16, 2022, Accessed: Apr. 16, 2022. [Online]. Available: <https://www.frontiersin.org/article/10.3389/fnins.2022.769983>
- [19] D. McDaid, A.-L. Park, and S. Chadha, “Estimating the global costs of hearing loss,” *International Journal of Audiology*, vol. 60, no. 3, pp. 162–170, Mar. 2021, doi: 10.1080/14992027.2021.1883197.
- [20] D. C. Peterson, V. Reddy, and R. N. Hamel, “Neuroanatomy, Auditory Pathway,” in *StatPearls*, Treasure Island (FL): StatPearls Publishing, 2022. Accessed: May 27, 2022. [Online]. Available: <http://www.ncbi.nlm.nih.gov/books/NBK532311/>

- [21] W. A. Yost and R. S. Schlauch, "Fundamentals of Hearing: An Introduction (4th edition)," *The Journal of the Acoustical Society of America*, vol. 110, no. 4, Oct. 2001, doi: 10.1121/1.1398047.
- [22] H. Liu *et al.*, "Organ of Corti and Stria Vascularis: Is there an Interdependence for Survival?," *PLoS One*, vol. 11, no. 12, p. e0168953, Dec. 2016, doi: 10.1371/journal.pone.0168953.
- [23] H. F. Schuknecht and M. R. Gacek, "Cochlear pathology in presbycusis," *Ann Otol Rhinol Laryngol*, vol. 102, no. 1 Pt 2, pp. 1–16, Jan. 1993, doi: 10.1177/00034894931020S101.
- [24] K.-Y. Lee, "Pathophysiology of Age-Related Hearing Loss (Peripheral and Central)," *Korean J Audiol*, vol. 17, no. 2, pp. 45–49, Sep. 2013, doi: 10.7874/kja.2013.17.2.45.
- [25] S. N. Merchant and J. B. Nadol, *Schuknecht's Pathology of the Ear*. PMPH-USA, 2010.
- [26] T. H. Chisolm, J. F. Willott, and J. J. Lister, "The aging auditory system: anatomic and physiologic changes and implications for rehabilitation," *Int J Audiol*, vol. 42 Suppl 2, pp. 2S3-10, Jul. 2003.
- [27] P. Melgar-Rojas, J. Alvarador, V. Fuentes-Santamaria, and J. Juiz, "Cellular Mechanisms of Age-Related Hearing Loss | SpringerLink," 2015. https://link.springer.com/chapter/10.1007/978-3-319-13473-4_15 (accessed Oct. 15, 2020).
- [28] J. Otte, H. F. Schunknecht, and A. G. Kerr, "Ganglion cell populations in normal and pathological human cochleae. Implications for cochlear implantation," *Laryngoscope*, vol. 88, no. 8 Pt 1, pp. 1231–1246, Aug. 1978, doi: 10.1288/00005537-197808000-00004.
- [29] C. A. Makary, J. Shin, S. G. Kujawa, M. C. Liberman, and S. N. Merchant, "Age-related primary cochlear neuronal degeneration in human temporal bones," *J Assoc Res Otolaryngol*, vol. 12, no. 6, pp. 711–717, Dec. 2011, doi: 10.1007/s10162-011-0283-2.
- [30] M. Pauler, H. F. Schuknecht, and A. R. Thornton, "Correlative studies of cochlear neuronal loss with speech discrimination and pure-tone thresholds," *Arch Otorhinolaryngol*, vol. 243, no. 3, pp. 200–206, 1986, doi: 10.1007/BF00470622.
- [31] K. K. Ohlemiller, J. M. Lett, and P. M. Gagnon, "Cellular correlates of age-related endocochlear potential reduction in a mouse model," *Hear Res*, vol. 220, no. 1–2, pp. 10–26, Oct. 2006, doi: 10.1016/j.heares.2006.06.012.

- [32] D. M. Mills and R. A. Schmiedt, "Metabolic presbycusis: differential changes in auditory brainstem and otoacoustic emission responses with chronic furosemide application in the gerbil," *J Assoc Res Otolaryngol*, vol. 5, no. 1, pp. 1–10, Mar. 2004, doi: 10.1007/s10162-003-4004-3.
- [33] M. Pauler, H. F. Schuknecht, and J. A. White, "Atrophy of the stria vascularis as a cause of sensorineural hearing loss," *Laryngoscope*, vol. 98, no. 7, pp. 754–759, Jul. 1988, doi: 10.1288/00005537-198807000-00014.
- [34] R. D. Frisina and J. P. Walton, "Age-related structural and functional changes in the cochlear nucleus," *Hear Res*, vol. 216–217, pp. 216–223, Jul. 2006, doi: 10.1016/j.heares.2006.02.003.
- [35] H. L. Seldon and G. M. Clark, "Human cochlear nucleus: comparison of Nissl-stained neurons from deaf and hearing patients," *Brain Res*, vol. 551, no. 1–2, pp. 185–194, Jun. 1991, doi: 10.1016/0006-8993(91)90932-l.
- [36] Y. Wang and P. B. Manis, "Synaptic transmission at the cochlear nucleus endbulb synapse during age-related hearing loss in mice," *J Neurophysiol*, vol. 94, no. 3, pp. 1814–1824, Sep. 2005, doi: 10.1152/jn.00374.2005.
- [37] G. I. Varghese, X. Zhu, and R. D. Frisina, "Age-related declines in distortion product otoacoustic emissions utilizing pure tone contralateral stimulation in CBA/CaJ mice," *Hear Res*, vol. 209, no. 1–2, pp. 60–67, Nov. 2005, doi: 10.1016/j.heares.2005.06.006.
- [38] M. Jacobson, S. Kim, J. Romney, X. Zhu, and R. D. Frisina, "Contralateral suppression of distortion-product otoacoustic emissions declines with age: a comparison of findings in CBA mice with human listeners," *Laryngoscope*, vol. 113, no. 10, pp. 1707–1713, Oct. 2003, doi: 10.1097/00005537-200310000-00009.
- [39] X. Zhu *et al.*, "Auditory efferent feedback system deficits precede age-related hearing loss: contralateral suppression of otoacoustic emissions in mice," *J Comp Neurol*, vol. 503, no. 5, pp. 593–604, Aug. 2007, doi: 10.1002/cne.21402.
- [40] S. Kim, D. R. Frisina, and R. D. Frisina, "Effects of age on contralateral suppression of distortion product otoacoustic emissions in human listeners with normal hearing," *Audiol Neurootol*, vol. 7, no. 6, pp. 348–357, Dec. 2002, doi: 10.1159/000066159.
- [41] C. Abdala and L. Visser-Dumont, "Distortion Product Otoacoustic Emissions: A Tool for Hearing Assessment and Scientific Study," *Volta Rev*, vol. 103, no. 4, pp. 281–302, 2001.
- [42] R. Frisina and X. Zhu, "Auditory sensitivity and the outer hair cell system in the CBA mouse model of age-related hearing loss," *Open access animal physiology*, vol. 2, pp. 9–16, Jun. 2010, doi: 10.2147/OAAP.S7202.

- [43] V. Ashok Murthy and G. Kirthi Kalyan, "Effects of Ageing on Otoacoustic Emission," *Indian J Otolaryngol Head Neck Surg*, vol. 65, no. Suppl 3, pp. 477–479, Dec. 2013, doi: 10.1007/s12070-011-0349-9.
- [44] L. Xie *et al.*, "The characterization of auditory brainstem response (ABR) waveforms: A study in tree shrews (*Tupaia belangeri*)," *J Otol*, vol. 13, no. 3, pp. 85–91, Sep. 2018, doi: 10.1016/j.joto.2018.05.004.
- [45] J. J. Eggermont and P. H. Schmidt, "The auditory brainstem response," in *Evoked Potential Manual: A Practical Guide to Clinical Applications*, E. J. Colon and S. L. Visser, Eds. Dordrecht: Springer Netherlands, 1990, pp. 41–77. doi: 10.1007/978-94-009-2059-0_2.
- [46] K. K. Ohlemiller, "Mouse methods and models for studies in hearing," *The Journal of the Acoustical Society of America*, vol. 146, no. 5, pp. 3668–3680, Nov. 2019, doi: 10.1121/1.5132550.
- [47] J. O. Pickles, "Mutation in Mitochondrial DNA as a Cause of Presbycusis," *AUD*, vol. 9, no. 1, pp. 23–33, 2004, doi: 10.1159/000074184.
- [48] M. F. Alexeyev, "Is there more to aging than mitochondrial DNA and reactive oxygen species?," *The FEBS Journal*, vol. 276, no. 20, pp. 5768–5787, 2009, doi: 10.1111/j.1742-4658.2009.07269.x.
- [49] C. Franceschi, P. Garagnani, P. Parini, C. Giuliani, and A. Santoro, "Inflammaging: a new immune–metabolic viewpoint for age-related diseases," *Nature Reviews Endocrinology*, vol. 14, no. 10, Art. no. 10, Oct. 2018, doi: 10.1038/s41574-018-0059-4.
- [50] N. Watson, B. Ding, X. Zhu, and R. D. Frisina, "Chronic inflammation - inflammaging - in the ageing cochlea: A novel target for future presbycusis therapy," *Ageing Res Rev*, vol. 40, pp. 142–148, Nov. 2017, doi: 10.1016/j.arr.2017.10.002.
- [51] C. Franceschi and J. Campisi, "Chronic Inflammation (Inflammaging) and Its Potential Contribution to Age-Associated Diseases," *The Journals of Gerontology: Series A*, vol. 69, no. Suppl_1, pp. S4–S9, Jun. 2014, doi: 10.1093/gerona/glu057.
- [52] M. Fujioka, H. Okano, and K. Ogawa, "Inflammatory and immune responses in the cochlea: potential therapeutic targets for sensorineural hearing loss," *Frontiers in Pharmacology*, vol. 5, 2014, Accessed: Jun. 03, 2022. [Online]. Available: <https://www.frontiersin.org/article/10.3389/fphar.2014.00287>
- [53] C. Verschuur, "'INFLAMMAGING' AND ITS MANAGEMENT IN PRESBYCUSIS," *J Hear Sci*, vol. 2, no. 4, pp. 46–48, Dec. 2012.

- [54] C. Verschuur, A. Agyemang-Prempeh, and T. A. Newman, "Inflammation is associated with a worsening of presbycusis: Evidence from the MRC national study of hearing," *International Journal of Audiology*, vol. 53, no. 7, pp. 469–475, Jul. 2014, doi: 10.3109/14992027.2014.891057.
- [55] M. Fujioka, S. Kanzaki, H. J. Okano, M. Masuda, K. Ogawa, and H. Okano, "Proinflammatory cytokines expression in noise-induced damaged cochlea," *Journal of Neuroscience Research*, vol. 83, no. 4, pp. 575–583, 2006, doi: 10.1002/jnr.20764.
- [56] V. Lobo, A. Patil, A. Phatak, and N. Chandra, "Free radicals, antioxidants and functional foods: Impact on human health," *Pharmacogn Rev*, vol. 4, no. 8, pp. 118–126, 2010, doi: 10.4103/0973-7847.70902.
- [57] A. Glasauer and N. S. Chandel, "ROS," *Curr Biol*, vol. 23, no. 3, pp. R100-102, Feb. 2013, doi: 10.1016/j.cub.2012.12.011.
- [58] H.-C. Lee and Y.-H. Wei, "Mitochondria and aging," *Adv Exp Med Biol*, vol. 942, pp. 311–327, 2012, doi: 10.1007/978-94-007-2869-1_14.
- [59] R. S. Balaban, S. Nemoto, and T. Finkel, "Mitochondria, oxidants, and aging," *Cell*, vol. 120, no. 4, pp. 483–495, Feb. 2005, doi: 10.1016/j.cell.2005.02.001.
- [60] A. J. Kowaltowski, N. C. de Souza-Pinto, R. F. Castilho, and A. E. Vercesi, "Mitochondria and reactive oxygen species," *Free Radic Biol Med*, vol. 47, no. 4, pp. 333–343, Aug. 2009, doi: 10.1016/j.freeradbiomed.2009.05.004.
- [61] M. D. Brand, "The sites and topology of mitochondrial superoxide production," *Exp Gerontol*, vol. 45, no. 7–8, pp. 466–472, Aug. 2010, doi: 10.1016/j.exger.2010.01.003.
- [62] M. D. Seidman, "Effects of dietary restriction and antioxidants on presbycusis," *Laryngoscope*, vol. 110, no. 5 Pt 1, pp. 727–738, May 2000, doi: 10.1097/00005537-200005000-00003.
- [63] M. D. Seidman, M. J. Khan, W. X. Tang, and W. S. Quirk, "Influence of lecithin on mitochondrial DNA and age-related hearing loss," *Otolaryngol Head Neck Surg*, vol. 127, no. 3, pp. 138–144, Sep. 2002, doi: 10.1067/mhn.2002.127627.
- [64] S. E. Heman-Ackah, S. K. Juhn, T. C. Huang, and T. S. Wiedmann, "A combination antioxidant therapy prevents age-related hearing loss in C57BL/6 mice," *Otolaryngol Head Neck Surg*, vol. 143, no. 3, pp. 429–434, Sep. 2010, doi: 10.1016/j.otohns.2010.04.266.

- [65] S. Someya *et al.*, "Age-related hearing loss in C57BL/6J mice is mediated by Bak-dependent mitochondrial apoptosis," *Proc Natl Acad Sci U S A*, vol. 106, no. 46, pp. 19432–19437, Nov. 2009, doi: 10.1073/pnas.0908786106.
- [66] E. C. Bielefeld, D. Coling, G.-D. Chen, and D. Henderson, "Multiple dosing strategies with acetyl L-carnitine (ALCAR) fail to alter age-related hearing loss in the Fischer 344/NHsd rat," *J Negat Results Biomed*, vol. 7, p. 4, Jul. 2008, doi: 10.1186/1477-5751-7-4.
- [67] S.-H. Sha, A. Kanicki, K. Halsey, K. A. Wearne, and J. Schacht, "Antioxidant-enriched diet does not delay the progression of age-related hearing loss," *Neurobiology of Aging*, vol. 33, no. 5, p. 1010.e15-1010.e16, May 2012, doi: 10.1016/j.neurobiolaging.2011.10.023.
- [68] I. K. Cheah and B. Halliwell, "Ergothioneine; antioxidant potential, physiological function and role in disease," *Biochimica et Biophysica Acta (BBA) - Molecular Basis of Disease*, vol. 1822, no. 5, pp. 784–793, May 2012, doi: 10.1016/j.bbadis.2011.09.017.
- [69] I. K. Cheah and B. Halliwell, "Ergothioneine, recent developments," *Redox Biol*, vol. 42, p. 101868, Jun. 2021, doi: 10.1016/j.redox.2021.101868.
- [70] P. A. Marone, J. Trampota, and S. Weisman, "A Safety Evaluation of a Nature-Identical L-Ergothioneine in Sprague Dawley Rats," *Int J Toxicol*, vol. 35, no. 5, pp. 568–583, Sep. 2016, doi: 10.1177/1091581816653375.
- [71] R. M. Y. Tang, I. K.-M. Cheah, T. S. K. Yew, and B. Halliwell, "Distribution and accumulation of dietary ergothioneine and its metabolites in mouse tissues," *Scientific Reports*, vol. 8, no. 1, Art. no. 1, Jan. 2018, doi: 10.1038/s41598-018-20021-z.
- [72] A. Dare, M. L. Channa, and A. Nadar, "L-ergothioneine; a potential adjuvant in the management of diabetic nephropathy," *Pharmacological Research - Modern Chinese Medicine*, vol. 2, p. 100033, Mar. 2022, doi: 10.1016/j.prmcm.2021.100033.
- [73] D. R. Frisina, "The Aging Cochlea," in *The Senses: A Comprehensive Reference - 2nd Edition*, Seond., Elsevier:Oxford, 2020, pp. 871–883. Accessed: Mar. 31, 2022. [Online]. Available: <https://www.elsevier.com/books/the-senses-a-comprehensive-reference/fritzs/978-0-12-805408-6>
- [74] G. A. Gates and J. C. Cooper, "Incidence of hearing decline in the elderly," *Acta Otolaryngol*, vol. 111, no. 2, pp. 240–248, 1991, doi: 10.3109/00016489109137382.
- [75] A. Howarth and G. R. Shone, "Ageing and the auditory system," *Postgrad Med J*, vol. 82, no. 965, pp. 166–171, Mar. 2006, doi: 10.1136/pgmj.2005.039388.

- [76] J. F. Willott, "Anatomic and physiologic aging: a behavioral neuroscience perspective," *J Am Acad Audiol*, vol. 7, no. 3, pp. 141–151, Jun. 1996.
- [77] J. Wang and J.-L. Puel, "Presbycusis: An Update on Cochlear Mechanisms and Therapies," *J Clin Med*, vol. 9, no. 1, p. E218, Jan. 2020, doi: 10.3390/jcm9010218.
- [78] T. Yamasoba, F. R. Lin, S. Someya, A. Kashio, T. Sakamoto, and K. Kondo, "Current concepts in age-related hearing loss: epidemiology and mechanistic pathways," *Hear Res*, vol. 303, pp. 30–38, Sep. 2013, doi: 10.1016/j.heares.2013.01.021.
- [79] P. Bazard *et al.*, "Cochlear Inflammaging in Relation to Ion Channels and Mitochondrial Functions," *Cells*, vol. 10, no. 10, p. 2761, Oct. 2021, doi: 10.3390/cells10102761.
- [80] N. Watson, B. Ding, X. Zhu, and R. D. Frisina, "Chronic inflammation - inflammaging - in the ageing cochlea: A novel target for future presbycusis therapy," *Ageing Res Rev*, vol. 40, pp. 142–148, Nov. 2017, doi: 10.1016/j.arr.2017.10.002.
- [81] E. M. Keithley, "Pathology and mechanisms of cochlear aging," *J Neurosci Res*, vol. 98, no. 9, pp. 1674–1684, Sep. 2020, doi: 10.1002/jnr.24439.
- [82] A. G. Cheng, L. L. Cunningham, and E. W. Rubel, "Mechanisms of hair cell death and protection," *Curr Opin Otolaryngol Head Neck Surg*, vol. 13, no. 6, pp. 343–348, Dec. 2005, doi: 10.1097/01.moo.0000186799.45377.63.
- [83] K. R. Martin, "The bioactive agent ergothioneine, a key component of dietary mushrooms, inhibits monocyte binding to endothelial cells characteristic of early cardiovascular disease," *J Med Food*, vol. 13, no. 6, pp. 1340–1346, Dec. 2010, doi: 10.1089/jmf.2009.0194.
- [84] I. Laurenza, R. Colognato, L. Migliore, S. Del Prato, and L. Benzi, "Modulation of palmitic acid-induced cell death by ergothioneine: evidence of an anti-inflammatory action," *Biofactors*, vol. 33, no. 4, pp. 237–247, 2008, doi: 10.1002/biof.5520330401.
- [85] J.-P. Bastard *et al.*, "Adipose tissue IL-6 content correlates with resistance to insulin activation of glucose uptake both in vivo and in vitro," *J Clin Endocrinol Metab*, vol. 87, no. 5, pp. 2084–2089, May 2002, doi: 10.1210/jcem.87.5.8450.
- [86] A. D. Pradhan, J. E. Manson, N. Rifai, J. E. Buring, and P. M. Ridker, "C-Reactive Protein, Interleukin 6, and Risk of Developing Type 2 Diabetes Mellitus," *JAMA*, vol. 286, no. 3, pp. 327–334, Jul. 2001, doi: 10.1001/jama.286.3.327.

- [87] I. K. Cheah, R. M. Y. Tang, T. S. Z. Yew, K. H. C. Lim, and B. Halliwell, "Administration of Pure Ergothioneine to Healthy Human Subjects: Uptake, Metabolism, and Effects on Biomarkers of Oxidative Damage and Inflammation," *Antioxid Redox Signal*, vol. 26, no. 5, pp. 193–206, 10 2017, doi: 10.1089/ars.2016.6778.
- [88] J. Y. Jang, A. Blum, J. Liu, and T. Finkel, "The role of mitochondria in aging," *J Clin Invest*, vol. 128, no. 9, Art. no. 9, Apr. 2021, doi: 10.1172/JCI120842.
- [89] C. Jara, A. K. Torres, M. A. Olesen, and C. Tapia-Rojas, "Mitochondrial Dysfunction as a Key Event during Aging: From Synaptic Failure to Memory Loss," *Mitochondria and Brain Disorders*, Aug. 2019, doi: 10.5772/intechopen.88445.
- [90] M. Strickland, B. Yacoubi-Loueslati, B. Bouhaouala-Zahar, S. L. F. Pender, and A. Larbi, "Relationships Between Ion Channels, Mitochondrial Functions and Inflammation in Human Aging," *Front Physiol*, vol. 10, Mar. 2019, doi: 10.3389/fphys.2019.00158.
- [91] A.-M. Lamhonwah and I. Tein, "Novel localization of OCTN1, an organic cation/carnitine transporter, to mammalian mitochondria," *Biochem Biophys Res Commun*, vol. 345, no. 4, pp. 1315–1325, Jul. 2006, doi: 10.1016/j.bbrc.2006.05.026.
- [92] H. Kawano, M. Otani, K. Takeyama, Y. Kawai, T. Mayumi, and T. Hama, "Studies on ergothioneine. VI. Distribution and fluctuations of ergothioneine in rats," *Chem Pharm Bull (Tokyo)*, vol. 30, no. 5, pp. 1760–1765, May 1982, doi: 10.1248/cpb.30.1760.
- [93] B. D. Paul and S. H. Snyder, "The unusual amino acid L-ergothioneine is a physiologic cytoprotectant," *Cell Death & Differentiation*, vol. 17, no. 7, Art. no. 7, Jul. 2010, doi: 10.1038/cdd.2009.163.
- [94] T. T. Williamson et al., "Inflammatory Cytokines are Associated with Aging Process in the Cochlea," presented at the Association for Research in Otolaryngology., San Diego, CA., 2018.
- [95] B. Ding, et al., "Detection of Mitochondrial DNA Mutations in the SV-K1 Cell Line and the Cochlea of CBA/CaJ Mice," presented at the Association for Research in Otolaryngology., Virtual, 2022.
- [96] J. Menardo et al., "Oxidative stress, inflammation, and autophagic stress as the key mechanisms of premature age-related hearing loss in SAMP8 mouse Cochlea," *Antioxid Redox Signal*, vol. 16, no. 3, pp. 263–274, Feb. 2012, doi: 10.1089/ars.2011.4037.
- [97] H. P. Misra, "Generation of Superoxide Free Radical during the Autoxidation of Thiols," *Journal of Biological Chemistry*, vol. 249, no. 7, pp. 2151–2155, Apr. 1974, doi: 10.1016/S0021-9258(19)42810-X.

- [98] C. Avendaño and J. C. Menéndez, "Chapter 15 - Cancer Chemoprevention," in *Medicinal Chemistry of Anticancer Drugs (Second Edition)*, C. Avendaño and J. C. Menéndez, Eds. Boston: Elsevier, 2015, pp. 712–713. doi: 10.1016/B978-0-444-62649-3.00015-6.
- [99] H. J. Forman, H. Zhang, and A. Rinna, "Glutathione: Overview of its protective roles, measurement, and biosynthesis," *Mol Aspects Med*, vol. 30, no. 1–2, pp. 1–12, 2009, doi: 10.1016/j.mam.2008.08.006.
- [100] J. Ey, E. Schömig, and D. Taubert, "Dietary sources and antioxidant effects of ergothioneine," *J Agric Food Chem*, vol. 55, no. 16, pp. 6466–6474, Aug. 2007, doi: 10.1021/jf071328f.
- [101] D. Gründemann *et al.*, "Discovery of the ergothioneine transporter," *PNAS*, vol. 102, no. 14, pp. 5256–5261, Apr. 2005, doi: 10.1073/pnas.0408624102.
- [102] M. Ben Said *et al.*, "A mutation in SLC22A4 encoding an organic cation transporter expressed in the cochlea stria endothelium causes human recessive non-syndromic hearing loss DFNB60," *Hum Genet*, vol. 135, no. 5, pp. 513–524, May 2016, doi: 10.1007/s00439-016-1657-7.
- [103] R. W. S. Li *et al.*, "Uptake and protective effects of ergothioneine in human endothelial cells," *J Pharmacol Exp Ther*, vol. 350, no. 3, pp. 691–700, Sep. 2014, doi: 10.1124/jpet.114.214049.
- [104] T. Nakamura *et al.*, "Decreased proliferation and erythroid differentiation of K562 cells by siRNA-induced depression of OCTN1 (SLC22A4) transporter gene," *Pharm Res*, vol. 24, no. 9, pp. 1628–1635, Sep. 2007, doi: 10.1007/s11095-007-9290-8.
- [105] D. Taubert, G. Grimberg, N. Jung, A. Rubbert, and E. Schömig, "Functional role of the 503F variant of the organic cation transporter OCTN1 in Crohn's disease," *Gut*, vol. 54, no. 10, pp. 1505–1506, Oct. 2005, doi: 10.1136/gut.2005.076083.
- [106] T. Nakamura, K. Yoshida, H. Yabuuchi, T. Maeda, and I. Tamai, "Functional characterization of ergothioneine transport by rat organic cation/carnitine transporter Octn1 (slc22a4)," *Biol Pharm Bull*, vol. 31, no. 8, pp. 1580–1584, Aug. 2008, doi: 10.1248/bpb.31.1580.
- [107] B. Halliwell, I. K. Cheah, and C. L. Drum, "Ergothioneine, an adaptive antioxidant for the protection of injured tissues? A hypothesis," *Biochem Biophys Res Commun*, vol. 470, no. 2, pp. 245–250, Feb. 2016, doi: 10.1016/j.bbrc.2015.12.124.
- [108] D. P. Hanlon, "Interaction of ergothioneine with metal ions and metalloenzymes," *J. Med. Chem.*, vol. 14, no. 11, pp. 1084–1087, Nov. 1971, doi: 10.1021/jm00293a017.

- [109] N. Motohashi, I. Mori, Y. Sugiura, and H. Tanaka, "Metal Complexes of Ergothioneine," *Chemical & Pharmaceutical Bulletin*, vol. 22, no. 3, pp. 654–657, 1974, doi: 10.1248/cpb.22.654.
- [110] N. Motohashi, I. Mori, and Y. Sugiura, "Complexing of Copper Ion by Ergothioneine," *Chemical & Pharmaceutical Bulletin*, vol. 24, no. 10, pp. 2364–2368, 1976, doi: 10.1248/cpb.24.2364.
- [111] D. B. Melville, "Ergothioneine," in *Vitamins & Hormones*, vol. 17, R. S. Harris, G. F. Marrian, and K. V. Thimann, Eds. Academic Press, 1959, pp. 155–204. doi: 10.1016/S0083-6729(08)60271-X.
- [112] R. S. Fraser, "Blood ergothioneine levels in disease," *J Lab Clin Med*, vol. 37, no. 2, pp. 199–206, Feb. 1951.
- [113] EFSA Panel on Dietetic Products, Nutrition and Allergies (NDA) *et al.*, "Safety of synthetic l-ergothioneine (Ergoneine®) as a novel food pursuant to Regulation (EC) No 258/97," *EFSA Journal*, vol. 14, no. 11, p. e04629, 2016, doi: 10.2903/j.efsa.2016.4629.
- [114] I. K. Cheah, L. Feng, R. M. Y. Tang, K. H. C. Lim, and B. Halliwell, "Ergothioneine levels in an elderly population decrease with age and incidence of cognitive decline; a risk factor for neurodegeneration?," *Biochem Biophys Res Commun*, vol. 478, no. 1, pp. 162–167, Sep. 2016, doi: 10.1016/j.bbrc.2016.07.074.
- [115] E. Smith *et al.*, "Ergothioneine is associated with reduced mortality and decreased risk of cardiovascular disease," *Heart*, vol. 106, no. 9, pp. 691–697, May 2020, doi: 10.1136/heartjnl-2019-315485.
- [116] T. Hatano, S. Saiki, A. Okuzumi, R. P. Mohny, and N. Hattori, "Identification of novel biomarkers for Parkinson's disease by metabolomic technologies," *J Neurol Neurosurg Psychiatry*, vol. 87, no. 3, pp. 295–301, Mar. 2016, doi: 10.1136/jnnp-2014-309676.
- [117] S. Zhang *et al.*, "Mushroom consumption and incident risk of prostate cancer in Japan: A pooled analysis of the Miyagi Cohort Study and the Ohsaki Cohort Study," *Int J Cancer*, vol. 146, no. 10, pp. 2712–2720, May 2020, doi: 10.1002/ijc.32591.
- [118] A. Shin *et al.*, "Dietary mushroom intake and the risk of breast cancer based on hormone receptor status," *Nutr Cancer*, vol. 62, no. 4, pp. 476–483, 2010, doi: 10.1080/01635580903441212.
- [119] EFSA Panel on Dietetic Products, Nutrition and Allergies (NDA) *et al.*, "Statement on the safety of synthetic l-ergothioneine as a novel food – supplementary dietary exposure and safety assessment for infants and young children, pregnant and breastfeeding women," *EFSA Journal*, vol. 15, no. 11, p. e05060, 2017, doi: 10.2903/j.efsa.2017.5060.

- [120] National University Hospital, Singapore, “Investigating the Efficacy of Ergothioneine to Delay Cognitive Decline in Mild Cognitively Impaired Subjects,” *clinicaltrials.gov*, Clinical trial registration NCT03641404, Aug. 2018. Accessed: Jun. 02, 2022. [Online]. Available: <https://clinicaltrials.gov/ct2/show/NCT03641404>
- [121] Midwest Center for Metabolic and Cardiovascular Research, “A Placebo-controlled, Randomized, Double-blind Trial to Assess the Effects of Ergothioneine on Cognition, Mood, and Sleep in Healthy Adult Men and Women,” *clinicaltrials.gov*, Clinical trial registration NCT04556032, Nov. 2020. Accessed: Jun. 02, 2022. [Online]. Available: <https://clinicaltrials.gov/ct2/show/NCT04556032>
- [122] R. B. Beelman, M. D. Kalaras, A. T. Phillips, and J. P. Richie, “Is ergothioneine a ‘longevity vitamin’ limited in the American diet?,” *J Nutr Sci*, vol. 9, p. e52, Nov. 2020, doi: 10.1017/jns.2020.44.
- [123] H.-Y. Pan *et al.*, “Ergothioneine exhibits longevity-extension effect in *Drosophila melanogaster* via regulation of cholinergic neurotransmission, tyrosine metabolism, and fatty acid oxidation,” *Food Funct*, vol. 13, no. 1, pp. 227–241, Jan. 2022, doi: 10.1039/d1fo02758a.
- [124] R. M. Y. Tang, I. K.-M. Cheah, T. S. K. Yew, and B. Halliwell, “Distribution and accumulation of dietary ergothioneine and its metabolites in mouse tissues,” *Scientific Reports*, vol. 8, no. 1, Art. no. 1, Jan. 2018, doi: 10.1038/s41598-018-20021-z.
- [125] T. T. Williamson, X. Zhu, J. P. Walton, and R. D. Frisina, “Auditory brainstem gap responses start to decline in mice in middle age: a novel physiological biomarker for age-related hearing loss,” *Cell Tissue Res.*, vol. 361, no. 1, pp. 359–369, Jul. 2015, doi: 10.1007/s00441-014-2003-9.
- [126] A. Cnaan, N. M. Laird, and P. Slasor, “Using the general linear mixed model to analyse unbalanced repeated measures and longitudinal data,” *Statistics in Medicine*, vol. 16, no. 20, pp. 2349–2380, 1997, doi: 10.1002/(SICI)1097-0258(19971030)16:20<2349::AID-SIM667>3.0.CO;2-E.
- [127] C. Krueger and L. Tian, “A Comparison of the General Linear Mixed Model and Repeated Measures ANOVA Using a Dataset with Multiple Missing Data Points,” *Biological Research For Nursing*, vol. 6, no. 2, pp. 151–157, Oct. 2004, doi: 10.1177/1099800404267682.
- [128] P. Martínez-Martín *et al.*, “Parkinson Symptoms and Health Related Quality of Life as Predictors of Costs: A Longitudinal Observational Study with Linear Mixed Model Analysis,” *PLOS ONE*, vol. 10, no. 12, p. e0145310, Dec. 2015, doi: 10.1371/journal.pone.0145310.

- [129] A. Larionov, A. Krause, and W. Miller, "A standard curve based method for relative real time PCR data processing," *BMC Bioinformatics*, vol. 6, p. 62, Mar. 2005, doi: 10.1186/1471-2105-6-62.
- [130] S. Dutta and P. Sengupta, "Men and mice: Relating their ages," *Life Sciences*, vol. 152, pp. 244–248, May 2016, doi: 10.1016/j.lfs.2015.10.025.
- [131] P. Dallos, "The active cochlea," *J Neurosci*, vol. 12, no. 12, pp. 4575–4585, Dec. 1992, doi: 10.1523/JNEUROSCI.12-12-04575.1992.
- [132] J.-P. Bai, A. Surguchev, S. Montoya, P. S. Aronson, J. Santos-Sacchi, and D. Navaratnam, "Prestin's Anion Transport and Voltage-Sensing Capabilities Are Independent," *Biophys J*, vol. 96, no. 8, pp. 3179–3186, Apr. 2009, doi: 10.1016/j.bpj.2008.12.3948.
- [133] G. I. Frolenkov, "Regulation of electromotility in the cochlear outer hair cell," *J Physiol*, vol. 576, no. Pt 1, pp. 43–48, Oct. 2006, doi: 10.1113/jphysiol.2006.114975.
- [134] H. Wang *et al.*, "Inner hair cell ribbon synapse plasticity might be molecular basis of temporary hearing threshold shifts in mice," *Int J Clin Exp Pathol*, vol. 8, no. 7, pp. 8680–8691, Jul. 2015.
- [135] F. Song, B. Gan, N. Wang, Z. Wang, and A. Xu, "Hidden hearing loss is associated with loss of ribbon synapses of cochlea inner hair cells," *Bioscience Reports*, vol. 41, no. 4, p. BSR20201637, Apr. 2021, doi: 10.1042/BSR20201637.
- [136] "Ergothioneine levels in an elderly population decrease with age and incidence of cognitive decline; a risk factor for neurodegeneration? - PubMed." <https://pubmed.ncbi.nlm.nih.gov/27444382/> (accessed May 08, 2022).
- [137] K. Obayashi, K. Kurihara, Y. Okano, H. Masaki, and D. B. Yarosh, "L-Ergothioneine scavenges superoxide and singlet oxygen and suppresses TNF-alpha and MMP-1 expression in UV-irradiated human dermal fibroblasts," *J Cosmet Sci*, vol. 56, no. 1, pp. 17–27, Feb. 2005.
- [138] V. Srivastava *et al.*, "Association of SOD2, a Mitochondrial Antioxidant Enzyme, with Gray Matter Volume Shrinkage in Alcoholics," *Neuropsychopharmacology*, vol. 35, no. 5, pp. 1120–1128, Apr. 2010, doi: 10.1038/npp.2009.217.
- [139] R. D. Williamson *et al.*, "L-(+)-Ergothioneine Significantly Improves the Clinical Characteristics of Preeclampsia in the Reduced Uterine Perfusion Pressure Rat Model," *Hypertension*, vol. 75, no. 2, pp. 561–568, Feb. 2020, doi: 10.1161/HYPERTENSIONAHA.119.13929.

- [140] J. C. Corona and M. R. Duchon, "PPAR γ as a therapeutic target to rescue mitochondrial function in neurological disease," *Free Radic Biol Med*, vol. 100, pp. 153–163, Nov. 2016, doi: 10.1016/j.freeradbiomed.2016.06.023.
- [141] J. B. Mackenzie and C. G. Mackenzie, "The effect of age, sex, and androgen on blood ergothioneine," *J Biol Chem*, vol. 225, no. 2, pp. 651–657, Apr. 1957.
- [142] M. C. Decaroli and V. Rochira, "Aging and sex hormones in males," *Virulence*, vol. 8, no. 5, pp. 545–570, Nov. 2016, doi: 10.1080/21505594.2016.1259053.
- [143] K. R. Henry, "Males lose hearing earlier in mouse models of late-onset age-related hearing loss; females lose hearing earlier in mouse models of early-onset hearing loss," *Hear Res*, vol. 190, no. 1–2, pp. 141–148, Apr. 2004, doi: 10.1016/S0378-5955(03)00401-5.
- [144] P. Guimaraes, X. Zhu, T. Cannon, S. Kim, and R. D. Frisina, "Sex differences in distortion product otoacoustic emissions as a function of age in CBA mice," *Hear Res*, vol. 192, no. 1–2, pp. 83–89, Jun. 2004, doi: 10.1016/j.heares.2004.01.013.
- [145] D. McFadden, "Masculinization of the Mammalian Cochlea," *Hear Res*, vol. 252, no. 1–2, pp. 37–48, Jun. 2009, doi: 10.1016/j.heares.2009.01.002.
- [146] D. L. Maney, D. Maney, and R. Pinaud, "Estradiol-dependent modulation of auditory processing and selectivity in songbirds," *Front Neuroendocrinol*, vol. 32, no. 3, pp. 287–302, Aug. 2011, doi: 10.1016/j.yfrne.2010.12.002.
- [147] S. W. Yeo, K.-H. Chang, S.-N. Park, and B.-D. Suh, "Effects of testosterone in the treatment of immune-mediated sensorineural hearing loss," *Eur Arch Otorhinolaryngol*, vol. 260, no. 6, pp. 316–319, Jul. 2003, doi: 10.1007/s00405-002-0570-y.
- [148] N. P. Zauber and A. G. Zauber, "Hematologic Data of Healthy Very Old People," *JAMA*, vol. 257, no. 16, pp. 2181–2184, Apr. 1987, doi: 10.1001/jama.1987.03390160067028.
- [149] R. Alis, O. Fuster, L. Rivera, M. Romagnoli, and A. Vaya, "Influence of age and gender on red blood cell distribution width," *Clin Chem Lab Med*, vol. 53, no. 2, pp. e25–28, Feb. 2015, doi: 10.1515/cclm-2014-0756.
- [150] M. V. Kameneva, K. O. Garrett, M. J. Watach, and H. S. Borovetz, "Red blood cell aging and risk of cardiovascular diseases," *Clinical Hemorheology and Microcirculation*, vol. 18, no. 1, pp. 67–74, Jan. 1998.
- [151] J. Dybas *et al.*, "Age-related and atherosclerosis-related erythropathy in ApoE/LDLR $^{-/-}$ mice," *Biochimica et Biophysica Acta (BBA) - Molecular Basis of Disease*, vol. 1866, no. 12, p. 165972, Dec. 2020, doi: 10.1016/j.bbdis.2020.165972.

- [152] W. Guo, M. Li, and S. Bhasin, "Testosterone Supplementation Improves Anemia in Aging Male Mice," *J Gerontol A Biol Sci Med Sci*, vol. 69, no. 5, pp. 505–513, May 2014, doi: 10.1093/gerona/glt127.
- [153] E. Bachman *et al.*, "Testosterone Induces Erythrocytosis via Increased Erythropoietin and Suppressed Hecpidin: Evidence for a New Erythropoietin/Hemoglobin Set Point," *J Gerontol A Biol Sci Med Sci*, vol. 69, no. 6, pp. 725–735, Jun. 2014, doi: 10.1093/gerona/glt154.
- [154] I. K. Cheah, R. M. Y. Tang, T. S. Z. Yew, K. H. C. Lim, and B. Halliwell, "Administration of Pure Ergothioneine to Healthy Human Subjects: Uptake, Metabolism, and Effects on Biomarkers of Oxidative Damage and Inflammation," *Antioxid Redox Signal*, vol. 26, no. 5, Art. no. 5, 10 2017, doi: 10.1089/ars.2016.6778.
- [155] D. Taubert *et al.*, "Association of rheumatoid arthritis with ergothioneine levels in red blood cells: a case control study," *J Rheumatol*, vol. 33, no. 11, pp. 2139–2145, Nov. 2006.
- [156] L. K. Schmitz, "Bioavailability and antioxidant effect of ergothioneine in human blood," *MaRBL*, vol. 6, 2015, doi: 10.26481/marble.2015.v6.375.
- [157] H. Mitsuyama and J. M. May, "Uptake and antioxidant effects of ergothioneine in human erythrocytes," *Clin Sci (Lond)*, vol. 97, no. 4, pp. 407–411, Oct. 1999.
- [158] S. Sotgia *et al.*, "Clinical and Biochemical Correlates of Serum L-Ergothioneine Concentrations in Community-Dwelling Middle-Aged and Older Adults," *PLOS ONE*, vol. 9, no. 1, p. e84918, Jan. 2014, doi: 10.1371/journal.pone.0084918.
- [159] B. Halliwell and J. M. C. Gutteridge, *Free Radicals in Biology and Medicine*, 5th ed. Oxford: Oxford University Press, 2015. doi: 10.1093/acprof:oso/9780198717478.001.0001.
- [160] S. S. Spicer, J. G. Wooley, and V. Kessler, "Ergothioneine Depletion in Rabbit Erythrocytes and Its Effect on Methemoglobin Formation and Reversion," *Proceedings of the Society for Experimental Biology and Medicine*, vol. 77, no. 3, pp. 418–420, Jul. 1951, doi: 10.3181/00379727-77-18799.
- [161] N. A. Chaves and D. G. H. da Silva, "Homeostasis of Oxidative-Related Metabolism in Human Erythrocyte: An Overview of the Hemoglobin S Presence Implications," *ABTD*, vol. 1, no. 4, pp. 1–5, Jun. 2018.
- [162] Z. Lu *et al.*, "PGC-1 α Regulates Expression of Myocardial Mitochondrial Antioxidants and Myocardial Oxidative Stress After Chronic Systolic Overload," *Antioxid Redox Signal*, vol. 13, no. 7, pp. 1011–1022, Oct. 2010, doi: 10.1089/ars.2009.2940.

- [163] A. Botta *et al.*, "Short term exercise induces PGC-1 α , ameliorates inflammation and increases mitochondrial membrane proteins but fails to increase respiratory enzymes in aging diabetic hearts," *PLoS One*, vol. 8, no. 8, p. e70248, 2013, doi: 10.1371/journal.pone.0070248.
- [164] S.-D. Chen, D.-I. Yang, T.-K. Lin, F.-Z. Shaw, C.-W. Liou, and Y.-C. Chuang, "Roles of Oxidative Stress, Apoptosis, PGC-1 α and Mitochondrial Biogenesis in Cerebral Ischemia," *Int J Mol Sci*, vol. 12, no. 10, pp. 7199–7215, Oct. 2011, doi: 10.3390/ijms12107199.
- [165] M. Ben Said *et al.*, "A mutation in SLC22A4 encoding an organic cation transporter expressed in the cochlea stria endothelium causes human recessive non-syndromic hearing loss DFNB60," *Hum Genet*, vol. 135, no. 5, Art. no. 5, May 2016, doi: 10.1007/s00439-016-1657-7.
- [166] L. M. Tiede, S. M. Rocha-Sanchez, R. Hallworth, M. G. Nichols, and K. Beisel, "Determination of hair cell metabolic state in isolated cochlear preparations by two-photon microscopy," *JBO*, vol. 12, no. 2, p. 021004, Mar. 2007, doi: 10.1117/1.2714777.
- [167] K. Ishii, W. G. Zhai, and M. Akita, "Effect of a Beta-Stimulant on the Inner Ear Stria Vascularis," *Ann Otol Rhinol Laryngol*, vol. 109, no. 7, pp. 628–633, Jul. 2000, doi: 10.1177/000348940010900703.
- [168] D. Coling, S. Chen, L.-H. Chi, S. Jamesdaniel, and D. Henderson, "Age-related Changes in Antioxidant Enzymes Related to Hydrogen Peroxide Metabolism in Rat Inner Ear," *Neurosci Lett*, vol. 464, no. 1, pp. 22–25, Oct. 2009, doi: 10.1016/j.neulet.2009.08.015.

Appendix A: EGT Injection Calculations

EGT injections were based on the weight of each individual mouse and administered according to Figure 2.1. Here, we calculated the delivered concentration for individual mice at both dose levels, low and high. Low dose mice were given injections of EGT equivalent to 35 mg/kg for the first 7 days of the study where the dose was then doubled (70 mg/kg) and given once a week until the test date end. Below, we start with the desired dose and convert into mol/kg.

$$1. \quad 35 \frac{\text{mg}}{\text{kg}} * \frac{1\text{g}}{1000\text{mg}} \text{ (Convert mg to grams)} * \frac{\text{mol}}{229.3\text{g}} \text{ (Multiply by MW)}$$

This number is then multiplied by a conversion factor and 25g (average mouse weight) to obtain the average amount of moles of EGT delivered in one dose.

$$2. \quad * \frac{1\text{kg}}{1000\text{g}} \text{ (Convert kg to grams)} * 25\text{g} \text{ (Multiply by assumed mouse BW, 25g)}$$
$$= 3.8159 * 10^{(-6)} \text{ moles or } 3.8159 \mu\text{mol} \text{ (convert to umoles)}$$

The amount of moles is then divided by 0.1 mL (desired injection volume) to get the concentration.

$$3. \quad 3.8159 \frac{\mu\text{mol}}{.1\text{mL}} \text{ (Divide } \mu\text{mol by desired injection volume)} * \frac{1000\text{mL}}{\text{L}} \text{ (convert mL to L)}$$
$$= 38159.61\mu\text{M} = 38.159\text{mM} \text{ (convert to mM)}$$

Lastly, in the event that a mouse weighs more than 25 g, the injection volume was adjusted as below:

$$4. \quad \frac{0.1\text{mL}}{25\text{g}} = \frac{X}{30\text{g}} \text{ (Use 30g as example BW); } \frac{.1\text{mL}}{25\text{g}} * 30\text{g} = X, X = 0.12\text{mL}$$

High dose mice then were calculated in much the same way, where 70 mg/kg was administered for the first 7 days and then once a week until the testing end date where the dose was doubled (140 mg/kg). Here we see that 70 mg/kg is simply double the amount of EGT in moles and concentration.

$$\begin{aligned}
 5. & \quad 70 \frac{mg}{kg} * \frac{1g}{1000mg} \text{ (Convert mg to grams)} * \frac{mol}{229.3g} \text{ (Multiply by MW)} \\
 6. & \quad * \frac{1kg}{1000g} \text{ (Convert kg to grams)} * 25g \text{ (Multiply by assumed mouse BW, 25g)} \\
 & \quad = 7.6319 * 10^{(-6)} \text{ moles or } 7.6319 \text{ } \mu\text{mol (convert to umoles)}
 \end{aligned}$$

In the below calculation, the moles will be used to calculate the concentration of EGT given in a 0.1 mL injection.

$$\begin{aligned}
 7. & \quad 7.6319 \frac{\mu\text{mol}}{.1\text{mL}} \text{ (Divide } \mu\text{mol by desired injection volume)} * \frac{1000\text{mL}}{L} \text{ (convert mL to L)} \\
 & \quad = 76319.23\mu\text{M} = 76.32\text{mM (convert to mM)}
 \end{aligned}$$

Lastly, in the event that a mouse weighs more than 25 g, the injection volume was adjusted as below:

$$\frac{0.1\text{mL}}{25\text{g}} = \frac{X}{30\text{g}} \text{ (Use 30g as example BW); } \quad \frac{0.1\text{mL}}{25\text{g}} * 30\text{g} = X, X = 0.12\text{mL}$$

Appendix B: Compiled Group Results for ABR and DPOAE

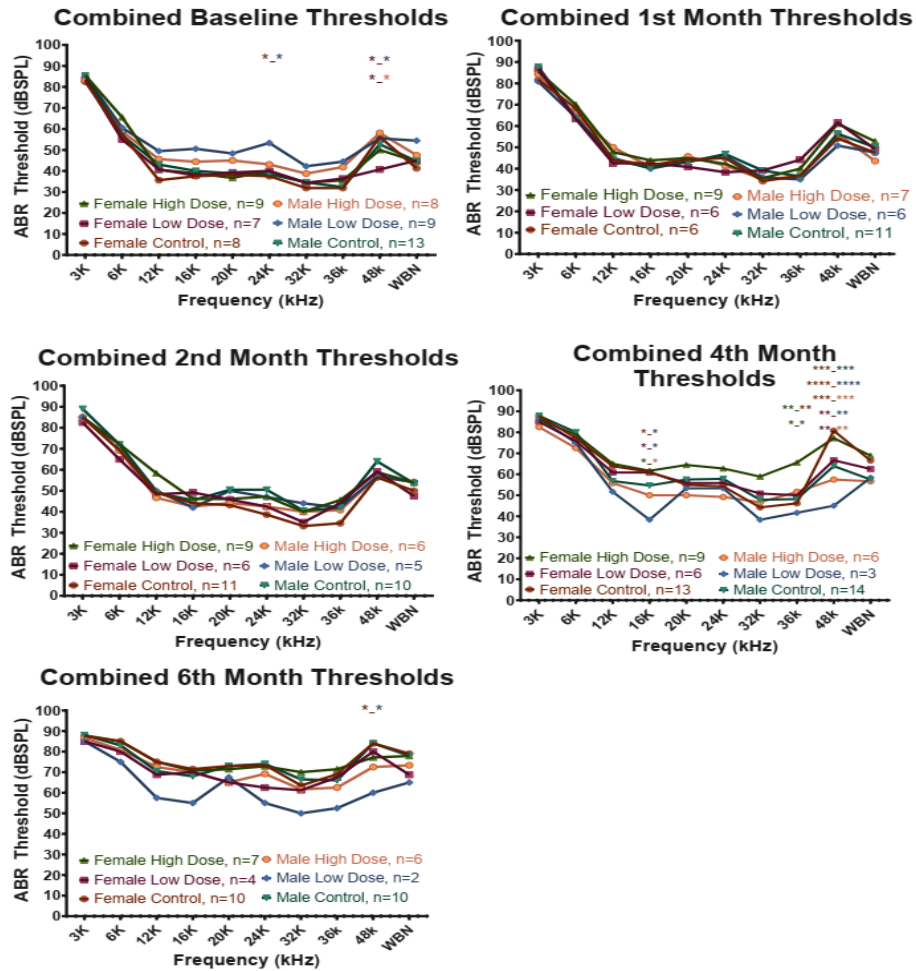


Figure B.1: Combined ABR Thresholds for All Test Groups. ABR Thresholds for all test groups were combined and analyzed at each time-point. Here we can see that the two male treated groups have slightly higher thresholds than all other groups at Baseline. However, by the 4th and 6th months, both male treated groups show *reduced* thresholds, while all other groups experienced elevated thresholds, consistent with the continued progression of age-related hearing loss. Data analyzed using 2-way ANOVA with Tukey's multiple comparison *post-hoc* corrections. Each dataset is compared to every other dataset and analyzed for significance. Significance between two groups is denoted by the colors of the two starred groups separated with an underscore where $P < 0.05$, $** P < 0.01$, $*** P < 0.001$, $**** P < 0.0001$.

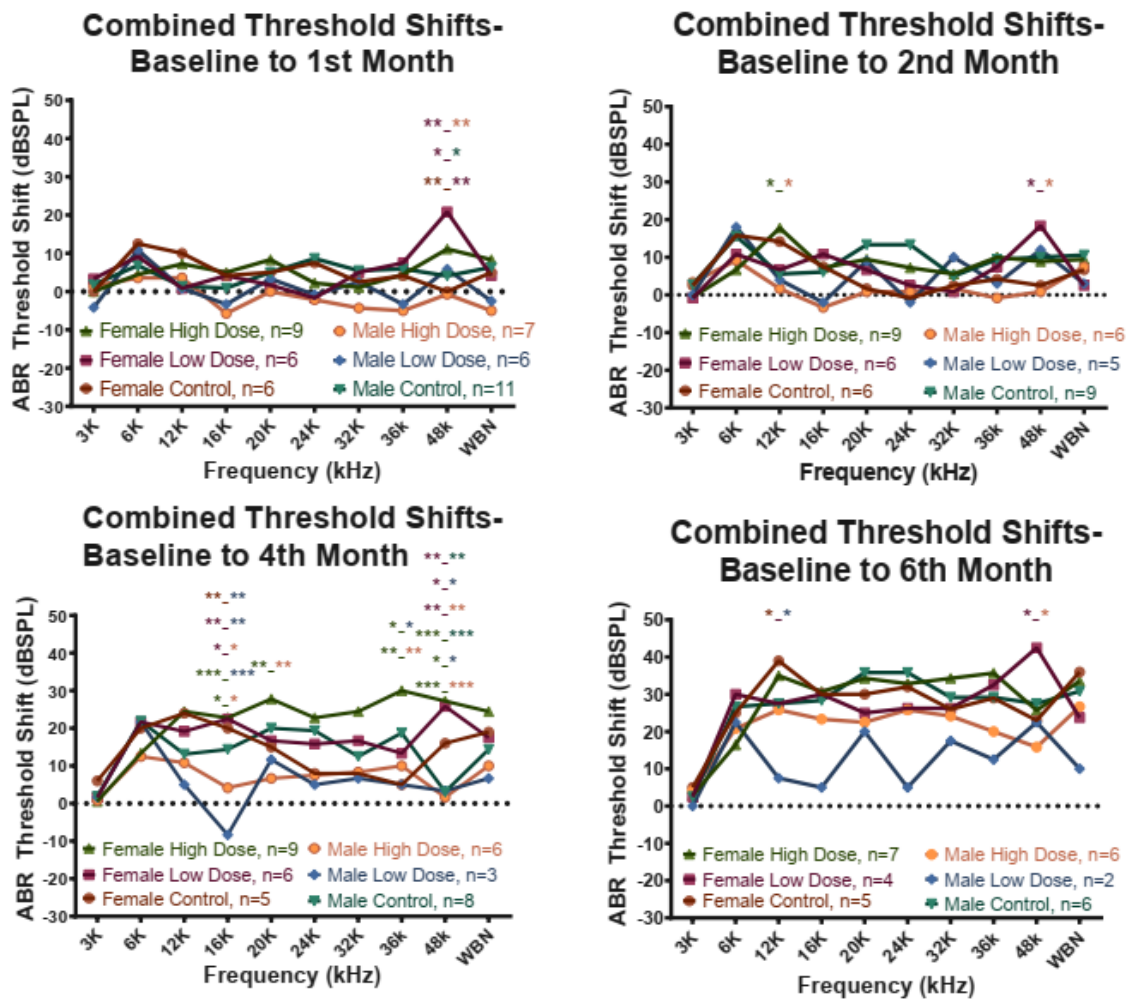


Figure B.2: Combined ABR Threshold Shifts for All Test Groups. ABR Thresholds Shifts analyses of all groups at each time-point. Even at the first time-point, it is clear that both male treated groups are outperforming all other groups. Additionally, female low-dose (LD) mice have already experienced elevated thresholds at 48 kHz. By the 4th and 6th Months from Baseline, both male treated groups continue to to have lower thresholds relative to all others, as seen in the 6th Month, where male LD mice show minimal threshold shifts at various frequencies. Data analyzed using 2-way ANOVA with Tukey’s multiple comparison *post-hoc* corrections. Each dataset is compared to every other dataset and analyzed for significance. Significance between two groups is denoted by the colors of the two starred groups separated with an underscore where $P < 0.05$, $** P < 0.01$, $*** P < 0.001$, $**** P < 0.0001$.

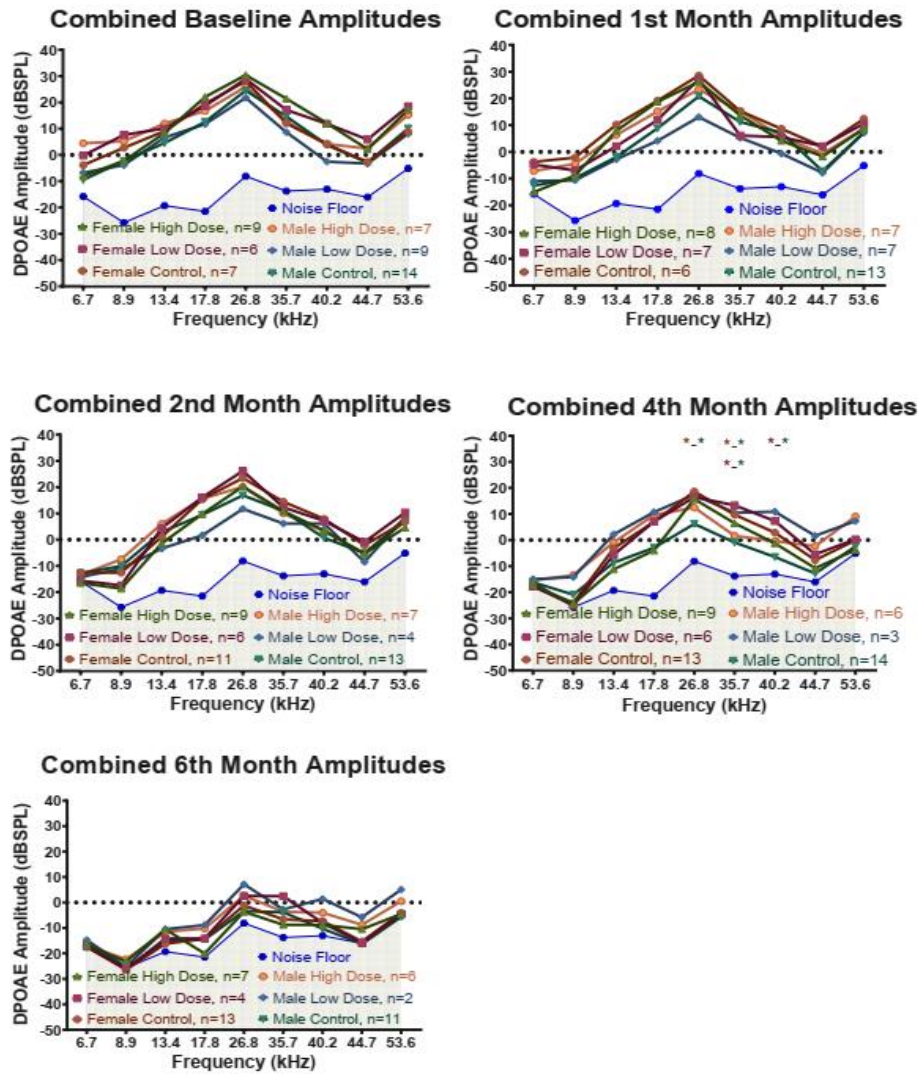


Figure B.3: Combined DPOAE Amplitudes for All Test Groups. DPOAE Amplitudes for all test groups were combined and analyzed at each time-point. All baseline groups look to have similar amplitudes where amplitude decline starts in the 1st month. Here female LD and male LD are noticeable in their decline. By the 2nd month, all female groups appear to show no decline while male LD continues to show amplitude decline. By the 4th and 6th months, male LD and HD exhibit amplitudes either in line or better than all other groups. This can be especially seen in the 6th month data. Data analyzed using 2-way ANOVA with Tukey's multiple comparison *post-hoc* corrections. Each dataset is compared to every other dataset and analyzed for significance. Significance between two groups is denoted by the colors of the two starred groups separated with an underscore where $P < 0.05$, ** $P < 0.01$, *** $P < 0.001$, **** $P < 0.0001$.

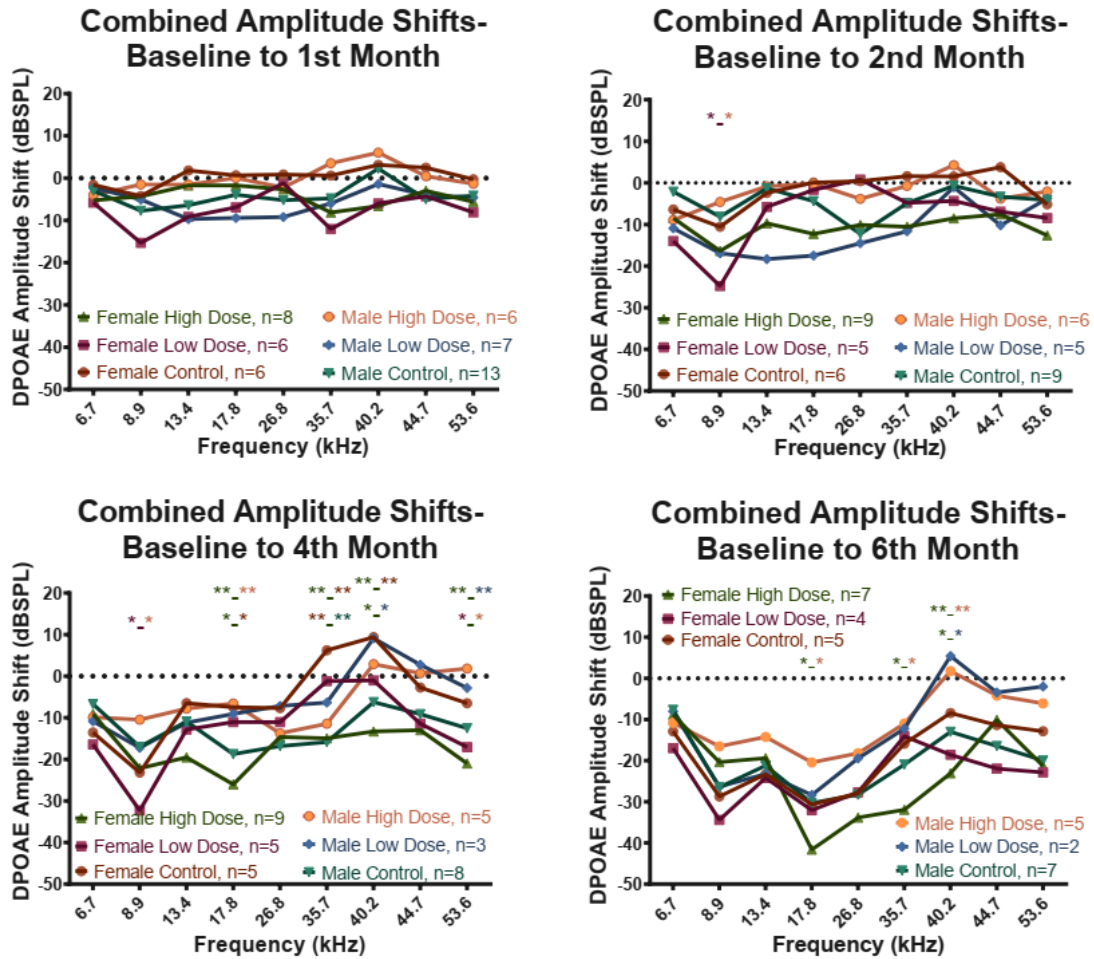


Figure B.4: Combined DPOAE Amplitude Shifts for All Test Groups. DPOAE Amplitude Shifts analyzes all groups at each time-point. Baseline to 1st month shifts show normal amplitude decline for all groups except for female control and male HD. In the next time-point, male HD and female control continue to exhibit no decline while male LD declines further. By the 4th month both male LD and HD exhibit improved amplitudes at 40.2 and 44.7 kHz where female control and LD also show improved amplitudes compared to previous months. 6th month data then exhibits male LD and HD separating from the other groups at 40.2-53.6 kHz. Data analyzed using 2-way ANOVA with Tukey’s multiple comparison *post-hoc* corrections. Each dataset is compared to every other dataset and analyzed for significance. Significance between two groups is denoted by the colors of the two starred groups separated with an underscore where $P < 0.05$, ** $P < 0.01$, *** $P < 0.001$, **** $P < 0.0001$.

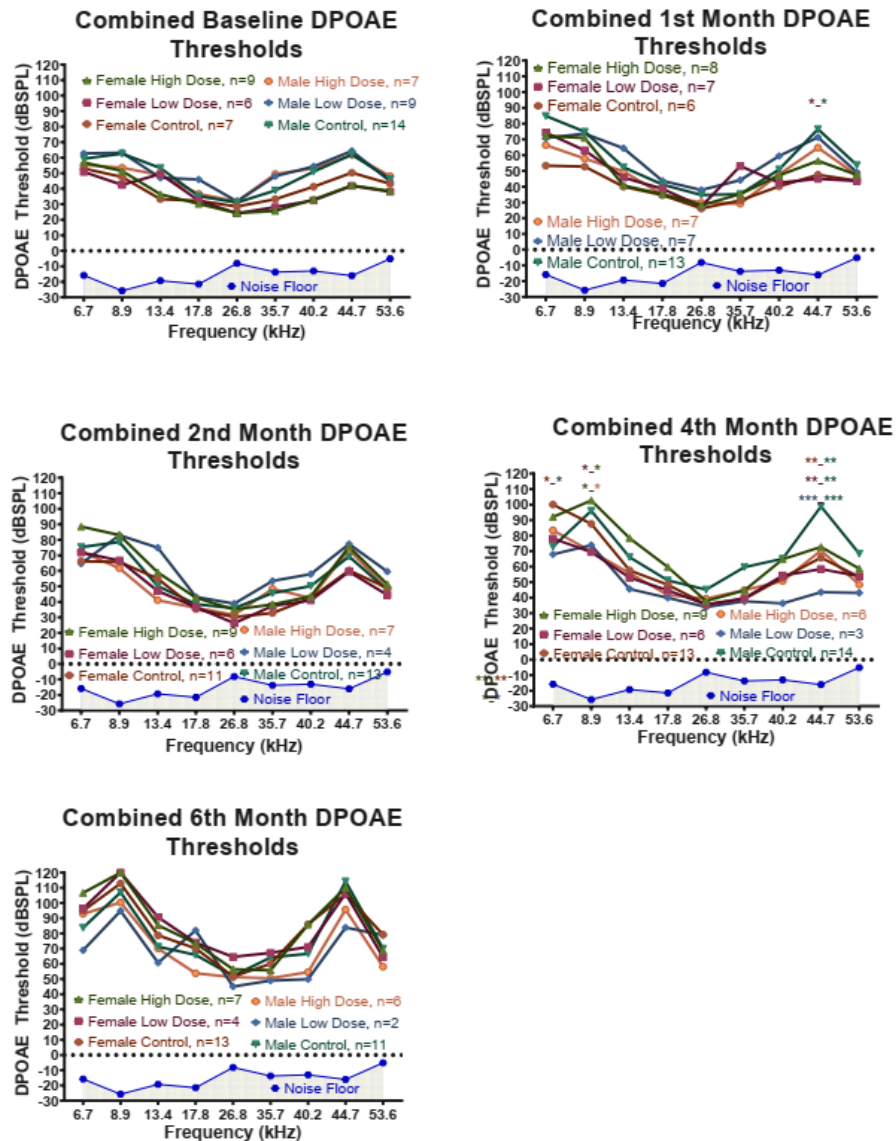


Figure B.5: Combined DPOAE Thresholds for All Test Groups. DPOAE Thresholds for all test groups were combined and analyzed at each time-point. All baseline groups look to have similar thresholds, and threshold elevation starts in the 1st month. Here male control and male LD are noticeable in their elevations at 44.7 kHz. 2nd month analysis then reveals no significant differences, where 4th month data reveals significant differences for female LD due to its threshold elevation. Interestingly, male LD has switched position in the group, showing noticeably reduced thresholds. 6th month data continues this trend as male LD and HD have lower thresholds than all other groups. Data analyzed using 2-way ANOVA with Tukey's multiple comparison *post-hoc* corrections. Each dataset is compared to every other dataset and analyzed for significance. Significance between two groups is denoted by the colors of the two starred groups separated with an underscore where $P < 0.05$, ** $P < 0.01$, *** $P < 0.001$, **** $P < 0.0001$.

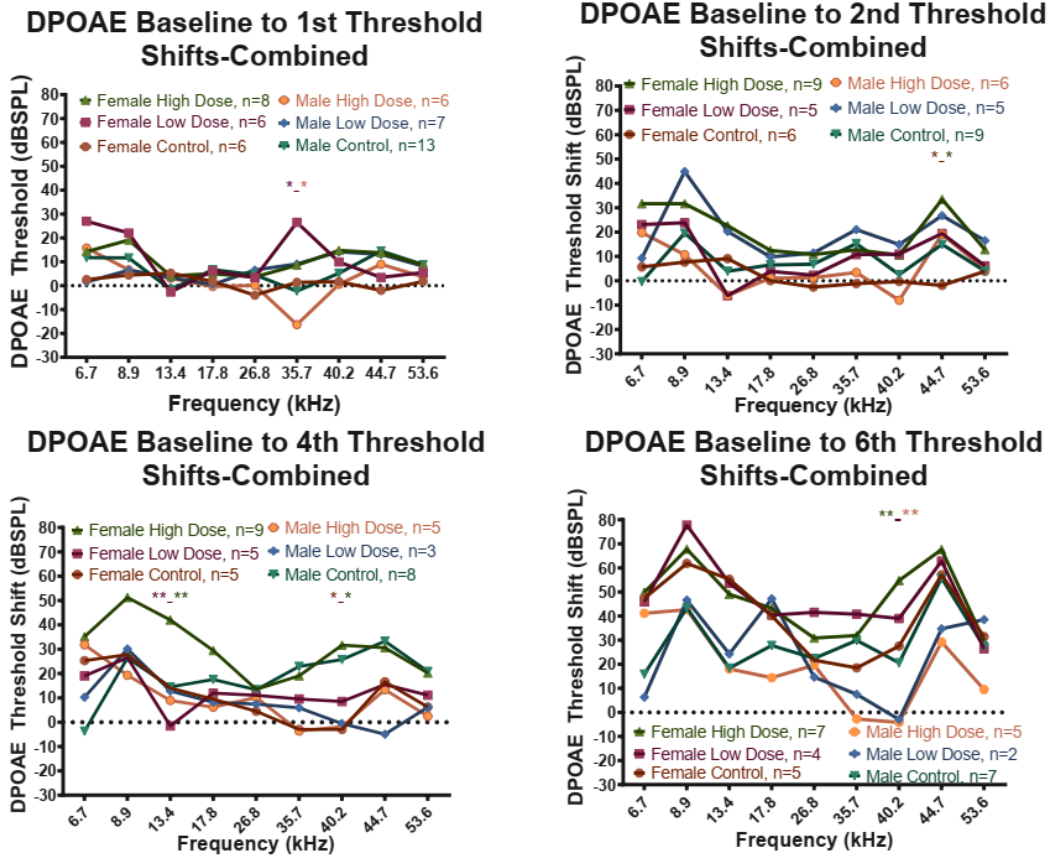


Figure B.6: Combined DPOAE Threshold Shifts for All Test Groups. DPOAE Threshold Shifts analyses of all groups at each time-point. Baseline to 1st month shifts show a negative threshold for male HD and significant elevation for female LD at 35.7 kHz. In the next time-point, male HD and female control exhibit no decline while male LD and female LD experience elevated threshold shifts. By the 4th month both male LD and HD exhibit low threshold shifts at 40.2 and 44.7 kHz, whereas female control and LD also show reduced threshold shifts. Here, female HD and male controls are shown to be experiencing significant age-related hearing loss threshold elevations, i.e. positive shifts. 6th month data then shows male LD and HD separating from the other groups at 35.7-53.6 kHz. Data analyzed using 2-way ANOVA with Tukey's multiple comparison *post-hoc* corrections. Each dataset is compared to every other dataset and analyzed for significance. Significance between two groups is denoted by the colors of the two starred groups separated with an underscore where $P < 0.05$, $** P < 0.01$, $*** P < 0.001$, $**** P < 0.0001$.

Appendix C: Peak Picking Results-Peak 1

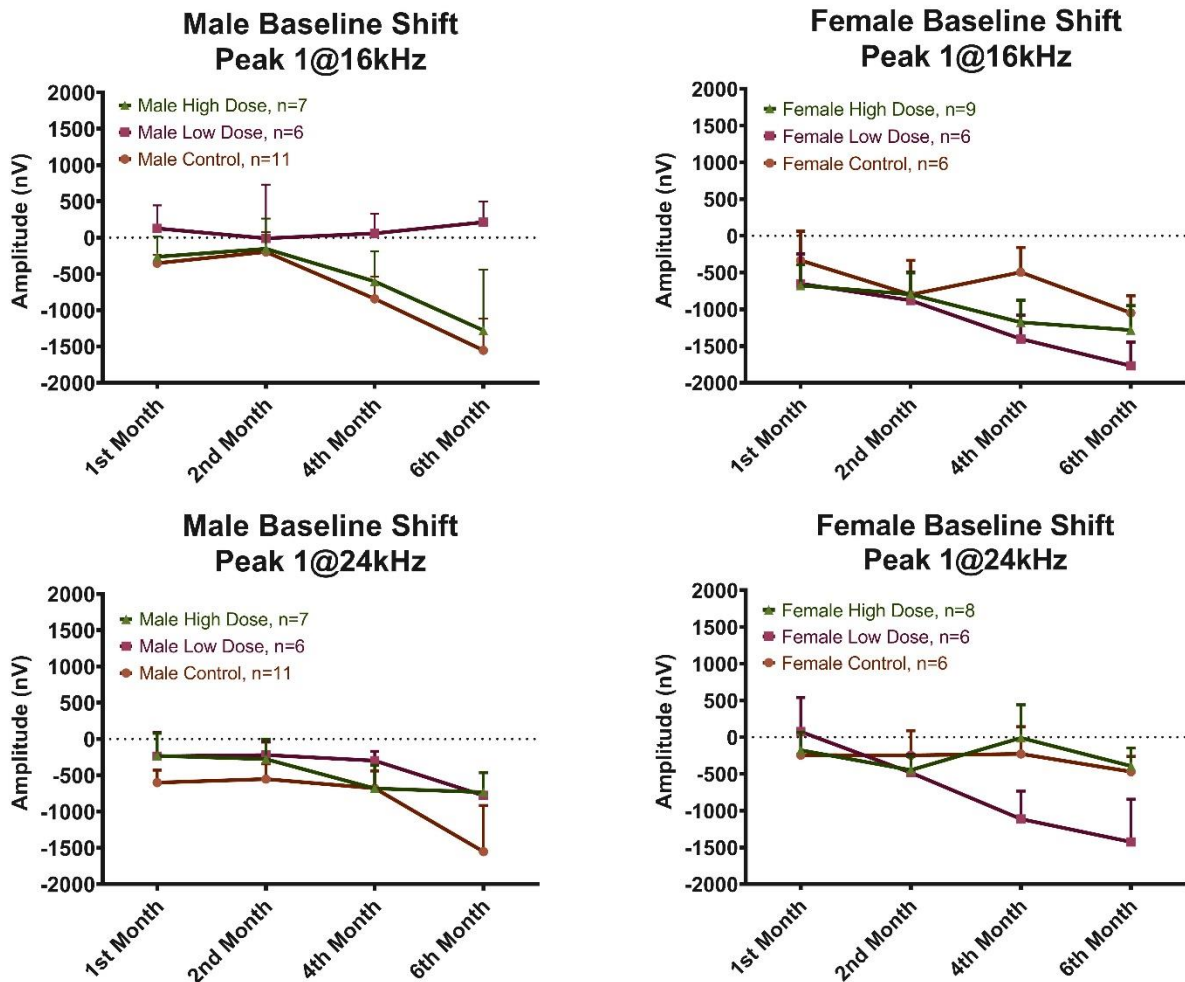


Figure C.1: ABR Amplitude Shift Analysis Peak 1. Here, Peak 1 shifts show better amplitudes for treated males relative to male Controls, for both frequencies. While female shifts for Controls are similar to, or are greater (better) than both female treated groups. Peak 1 amplitudes for subsequent months were subtracted from Baseline data to determine the Baseline shift. Data were analyzed using 2-way ANOVA with Dunnett's multiple comparison *post-hoc* corrections. Each dataset was compared to every other dataset and analyzed for significance. None of the Peak 1 amplitude main effects was statistically significant.

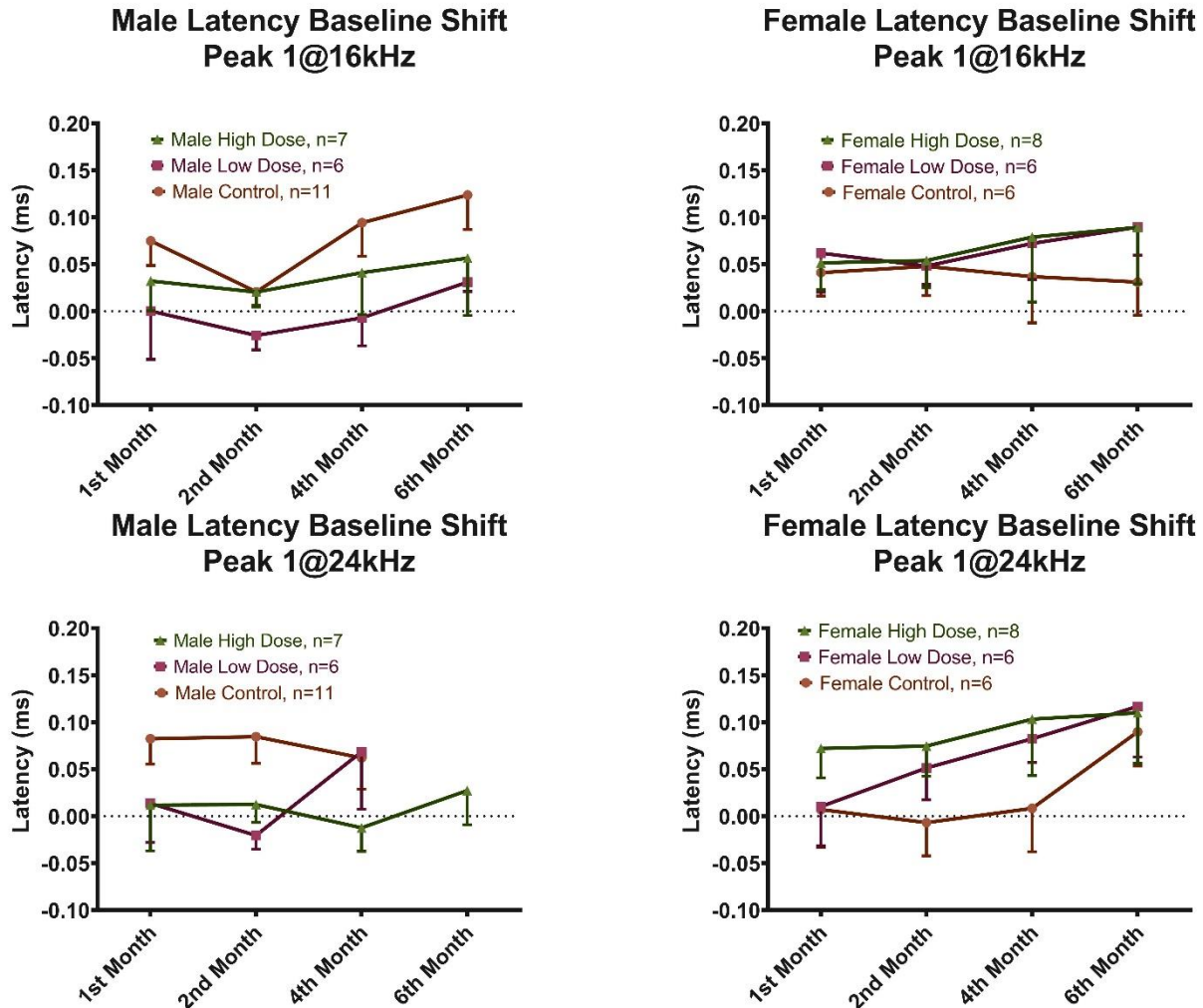


Figure C.2: ABR Latency Shift Analysis Peak 1. Here, Peak 1 Latency shifts show improvements for treated males, for both frequencies; while female shifts for Controls are better (shorter latencies) than both female treated groups. Peak 1 Latencies for subsequent months were subtracted from Baseline data to determine the Baseline shift. Data were analyzed using 2-way ANOVA with Dunnett's multiple comparison *post-hoc* corrections. Each dataset is compared to every other dataset and analyzed for significance. None of the Peak 1 Latency main effects was statistically significant.